Radio Science Bulletin

ISSN 1024-4530

INTERNATIONAL
UNION OF
RADIO SCIENCE

UNION
RADIO-SCIENTIFIQUE
INTERNATIONALE

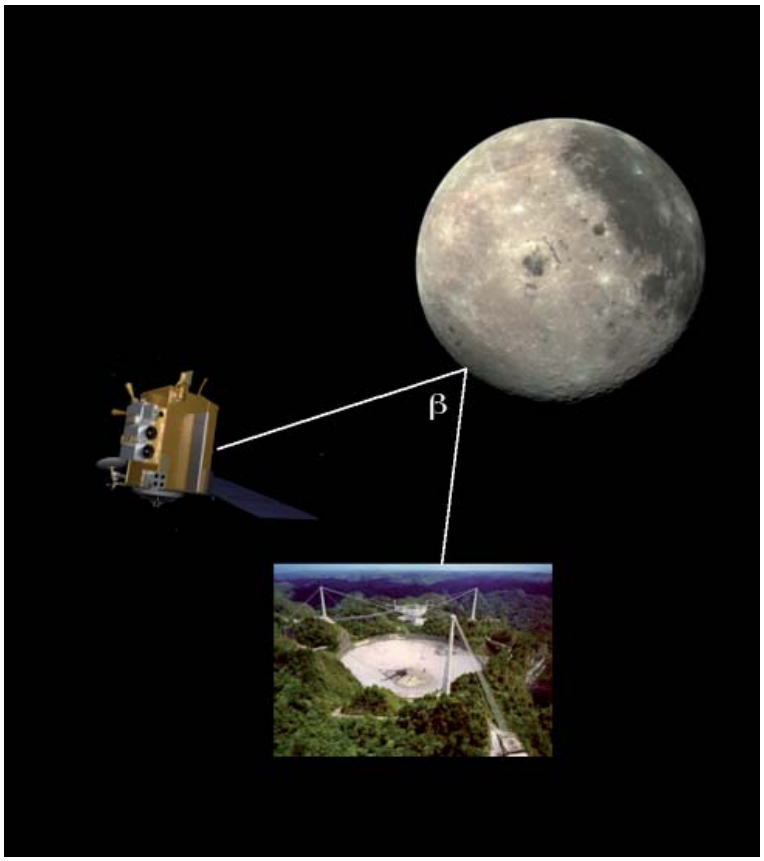

No 357
June 2016

URSI, c/o Ghent University (INTEC)
St.-Pietersnieuwstraat 41, B-9000 Gent (Belgium)

Contents

Front cover: A schematic overview of S-band (13 cm wavelength) Arecibo-Lunar Reconnaissance Orbiter mapping of the moon. See the paper by Thomas W. Thompson, Bruce A. Campbell, and D. Benjamin J. Bussey, pp. 23-35.

The International Union of Radio Science (URSI) is a foundation Union (1919) of the International Council of Scientific Unions as direct and immediate successor of the Commission Internationale de Télégraphie Sans Fil which dates from 1914.

Radio Science Bulletin Staff

Editor

W. R. Stone
Stoneware Limited
840 Armada Terrace
San Diego, CA 92106, USA
Tel: +1-619 222 1915, Fax: +1-619 222 1606
E-mail: r.stone@ieee.org

Editor-in-Chief

P. Lagasse
URSI Secretariat
Ghent University - INTEC
Technologiepark - Zwijnaarde 15
B-9052 Gent, BELGIUM
Tel: +32 9-264 33 20, Fax: +32 9-264 42 88
E-mail: lagasse@intec.ugent.be

Production Editors

I. Lievens
I. Heleu
URSI Secretariat / Ghent University - INTEC
Technologiepark - Zwijnaarde 15
B-9052 Gent, BELGIUM
Tel: +32 9-264.33.20, Fax: +32 9-264.42.88
E-mail: ingeursi@intec.ugent.be, info@ursi.org

Senior Associate Editors

A. Pellinen-Wannberg
Department of Physics
Umea University
BOX 812
SE-90187 Umea, SWEDEN
Tel: +46 90 786 74 92, Fax: +46 90 786 66 76
E-mail: asta.pellinen-wannberg@umu.se

O. Santolik
Institute of Atmospheric Physics
Academy of Sciences of the Czech Republic
Bocni II
1401, 141 31 Prague 4, CZECH REPUBLIC
Tel: +420 267 103 083, Fax +420 272 762 528
E-mail os@ufa.cas.cz, santolik@gmail.com

Associate Editors, Commissions

Commission A

P. Tavella
INRIM
Strada delle Cacce 91
10135 Torino, ITALY
Tel: +39 011 3919235, Fax: +39 011 3919259
E-mail: tavella@inrim.it

P. M. Duarte Cruz
Instituto de Telecomunicações
Campus Universitário de Santiago
P-3810-193 Aveiro, PORTUGAL
Tel: +351 234377900
E-mail: pcruz@av.it.pt

Commission B

K. Kobayashi
Dept. of Electrical, and Communication Engineering
Chuo University
1-13-27 Kasuga, Bunkyo-ku
Tokyo, 112-8551, JAPAN
Tel: +81 3 3817 1846/69, Fax: +81 3 3817 1847
E-mail: kazuya@tamacc.chuo-u.ac.jp

L. Li
School of EECS
Peking University
Room 2843N, Science Building#2
Beijing 100871, CHINA CIE
Tel: +86-10-62754409-2 , Fax: +86-10-62754409
E-mail: lianlin.li@pku.edu.cn

Commission C

S. E. El-Khamy
Dept. of Electrical Engineering
Alexandria University - Faculty of Engineering
Abou-Keer Street
Alexandria 21544, EGYPT
Tel: +2010-1497360, Fax: +203 5971853
E-mail: elkhamy@ieee.org, said.elkhamy@gmail.com

A. I. Zaghloul
Ece, Virginia Tech
7054 Haycock Rd
22043 Falls Church, USA
Tel: +1-703-538-8435, Fax: +1-703-538-8450
E-mail: amirz@vt.edu

Commission D

G. Gradoni
School of Mathematical Sciences
University of Nottingham
University Park
Nottingham NG7 2RD, UNITED KINGDOM
Tel: +44(0)7745368300, Fax: +44(0)1159514951
E-mail: gabriele.gradoni@gmail.com, gabriele.gradoni@nottingham.ac.uk

Commission E

F. Gronwald
Hamburg University of Technology
Harburger Schloss Strasse 20
21079 Hamburg, GERMANY
Tel: +49-40-42878-2177
E-mail: gronwald@tuhh.de

G. Gradoni
School of Mathematical Sciences
University of Nottingham
University Park
Nottingham NG7 2RD, UNITED KINGDOM
Tel: +44(0)7745368300, Fax: +44(0)1159514951
E-mail: gabriele.gradoni@gmail.com, gabriele.gradoni@nottingham.ac.uk

Commission F

V. Chandrasekar
Engineering B117
Colorado State University
Fort Collins, Colorado 80523 , USA
Tel: +1 970 491 7981, Fax: +1 970 491 2249
E-mail: chandra@engr.colostate.edu, chandra.ve@gmail.com

M. Kurum
Department of Electrical and Computer Engineering
The George Washington University
800 22nd Street
NW, Washington, DC 20052, USA
Tel: +1 202 994 6080
E-mail: mkurum@gmail.com

Commission G

P. Doherty
Institute for Scientific Research
Boston College
140 Commonwealth Avenue
Chestnut Hill, MA 02467, USA
Tel: +1 617 552 8767, Fax: +1 617 552 2818
E-mail: Patricia.Doherty@bc.edu

Commission H

J. Lichtenberger
Eötvös University
Pazmany Peter Setany 1/a
H-1111 Budeapest
HUNGARY
Tel: +36 1 209 0555 x6654, Fax +36 1 372 2927
E-mail lityi@sas.elte.hu

W. Li
UCLA
7127 Math Sciences Bldg
405 Hilgard Avenue
Los Angeles, CA, 90095, USA
E-mail: moonli@atmos.ucla.edu

Commission J

J. W. M. Baars
Mm-astronomy
Max Planck Institute for Radio Astronomy
Auf dem Hügel 69
53121 Bonn, GERMANY
Tel: +49-228-525303
E-mail: jacobbaars@arcor.de

Commission K

P. Mojabi
Room E3-504B, EITC Building
Electrical and Computer Engineering Department
University of Manitoba
Winnipeg, R3T5V6, CANADA
Tel: +1 204 474 6754 , Fax: +1 204 261 4639
E-mail: Puyan.Mojabi@umanitoba.ca

Associate Editors, Columns

Book Reviews

G. Trichopoulos
Electrical, Computer & Energy Engineering ISTB4 555D
Arizona State University
781 E Terrace Road, Tempe, AZ, 85287 USA
Tel: +1 (614) 364-2090
E-mail: gtrichop@asu.edu

Historical Papers

J. D. Mathews
Communications and Space Sciences Lab (CSSL)
The Pennsylvania State University
323A, EE East
University Park, PA 16802-2707, USA
Tel: +1(814) 777-5875, Fax: +1 814 863 8457
E-mail: JDMathews@psu.edu

Et Cetera

T. Akgül
Dept. of Electronics and Communications Engineering
Telecommunications Division
Istanbul Technical University
80626 Maslak Istanbul, TURKEY
Tel: +90 212 285 3605, Fax: +90 212 285 3565
E-mail: tayfun.akgul@ieee.org

Women in Radio Science

A. Pellinen-Wannberg
Department of Physics and Swedish Institute of Space Physics
Umeå University
S-90187 Umeå, Sweden
Tel: +46 90 786 7492
E-mail: asta.pellinen-wannberg@umu.se

Ethically Speaking

Randy L. Haupt
Colorado School of Mines
Brown Building 249
1510 Illinois Street, Golden, CO 80401 USA
Tel: +1 (303) 273 3721
E-mail: rhaupt@mines.edu

Solution Box

Ö. Ergül
Department of Electrical and Electronics Engineering
Middle East Technical University
TR-06800, Ankara, Turkey
E-mail: ozgur.ergul@eee.metu.edu.tr

Telecommunications Health & Safety

J. C. Lin
University of Illinois at Chicago
851 South Morgan Street, M/C 154
Chicago, IL 60607-7053 USA
Tel: +1 312 413 1052, Fax: +1 312 996 6465
E-mail: lin@uic.edu

Historical Column

G. Pelosi
Department of Information Engineering
University of Florence
Via di S. Marta, 3, 50139 Florence, Italy
E-mail: giuseppe.pelosi@unifi.it

Early Career Representative Column

S. J. Wijnholds
Netherlands Institute for Radio Astronomy
Oude Hoogeveensedijk 4
7991 PD Dwingeloo, The Netherlands
E-mail: wijnholds@astron.nl

URSI Officers and Secretariat

Current Officers triennium 2014-2017

President

P. S. Cannon
Gisbert Kapp Building
University of Birmingham
Edgbaston , Birmingham, B15 2TT,
UNITED KINGDOM
Tel: +44 (0) 7990 564772
Fax: +44 (0)121 414 4323
E-mail: p.cannon@bham.ac.uk
president@ursi.org

Vice President

M. Ando
Dept. of Electrical & Electronic Eng.
Graduate School of Science and Eng.
Tokyo Institute of Technology
S3-19, 2-12-1 O-okayama, Meguro
Tokyo 152-8552
JAPAN
Tel: +81 3 5734-2563
Fax: +81 3 5734-2901
E-mail: mando@antenna.ee.titech.ac.jp

Past President

P. Wilkinson
Bureau of Meteorology
P.O. Box 1386
Haymarket, NSW 1240
AUSTRALIA
Tel: +61 2-9213 8003
Fax: +61 2-9213 8060
E-mail: p.wilkinson@bom.gov.au

Vice President

Y. M. M. Antar
Electrical Engineering Department
Royal Military College
POB 17000, Station Forces
Kingston, ON K7K 7B4
CANADA
Tel: +1-613 541-6000 ext.6403
Fax: +1-613 544-8107
E-mail: antar-y@rmc.ca

Secretary General

P. Lagasse
URSI Secretariat
Ghent University - INTEC
Technologiepark - Zwijnaarde 15
B-9052 Gent
BELGIUM
Tel: +32 9-264 33 20
Fax: +32 9-264 42 88
E-mail: lagasse@intec.ugent.be

Vice President

U. S. Inan
Director, STAR Laboratory
Electrical Eng. Dept
Stanford University
Packard Bldg. Rm. 355
350 Serra Mall
Stanford, CA 94305, USA
Tel: +1-650 723-4994
Fax: +1-650 723-9251
E-mail: inan@stanford.edu
uinan@ku.edu.tr

Vice President

S. Ananthakrishnan
Electronic Science Department
Pune University
Ganeshkhind, Pune 411007
INDIA
Tel: +91 20 2569 9841
Fax: +91 20 6521 4552
E-mail: subra.anan@gmail.com

URSI Secretariat

Secretary General

P. Lagasse
URSI Secretariat
Ghent University - INTEC
Technologiepark - Zwijnaarde 15
B-9052 Gent
BELGIUM
Tel: +32 9-264 33 20
Fax: +32 9-264 42 88
E-mail: lagasse@intec.ugent.be

Assistant Secretary General AP-RASC

K. Kobayashi
Dept. of Electr and Commun. Eng,
Chuo University
1-13-27 Kasuga, Bunkyo-ku
Tokyo, 112-8551
JAPAN
Tel: +81 3 3817 1846/69
Fax: +81 3 3817 1847

Assistant Secretary General

P. Van Daele
INTEC- IBBT
Ghent University
Technologiepark - Zwijnaarde 15
B-9052 Gent
BELGIUM
Tel: +32 9 331 49 06
Fax +32 9 331 48 99
E-mail peter.vandaele@intec.Ugent.be

Executive Secretary

I. Heleu
URSI Secretariat
Ghent University - INTEC
Technologiepark - Zwijnaarde 15
B-9052 Gent
BELGIUM
Tel. +32 9-264.33.20
Fax +32 9-264.42.88
E-mail info@ursi.org

Assistant Secretary General Publications & GASS

W.R. Stone
840 Armada Terrace
San Diego, CA 92106
USA
Tel: +1-619 222 1915
Fax: +1-619 222 1606
E-mail: r.stone@ieee.org

Administrative Secretary

I. Lievens
URSI Secretariat
Ghent University - INTEC
Technologiepark - Zwijnaarde 15
B-9052 Gent
BELGIUM
Tel: +32 9-264.33.20
Fax: +32 9-264.42.88
E-mail: ingeursi@intec.ugent.be

Assistant Secretary General AT-RASC

P. L. E. Uslenghi
Dept. of ECE (MC 154)
University of Illinois at Chicago 851
S. Morgan Street
Chicago, IL 60607-7053
USA
Tel: +1 312 996-6059
Fax: +1 312 996 8664
E-mail: uslenghi@uic.edu

Editor's Comments

Ross Stone
Stoneware Limited
840 Armada Terrace
San Diego, CA 92106, USA
Tel: +1-619 222 1915, Fax: +1-619 222 1606
E-mail: r.stone@ieee.org

Our Papers

We have three papers in this issue. They span a wide range of radio-science topics, cover more than 50 years of history, and the authors cover the spectrum from students to senior researchers.

Our first paper, by G. Ya. Khachikyan, B. T. Zhumabayev, and A. V. Streltsov, is an invited contribution that resulted from a very interesting presentation I heard at the USNC-URSI National Radio Science Meeting in January of this year. The paper reviews results from numerical simulations and experiments showing that the precursors to earthquakes with a magnitude greater than seven can produce measurable modifications to ionospheric parameters over periods ranging from several hours to several days before the start of the earthquake. The paper begins with a review of 50 years of reports of observations of such ionospheric modifications. A review of simulations of how ionospheric parameters can be modified by earthquakes is then presented. These models are based on the global electric circuit concept, which is explained. The use of the models to explain the DEMETER satellite observations of the ionosphere above strong earthquakes and their precursors is analyzed. One of the results of this analysis is the conclusion that there is a relationship among where strong earthquakes occur, where geomagnetic field lines penetrate the Earth's surface near the earthquake's epicenter, and the occurrence of modifications to the ionosphere as a precursor to the earthquake. This also leads to some interesting conclusions regarding the likely ability to observe such relationships over the next few years. I think you will find this a fascinating paper.

John Mathews has brought us an invited paper by Thomas Thompson, Bruce Campbell, and Ben Bussey, tracing 50 years of radar mapping of the Earth's moon using the Arecibo Observatory. The paper begins with the recognition before Arecibo was built by William Gordon – who conceived Arecibo and made it a reality – that the facility could be used for radar studies of the moon. It recounts the first lunar radar observations done as part of Arecibo's commissioning in 1964, and traces the various lunar-mapping programs done using the delay-Doppler technique from the 1960s through the 1980s. The use of synthetic-aperture-radar techniques combined with bistatic measurements that begin in the 1990s is then described. These techniques resulted in a significant improvement in resolution, and in the information that could be obtained using the polarization of the signals. The more-recent use of satellite-based radar combined with the Arecibo Observatory is explained. The features that can be determined from lunar radar scattering, and how they are derived, are then considered. This is followed by an annotated bibliography tracing Arecibo lunar radar measurements. This paper is both a significant contribution to the record of the history of radio science, and a most interesting look at one way the world's largest radio telescope has been used for 50 years.

Special Section: BeNeLux Student Paper Winner

Our third paper is one of the winners of the Student Paper Contest from a BeNeLux symposium held in December, 2015. The paper is by J. Vanhamel, with coauthors S. Berkenbosch, E. Dekemper, D. Fussen, P. Leroux, E. Neefs, and E. Van Lil. The topic is the implementation of RF drivers for tunable acousto-optical filters for a space mission. The challenges faced in the work reported were to design RF chains to drive the filters in each of the three operating-wavelength ranges – ultraviolet (UV), visible, and near-infrared (NIR) – using space-qualified parts. The paper begins with a discussion of the requirements and the challenges. Possible RF-generator architectures are examined, and the bases for focusing on the phased-locked-loop and Hilbert transform architectures are explained. The designs for implementing these architectures are presented. The results obtained from tests of the systems built for each channel are analyzed. The paper concludes with a discussion of planned future work. This paper provides

an excellent introduction to the realities of designing and building circuits to meet the requirements of space flight.

Our Other Contributions

Stefan Wijnholds has provided us with a tutorial on academic publishing, authored by W. Ross Stone, Stefan Wijnholds, and Phil Wilkinson. Put simply, the Editor of the *Radio Science Bulletin*, the Chair of the URSI Early Career Representatives, and the Editor-in-Chief of *Radio Science* have written an article describing the process of academic publishing, intended for those who may be new to the process or who would like more information about the details of the process – and using those two publications as examples. Some of this may also be of interest to those who are experienced authors.

In his Ethically Speaking column, Randy Haupt looks at the age-old question, "How full is your glass?" He explains why the meaning attached to the answer to that question is what really matters.

In the Solution Box, Özgür Ergül has brought us solutions to a pair of problems by Ismail E. Uysal, H. Arda Ülkü, and Hakan Bağcı. They provide solutions to the computation of the fields scattered from gold spheres incorporating plasmonic effects that dominate at optical frequencies. There were several computational challenges to be overcome in solving these problems, and alternative solutions are sought.

In his Telecommunications Health and Safety column, Jim Lin reviews recent developments in transcranial magnetic stimulation. This uses transient, high-strength, pulsed magnetic fields to stimulate nerve cells in the brain. The goal is to improve symptoms of depression or other psychiatric diseases that are resistant to drug therapy.

Asta Pellinen-Wannberg's Women in Radio Science column has a contribution from Anthea Coster, who is Assistant Director for the Haystack Observatory. She describes her career path and how it was influenced over the years. She also offers some suggestions for those trying to work out their own career paths, and for those who would help them do so.

Important Dates

The calls for papers – and the paper-submission deadlines – for several important conferences appear in this issue. The XXXIInd General Assembly and Scientific Symposium of URSI, to be held August 19-26, 2017, in Montréal, Quebec, Canada, is one of those. The paper-submission deadline for the GASS is January 30, 2017. That is also the deadline for submission for applications for Young Scientist Awards, and for submissions to the Student Paper Contest. More information can be found on the Web site: www.GASS2017.org.

The Asia-Pacific Radio Science Conference (AP-RASC 2016) will be held August 21-25, 2016, at the Grand Hilton Seoul Hotel in Seoul, Korea. 678 papers from 34 countries have been submitted, with all 10 URSI Commissions well represented. There is still time to make plans to attend this conference, which promises to be an outstanding gathering of radio scientists. Visit the Web site at aprasc2016.org immediately to make hotel reservations at the conference venue. I look forward to seeing you there!

XXXIInd General Assembly and Scientific Symposium of the International Union of Radio Science

Union Radio Scientifique Internationale

August 19-26, 2017 Montréal, Québec, Canada

Announcement and Call for Papers

The XXXIInd General Assembly and Scientific Symposium (GASS) of the International Union of Radio Science (Union Radio Scientifique Internationale: URSI) will be in Montréal. The XXXIInd GASS will have a scientific program organized around the ten Commissions of URSI, including oral sessions, poster sessions, plenary and public lectures, and tutorials, with both invited and contributed papers. In addition, there will be workshops, short courses, special programs for young scientists, a student paper competition, programs for accompanying persons, and industrial exhibits. More than 1,500 scientists from more than 50 countries are expected to participate. The detailed program, the link to the electronic submission site for papers, the registration form, the application for the Young Scientists program, and hotel information are available on the GASS Web site: **http://www.gass2017.org**

Submission Information

All papers should be submitted electronically via the link provided on the GASS Web site: http://www.gass2017.org. Please consult the symposium Web site for the latest instructions, templates, and sample formats. Accepted papers that are presented at the GASS may be submitted for posting to IEEE Xplore if the author chooses.

Important Deadlines: Paper submission: January 30, 2017
Acceptance Notification: March 20, 2017

Topics of Interest

Commission A: Electromagnetic Metrology
Commission B: Fields and Waves
Commission C: Radiocommunication and Signal Processing Systems
Commission D: Electronics and Photonics
Commission E: Electromagnetic Environment and Interference
Commission F: Wave Propagation and Remote Sensing
Commission G: Ionospheric Radio and Propagation
Commission H: Waves in Plasmas
Commission J: Radio Astronomy
Commission K: Electromagnetics in Biology and Medicine

Young Scientists Program and Student Paper Competition

A limited number of awards are available to assist young scientists from both developed and developing countries to attend the GASS. Information on this program and on the Student Paper Competition is available on the Web site.

Contact

For all questions related to paper submissions for the GASS, please contact the URSI Secretariat: gass@ursi.org
For all questions related to registration and attendance at the GASS, please see the GASS2017 Web site:

www.gass2017.org

AWARDS FOR YOUNG SCIENTISTS

CONDITIONS

A limited number of awards are available to assist young scientists from both developed and developing countries to attend the General Assembly and Scientific Symposium of URSI.

To qualify for an award the applicant:

1. must be less than 35 years old on September 1 of the year (2017) of the URSI General Assembly and Scientific Symposium;
2. should have a paper, of which he or she is the principal author, submitted and accepted for oral or poster presentation at a regular session of the General Assembly and Scientific Symposium.

Applicants should also be interested in promoting contacts between developed and developing countries. Applicants from all over the world are welcome, including from regions that do not (yet) belong to URSI. All successful applicants are expected to participate fully in the scientific activities of the General Assembly and Scientific Symposium. They will receive free registration, and financial support for board and lodging at the General Assembly and Scientific Symposium. Limited funds will also be available as a contribution to the travel costs of young scientists from developing countries.

The application needs to be done electronically by going to the same Web site used for the submission of abstracts/papers via **http://www.gass2017.org**. The deadline for paper submission for the URSI GASS2017 in Montréal is **30 January 2017**.

A Web-based form will appear when applicants check "Young Scientist paper" at the time they submit their paper. All Young Scientists must submit their paper(s) and this application together with a CV and a list of publications in PDF format to the GA submission Web site.

Applications will be assessed by the URSI Young Scientist Committee taking account of the national ranking of the application and the technical evaluation of the abstract by the relevant URSI Commission. Awards will be announced on 1 May 2017 on the URSI Web site.

For more information about URSI, the General Assembly and Scientific Symposium and the activities of URSI Commissions, please look at the URSI Web site at: http://www.ursi.org and the GASS 2017 Web site at http://www.gass2017.org.

If you need more information concerning the Young Scientist Program, please contact:

The URSI Secretariat
Ghent University/INTEC
Technologiepark-Zwijnaarde 15
B-9052 Gent
Belgium
E-mail: ingeursi@intec.ugent.be

Modification of the Ionosphere by Precursors of Strong Earthquakes

G. Ya. Khachikyan[1], B.T. Zhumabayev[1], and A.V. Streltsov[2]

[1]Institute of Ionosphere
Kamenskoe Plato, Almaty, Kazakhstan

[2]Embry-Riddle Aeronautical University
Daytona Beach, Florida, USA
E-mail: streltsa@erau.edu

Abstract

We present results from experimental and numerical studies demonstrating that earthquakes with a magnitude $M > 7$ can significantly modify parameters of the ionospheric plasma in the region mapped by the geomagnetic filed lines to the epicenter several days or hours before the commencement of the earthquake. Continuous monitoring of the parameters of the ionosphere (in particular, the electron temperature and the density in the F region) with ground-based ionosondes can thus make the early detection of the forerunners of strong earthquakes possible. Our analysis suggested that during the years 2016-2020, particular attention should be given to the seismic regions located near the ground "footprint" of the $L = 2.0$ magnetic shell. This is because strong earthquakes have a tendency to predominantly occur there in the declining phase of the 11-year solar cycle, and the declining phase of the current solar cycle will last until year 2020. We concluded that monitoring of the ionospheric F region near the epicenters of strong earthquakes can significantly contribute to the development of the global, comprehensive understanding of earthquakes and their precursors.

1. Observations of the Modification of the Ionosphere by Strong Earthquakes

On March 27, 1964, at 03:36 UT, a strong earthquake with a magnitude $M = 9.2$ occurred in Alaska. The epicenter was located at 61.1°N and 147.6°W at a depth of ~ 25 km. About 19 minutes later, an ionospheric station in Adak (coordinates 51.9°N, 176.6°W) recorded disturbances in the ionosphere [1]. This paper was the first written report of the existence of lithosphere-ionosphere connections. In Figure 1, six ionograms (adapted from [1]) from 03:15 UT (top) to 04:00 UT (bottom) are presented. These ionograms showed that the ionosphere was relatively quiet for the time period 03:15 UT to 03:45 UT. It became disturbed at 03:55 UT, approximately 19 minutes after a seismic shock. After the great Alaskan earthquake in 1964, the first published observations showed that the earthquake generated Rayleigh waves that propagated along the Earth's surface, producing upward-traveling acoustic waves that caused the ionosphere to move up and down. The author of [2] observed air-pressure waves on a Berkeley barogram arriving in two distinct packets of signals: the first packet was excited by propagating seismic waves, and the second packet was

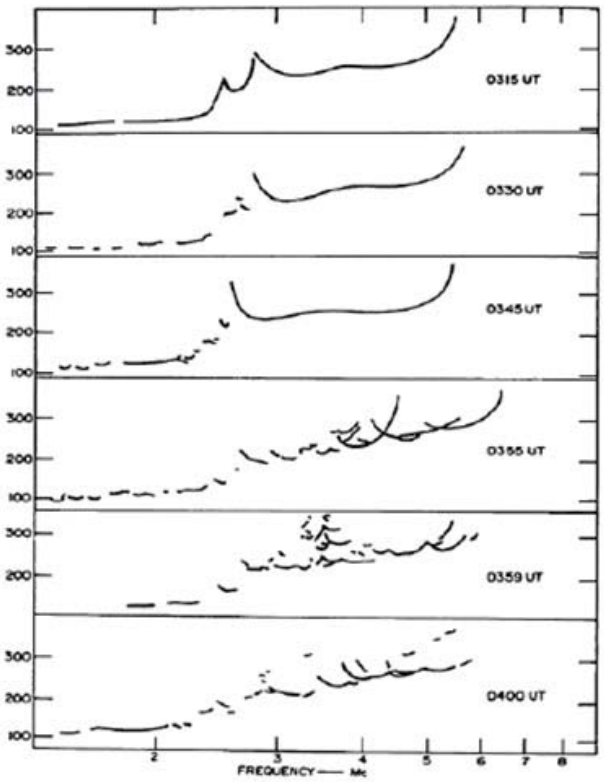

Figure 1. The variation of the ionospheric density over Adak (51.9°N, 176.6°W) after the Alaska March 28, 1964 earthquake with magnitude M = 9.2 [1].

excited by big ground upheavals in the earthquake's source zone. The authors of [3] observed ionospheric disturbances due to the Alaskan earthquake using data at four ionosonde sites in Alaska and California. Recent analyses of ionosonde data after the great Sumatra earthquake of December 26, 2004, showed that the earthquake may have caused the ionosphere to move up and down by about 40 km [4].

Over the past 50 years after the publication of the pioneering works [1-3], numerous experimental studies of lithosphere-ionosphere interactions have been performed. These studies demonstrated that ionospheric disturbances not only follow strong earthquakes, but also precede them [5]. Results from these studies include:

- Variations of the parameters of the ionospheric D layer before an earthquake, which was first documented as a change in the parameters of VLF signals received by ground-based receivers from remote transmitters [6];
- An increase in the ionospheric E-layer critical frequency [5];
- The appearance of a strong sporadic E layer several days before the earthquake [7];
- The decrease of the critical F2-layer frequency days before the 1960 Chile earthquake, with M = 9.5 (which was the largest earthquake recorded) [8];
- Anomalous variations in the maximum plasma frequency [9, 10], the ionospheric electron density [11-15], and the electron temperature [16];
- Disturbances of the total electron content (TEC) before strong earthquakes [17-21]; and
- Various electromagnetic phenomena in the ionosphere related to strong earthquakes [22-27].

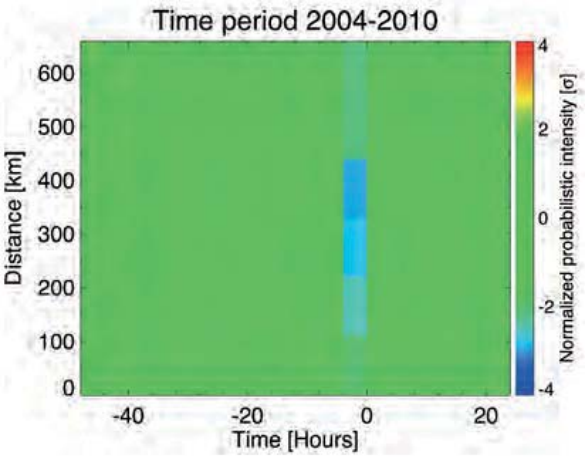

Figure 2. The decrease in the natural VLF (~1.7 kHz) wave intensity related to 8400 nighttime earthquakes with M ≥ 5.0 within 440 km of the epicenters [29].

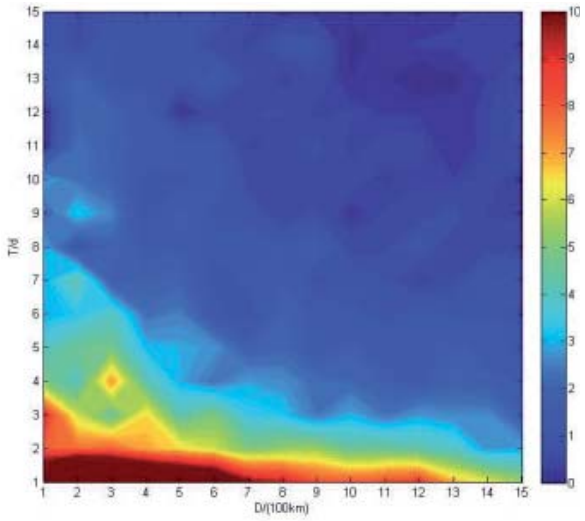

Figure 3. A two-dimensional histogram of the ionospheric anomalies as functions of the days, *T*, before the earthquakes, and the distances, *D*, between the epicenters and the projection of the DEMETER orbit on the Earth's surface. The color scale on the right is related to the number of events in each bin (adapted from [32]).

The recent significant results in this field were data obtained by the Detection of Electro-Magnetic Emissions Transmitted from Earthquake Regions (DEMETER) satellite during almost 6.5 years of its mission (years 2004-2010) [28-32]. In particular, DEMETER revealed that a small but statistically significant decrease (~ 3 dB) in the natural VLF wave intensity at a frequency of ~ 1.7 kHz was observed within 440 km of the epicenters of 8400 earthquakes with magnitudes of M ≥ 5.0 [28, 29]. This decrease was observed for a few hours before the time of the main shock. It is illustrated in Figure 2, reproduced from [29].

Data on the ion density recorded by the DEMETER satellite from 2004 to 2010 were analyzed in references [30-32]. The search for ion-density anomalies was done at less than 1500 km from the anomaly positions, and until 15 days after the anomaly time. The earthquakes were classified depending on their magnitude, depth, and position (below the sea or inland). Recently [32], a statistical analysis of 6263 ion-density perturbations associated with the earthquakes was performed. A spatio-temporal histogram related to these detected earthquake perturbations is shown in Figure 3, as adapted from [32].

On the basis of the statistical results in Figure 3, it was suggested [32] that:

1. The number of ion-density perturbations increased with the earthquake's magnitude;
2. The number of perturbations was maximum just the day before the earthquake;

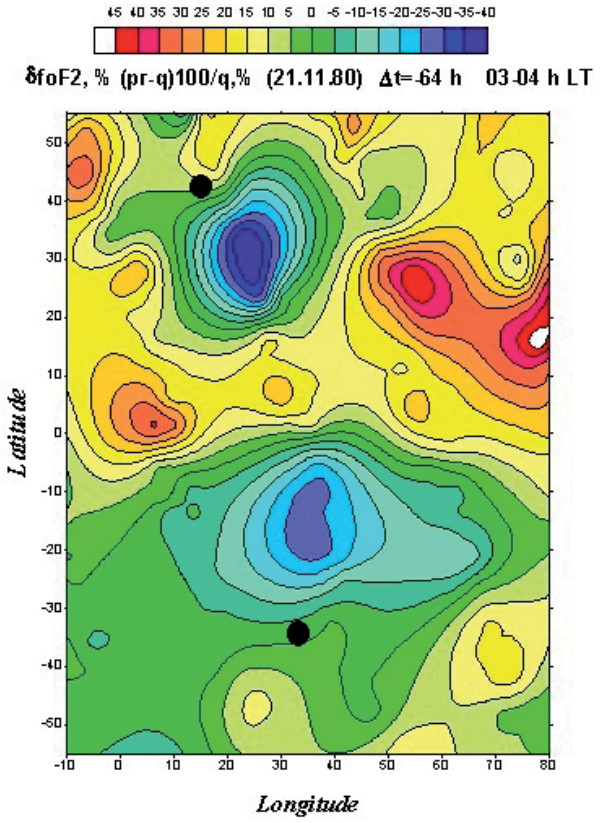

Figure 4. A map of the F2 layer's critical-frequency deviations (ΔfoF2) for the region 60°N - 60°S; 10°W - 80°E for the time of about 64 hours before the strong Irpinia earthquake (M = 6.9) that occurred in Italy on November 23, 1980, at 18:34 UT. The black circle in the northern hemisphere marks the epicenter (40.91°N, 15.37°E), and the black circle in the southern hemisphere marks the epicenter's magnetic-conjugate location [34]

3. The average amplitude of the perturbations increased with the earthquake's magnitude.

The results of [30-32] were in a good agreement with the results [33] on the pre-earthquake anomaly of the total electron content (TEC) obtained from ground-based GPS receivers. More than 700 earthquakes with $M \geq 6.0$ that occurred during 2002-2010 were analyzed. It was concluded that there was a larger occurrence rate of anomalies for the larger-magnitude earthquakes, and that the occurrence rate of anomalies decreased with increasing T (the number of days before the earthquake).

The authors of [34] used data from the Interkosmos-19 satellite and data from ground ionosondes to construct a map of critical-frequency deviations (ΔfoF2) before the strong Irpinia earthquake (M = 6.9), which occurred on November 23, 1980, at 18:34 UT in Italy, with epicenter coordinates of 40.91°N and 15.37°E (Figure 4). Data were contributed by the Intercosmos-19 satellite to the results shown in Figure 4, which were measured in a latitudinal region from 60°N to 60°S with a step in latitude of 5°, and from two ionosonde stations: Rome (41.8°N, 12.5°E) and Athens (38°N, 23.5°E), which were located close to the Irpinia epicenter. The Intercosmos-19 satellite passed over the epicenter in the early morning hours (03-04 h LT) for $\Delta t \approx -112$ h, −87 h, −64 h, −42 h, −40 h, and +9 h in relation to the instant of the main shock instant; and at evening hours (18-19 h LT) for $\Delta t \approx -120$ h, −96 h, −72 h, and −1.39 h, accordingly. Since the satellite passed over the epicenter region only twice per day at moments that did not coincide with the moments of ground-based sounding, the data from the ground-based stations were interpolated between neighboring values at the moment of the satellite's passage. The data of November 18-19 were taken as the quiescent background. Figure 4 presents the deviation of the F2 layer's critical frequency, which was defined as $\delta \text{foF2}\% = \left[\left(\text{foF2}pr - \text{foF2}q\right)/\text{foF2}q\right]100\%$, where (pr) means "present," and (q) means "quiescent background." The procedure for the ionospheric mapping was given in more detail in [35].

The map in Figure 4 demonstrated that 64 hours before the earthquake, the deviations of the F2 layer's critical frequencies were decreased in the area located to the south of the epicenter (the blue area in the northern hemisphere), and in the area located to the north of the magnetically conjugate location of the epicenter (the blue area in the southern hemisphere). An appearance of a ΔfoF2 anomaly in the magnetic-conjugate region suggested that the entire magnetic-flux tube mapped into the area of the earthquake was modified by some electromagnetic processes associated with the preparation for the earthquake.

1.1 Simulations of the Modulation of the Ionosphere by the Precursors of Strong Earthquakes

A number of numerical models for lithosphere-ionosphere coupling have been developed ([36-42] and references therein) to explain the experimental findings. These models were developed on the basis of a global electric circuit (GEC) concept, which links the electric fields and currents flowing in different parts of the coupled atmosphere-ionosphere-magnetosphere system ([43-45] and references therein). Figure 5 presents a schematic plot of the global electric circuit created in [46], which in turn was based on [44]. There are three main generators of fields and currents in the global electric circuit [44]: 1) the troposphere generator (continuous thunderstorm activity of the Earth, with about 46 lightning strikes per every second); 2) the ionospheric wind dynamo; and 3) the solar wind/magnetosphere dynamo. The troposphere generator may provide a 200 kV to 600 kV potential difference between the ground and the ionosphere. The ionosphere generator (ionospheric wind dynamo) may provide about 5 kV to 15 kV potential difference between the high and low latitudes. The magnetospheric generator (solar wind/magnetospheric dynamo) can provide about 40 kV to 130 kV potential drop across the polar cap. The

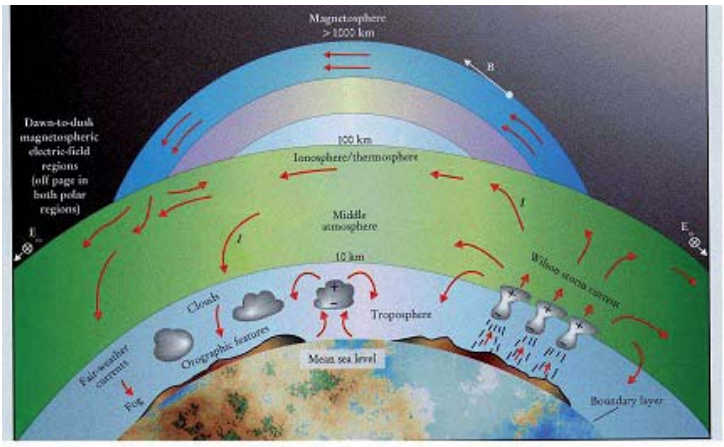

Figure 5. Electric currents in the global electric circuit [46]. Arrows represent current flow. The main sources of the voltage/current in this circuit are thunderstorms. The fair-weather currents are shown with downward-pointing arrows.

strongest source of voltages/currents in this circuit is the thunderstorms in the troposphere.

The arrows in Figure 5 represent currents. The electric current flows upward from the thunderstorm areas, spreads out all over the globe through the ionosphere, and also through the magnetosphere along magnetic field lines to the opposite hemisphere. The current returns to the surface of the Earth as the fair-weather troposphere-to-Earth current. The density of the vertical electric conduction current in the global electric circuit depends on conductivity, and, on average, is about 10^{-12} A/m^2. A detailed discussion of the global electric circuit concept (e.g., how a significant current can flow down because the electrical resistance increases in that direction, or how the currents flowing up to the magnetosphere become dissipated as they flow) is far beyond the scope of this paper, so we prefer to not include it in the present manuscript. We present Figure 5 as a simple but still very good conceptual illustration of the global electric circuit.

The concept of the global electric circuit was used in [36, 40] to explain the results from the DEMETER satellite observations, which showed a statistically significant change in the radio-noise spectrum. There was an ~ 3 dB decrease of the electromagnetic-wave intensity at a frequency of 1.7 kHz at night within 440 km of the epicenters of 8400 earthquakes with magnitudes greater than 5.0 and depths of the epicenters less than 40 km (Figure 2). The explanation of this fact is based on an assumption that the lithosphere-ionosphere coupling occurs through changes of the downward current density flowing in the global electric circuit in the fair-weather regions, as was shown in [47, 48]. A local modulation of the current density can arise from changes in the conductivity of the surface-layer air (the tropospheric part of the global electric circuit), which, for example, can arise from radon emanation [5]. The continuous nature of the current provides coupling between the ionosphere and the ground radioactivity sources. This coupling transports the effects associated with the changes in the local rate of charge generation at low altitudes to the ionosphere. Figure 6 shows a schematic plot developed in [36] to explain the DEMETER results presented in [28, 29]. This plot shows that the density, J_c,of the current flowing between the ionosphere and the ground in the fair-weather regions as a result of the potential difference, V_1, between the ionosphere and the ground is maintained by the generators in the global electric circuit. The current depends on the local columnar resistance, R_c, which has main contributions from the lower columnar resistance, R_{BL} (boundary layer), and the upper columnar resistance, R_{FT} (free troposphere). A decrease in R_{BL} due to the release of radioactive gases into the boundary layer reduces the total ground-ionosphere electrical resistance, R_c. This, in turn, increases the vertical fair-weather current in the global electric circuit, and lowers the ionosphere (to maintain the continuity of the electron flow).

It was shown in [36] that the change in 1.7 kHz signals indicated a change in the earth-ionosphere waveguide cutoff frequency, $f_c = c/2h$, where h is the effective height and c is the speed of light. It was estimated that perturbations to h of ~ 10 km per 12 hours represented a 13% change in f_c ~ 2 kHz, which is easily detectable. At the same time, the model [36, 40] raised a number of questions. Examples of these questions include how the electric current can flow directly from the E-region of the ionosphere to the ground; how to take into account the Pedersen and Hall conductivities at altitudes where the conductivity becomes anisotropic; how this model will work at the geomagnetic equator; where the geomagnetic field lines are horizontal, since an electric current can flow only along the geomagnetic field lines, the conductive electric field cannot be vertical in the E-region at all. The results of references [36, 40] may thus be considered only as a first attempt to use the concept of a global electric circuit to explain the VLF anomalies measured by DEMETER.

The concept of the global electric circuit was also used in [37-39, 41, 42] to explain the anomalous variations in the ionospheric F2-layer electron density and the total electron content (TEC) observed above regions of strong earthquake preparation. One of the currently accepted hypothesis about the origin of the ionospheric-density variations over the region of earthquake preparation is that they are caused by surface charges/currents of the Earth associated with stressed rock [41]. This hypothesis is also based on the suggestion that the electric fields generated in the regions

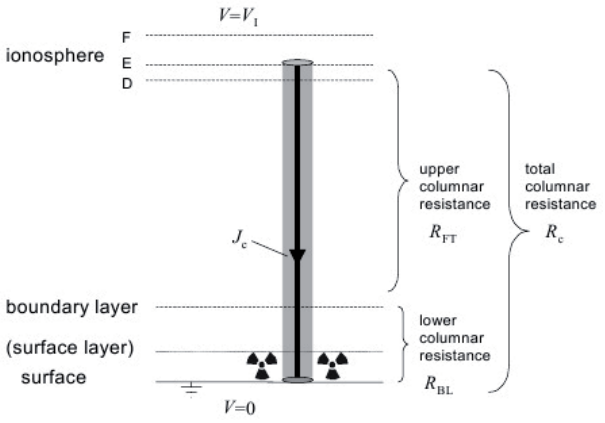

Figure 6. A conceptual model of the lithosphere-ionosphere coupling, developed in [36] to explain the DEMETER observations of the decreasing intensity of electromagnetic waves with a frequency of ~1.7 kHz above the regions of the strong earthquake preparation.

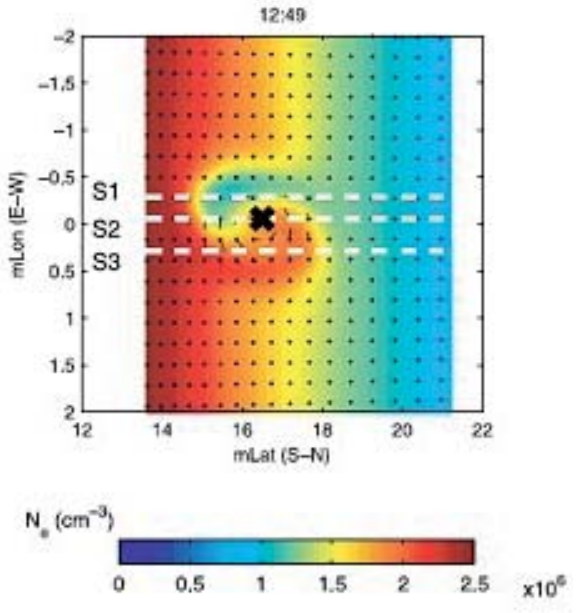

Figure 7. The distribution of the variation of the ionospheric electron density above the maximum of the ionospheric F2 layer, due to electric current of seismic origin (adapted from [41]). The black cross marks the projection of the epicenter to the ionospheric height.

of earthquake preparation are important elements of the global electric circuit (GEC), in which small currents with a mean density of about 10^{-12} A/m^2 flow in the regions of fair weather [44]. These areas are close to the areas of anticyclone, with diameters of thousands of kilometers. In areas of earthquake preparation, the stressed rocks could generate an electric current with a density of 0.5 μA/m^2 to 1.25 μA/m^2 [49]. This area can occupy up to several hundred thousands of square kilometers, as shown by satellites that measure thermal anomalies over the area of earthquake preparation [50]. It was shown in [37] that such currents are able to create ionospheric electric-field disturbances of several mV/m within an area about 200 km in radius. In turn, it was shown in [38, 41] that such electric fields may disturb the ionospheric parameters up to 50% and more.

Simulations in [41] used the electric current of seismic origin with a current density of about 0.2 μA/m^2 to 10 μA/m^2, distributed over an area of 200 km × 30 km, to cause TEC variations of ~ 2% to 25% in the daytime ionosphere. Currents with a density of 0.01 μA/m^2 to 1 μA/m^2 were used to obtain nighttime TEC variations of 1% to 30%. Such a current density is rather large. In the improved model [51], the dynamo current density required to generate the same amount of TEC variation was found to be smaller by a factor of 30. The simulations presented in [42] used a larger area of seismic current generation, 200 km × 3000 km, and a smaller current density, ~ 4×10^{-8} A/m^2, and produced the same TEC variations. Simulated pre-earthquake anomalies in the TEC were in agreement with experimental results (e.g., [17-21]). They were also in agreement with statistical results [52], where superposed epoch analyses of TEC anomalies associated with M ≥ 6.0 earthquakes in Japan that occurred in the years 1998-2011 were performed, and significant positive TEC anomalies one to five days before earthquakes within 1000 km from the epicenter were revealed. The main linear forces acting on the ionospheric plasma included the pressure gradient, the electric E×B force, and the friction of ions with neutrals. The magnitudes of these forces depended on local conditions, and they were carefully and self-consistently estimated in comprehensive numerical simulations (such as the simulations of the *SAMI3* model described in [41]).

The model simulations in [42] showed that electric current of seismic origin can produce modifications of the ionosphere above the epicenter of the earthquake, and above the magnetically conjugate location, as well. That finding could explain a spatial pattern of the ΔfoF2 deviations before the Irpinia earthquake shown in Figure 4. It was first shown in [39] that an electric current of seismic origin can produce both positive and negative ionospheric disturbances, relative to the magnetic meridian crossing the earthquake's epicenter area, and simulations in [41, 42] proved that result. In [41], the epicenter of the earthquake had magnetic coordinates mLat = 20°N and mLon = 0.0° The seismic electric field was "turned on" during the time interval from 12:00 to 13:00 LT. Figure 7 presents the part of Figure 5 from [41] showing the distribution of the ionospheric electron density at time 12:49 LT above the maximum ionospheric height (*hmF2*) in three meridian planes (shown with white dashed lines): S1 – magnetic longitude 0.3°W (6a); S2 – magnetic longitude 0.0° (6b); and S3 – magnetic longitude 0.3°E (6c). The black cross in Figure 7 marks the projection of the epicenter onto the ionospheric height, the longitude of which is noticeably shifted relative to the value on the Earth's surface (mLat = 20°N). This effect happens due to the inclination of the geomagnetic-field line passing through the epicenter.

The magnetic field in Figure 7 is directed into the paper. The E×B force therefore rotates the plasma

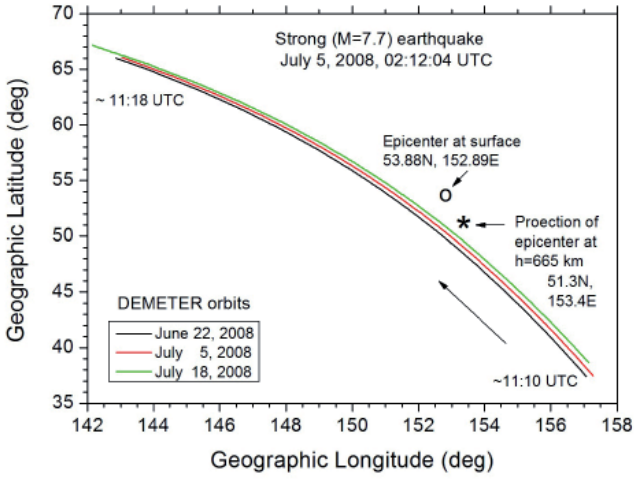

Figure 8. DEMETER satellite orbits (black, red, and green curves) near the epicenter of the strong earthquake (M = 7.7) that occurred in the Sea of Okhotsk on July 5, 2008, at 02:12:04 UT.

counterclockwise (black arrows). As a result, above the *hmF2*, the seismic electric field causes an electron-density enhancement on the east side (longitude > 0) of the mapped earthquake epicenter, and an electron-density reduction on the west side (longitude < 0) of the mapping epicenter. Simulations [41] showed that the electron temperature changed in the opposite way. It is reasonable to expect that N and T change in a way so as to maintain the pressure balance. At heights below *hmF2*, the model [41] shows the opposite distribution of electron density and electron temperature with respect to the epicenter compared to heights above *hmF2*.

2. Application of Results by Kuo et al. [2011] to the DEMETER Satellite Data

Figures 8 and 9 show the results obtained in [53] from applying the model [41] to the observations performed by the DEMETER satellite above the strong earthquake with M = 7.7 that occurred in the Sea of Okhotsk on July 5, 2008, at 02:12:04 UT. The coordinates of the epicenter were 53.88°N and 152.89°E. Figure 8 shows that during this event, the DEMETER satellite passed near the epicenter on June 22 (13 days before the earthquake: black curve), July 5 (nine hours after the earthquake: red curve), and July 18 (13 days after the event: green curve). DEMETER moved along the marked traces from the southeast to the northwest during about eight minutes from 11:10 to 11:18 UT. The black circle and star in Figure 8 respectively mark the epicenter and its projection along the geomagnetic-field line to the height of the DEMETER orbit, 665 km.

Figure 9 shows longitudinal variations between July 5 and June 22, 2008, of the relative difference in the electron density (the grey area in the bottom panel) and the electron

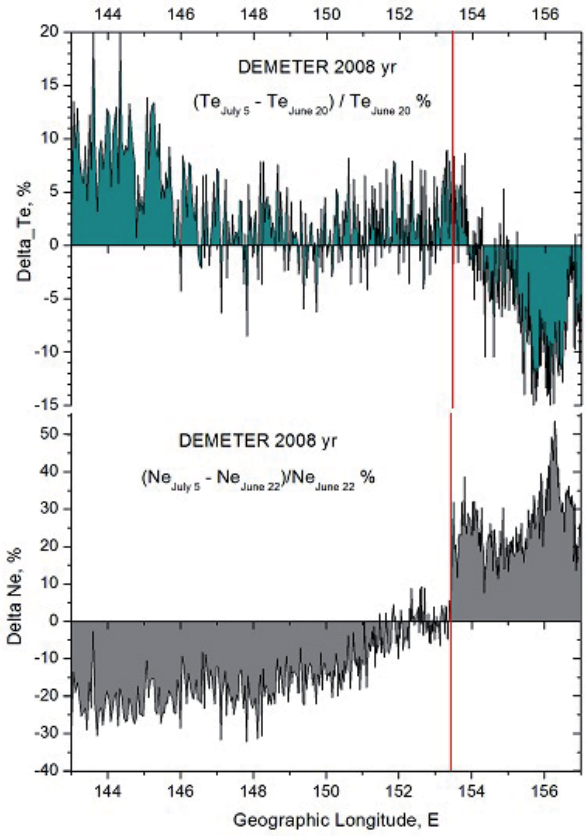

Figure 9. The relative difference in the electron density (the gray area at the bottom) and the electron temperature (the green area at the top), measured by the DEMETER satellite on July 5, 2008, and June 22, 2008, in the vicinity of the earthquake in the Sea of Okhotsk. The vertical red line marks the longitude of projection of the epicenter to the height of the DEMETER orbit at ~665 km [53].

temperature (the green area in the top panel). These were calculated as follows:

$$\Delta Ne\% = \left[\left(Ne_{5\,July} - Ne_{22\,June}\right)\Big/ Ne_{22\,June}\right]100\% ,$$

$$\Delta Te\% = \left[\left(Te_{5\,July} - Te_{22\,June}\right)\Big/ Te_{22\,June}\right]100\% .$$

The vertical red line in Figure 9 marks the longitude of the epicenter projection at the height of the DEMETER orbit (which was equal to 665 km). It is seen from Figure 9 that the electron density was increased on July 5 compared with the magnitude of the density on June 22 on the east side of the epicenter, and was decreased on the west side. The electron-temperature difference, centered according to zero ΔTe value, behaved in the opposite way. These results were in good qualitative agreement with the numerical simulations [41] illustrated in Figure 7.

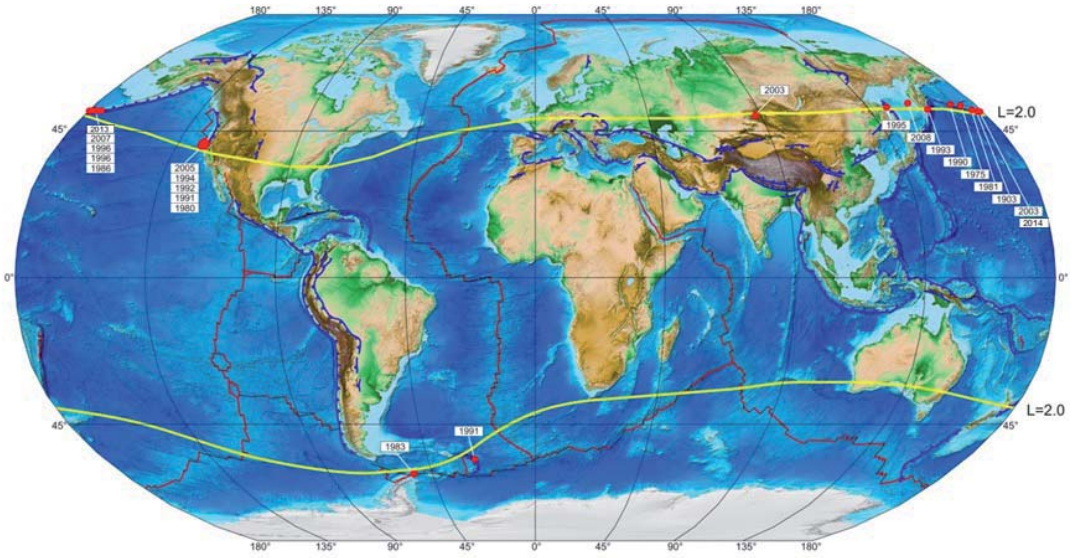

Figure 10. The yellow lines show the footprint of the L = 2 geomagnetic shell. The red circles show the epicenters of 22 strong earthquakes (M ≥ 7.0) the occurred in 1973-2014 in regions with L = 2.0 to 2.2 (Table 1).

3. Instrumentation for Monitoring the Ionosphere in the Magnetic Flux Tube Passing Through the Regions of the Earthquake Preparation

Data form the DEMETER satellite and results from the numerical simulations allowed us to identify ionospheric modifications related to the strong earthquake in the Sea of Okhotsk that occurred on July 5, 2008. Similar information could be obtained from a ground ionosonde continuously monitoring the state of the ionospheric F2 layer mapped by the geomagnetic field into the region on the ground where the earthquake was expected to happen. In particular, in the northern hemisphere, the ionosonde must be shifted some distance to the south relative to the expected epicenter. That distance can be estimated from the geometry of the geomagnetic field line passing through the epicenter on the ground.

Table 1. Earthquakes with M ≥ 7.0 that occurred in regions near the footprint of the geomagnetic field lines L = 2.0 to 2.2. The data were taken from the global NEIC catalog of the USGS (http://neic.usgs.gov/neis/epic/epic_global.htm).

#	Date & Time (dd.mm.yyyy UTC)	Geographic Latitude (deg)	Geographic Longitude (deg)	Depth (km)	Magnitude	L-Shell
1	02.02.1975 8:43	53.11	173.5	10	7.6	2.16
2	08.11.1980 10:27	41.12	–124.25	19	7.2	2.12
3	30.01.1981 8:52	51.74	176.27	33	7.1	2.08
4	11.07.1983 12:56	–60.89	–53.02	10	7.0	2.07
5	07.05.1986 22:47	51.52	–174.78	33	8.0	2.15
6	06.11.1990 20:14	53.45	169.87	24	7.1	2.19
7	17.08.1991 22:17	41.82	–125.4	13	7.0	2.15
8	27.12.1991 4:06	–56.03	–25.27	10	7.2	2.19
9	25.04.1992 18:06	40.37	–124.32	15	7.2	2.05
10	13.11.1993 1:18	51.93	158.65	34	7.0	2.03
11	01.09.1994 15:15	40.40	–125.68	10	7.0	2.03
12	27.05.1995 13:03	52.63	142.83	11	7.1	2.09
13	10.06.1996 4:03	51.56	–177.63	33	7.9	2.14
14	10.06.1996 15:24	51.48	–176.95	26	7.3	2.14
15	17.03.2003 16:36	51.27	177.98	33	7.1	2.08
16	27.09.2003 11:33	50.04	87.81	16	7.3	2.06
17	17.11.2003 6:43	51.15	178.65	33	7.8	2.08
18	15.06.2005 2:50	41.29	–125.95	16	7.2	2.08
19	19.12.2007 9:30	51.36	–179.51	34	7.2	2.11
20	05.07.2008 2:12	53.88	152.89	632	7.7	2.20
21	30.08.2013 16:25	51.54	–175.23	29	7.0	2.20
22	23.06.2014 20:33	51.85	178.73	109	7.9	2.17

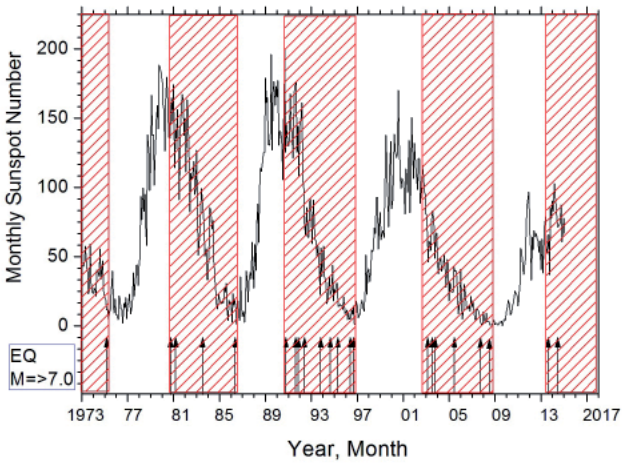

Figure 11. The monthly sunspot numbers and dates of strong (M ≥ 7.0) earthquakes that occurred near the footprint of L = 2.0 to 2.2 magnetic shells.

To use this idea, one needs to know an approximate region of strong earthquake preparation. In general, experts in seismology may give an answer to this question, because they determine rather correctly the areas of possible strong earthquakes. It is also reasonable to focus attention on areas where the results of a strong earthquake will be particularly disastrous: large urban areas, power plants, military bases, industrial installations, oil/gas fields, etc. The main problem is to determine the time interval (at least within several years) when a strong earthquake may occur. Here, we will present some results that might shed some light on this problem.

The geomagnetic field lines (L) penetrated in the epicenters of 173477 earthquakes with magnitudes $M \geq 4.5$ that occurred around the globe in the years 1973-2010 years were estimated in [54] using the International Geomagnetic Reference Field model (IGRF-10). This study showed that earthquakes preferentially occurred in the areas penetrated by an L-line in the range L = 1.0 to 1.2. The earthquake count then decreased with increasing L, but there was a local maximum in the distribution of the number of earthquakes as a function of the magnetic L-line in the range of L = 2.0 to 2.2. For example, there were 2898 earthquakes in the range of L = 1.8 to 2.0, and two times more (namely, 6234) in the range of L = 2.0 to 2.2. The fraction of the Earth's surface area lying between L = 2.0 and 2.2 is restricted by two narrow belts (of about 2.5° in latitude) starting from the yellow lines at their equatorial side (Figure 10). For example, in year 2015 at a longitude of 125°W, in the seismic region located closely to Oregon, USA, L = 2.0 penetrated into the crust at $\sim 40.2°N$, and L = 2.2 penetrated into the crust at $\sim 42.8°N$. One may speculate that an observed local peak of seismicity may be the result of any external earthquake triggering in seismic areas penetrated by an L of 2.0 to 2.2. It is known that in the radiation belt, the geomagnetic shell of 2.0 is occupied by the anomalous cosmic rays [55], which are one of the sources of air ionization in the global electric circuit (Figure 5). We therefore decided to analyze whether any systematic behavior over time took place for earthquake occurrence in seismic regions penetrated by an L of 2.0 to 2.2. As shown in [56], the worldwide rate of occurrence of smaller ($M < 7$) earthquakes does not systematically change over time (smaller earthquakes may be only aftershocks of the larger earthquakes). Taking this into account, we analyzed only $M \geq 7.0$ events. In 1973-2010, twenty earthquakes with $M \geq 7.0$ occurred in regions with an L of 2.0 to 2.2, and two events occurred afterward (Table 1 and Figure 10).

It is believed at present that cosmic rays show systematic behavior in the 11-year sunspot cycle. In Figure 11, we thus plotted the monthly number of sunspots for the years 1973-2015 (www.ngdc.noaa.gov/stp/solar/ssndata.html), and marked the dates of 22 strong earthquakes (see Table 1) with black arrows. It was seen from Figure 11 that all of these earthquakes occurred in the declining phases of the 11-year solar cycles (red boxes), while they were absent in the ascending phases. At present, we are living in the declining phase of the 24th solar cycle, which may be lasting approximately to 2019-2020 (https://en.wikipedia.org/wiki/Solar_cycle_24). Two strong earthquakes have already occurred in this phase, in the years 2013 and 2014 (Figure 10 and Table 1). It is reasonable to expect that several more similar events will occur during the next four to five years, because they regularly occurred in the declining phases of the three previous solar cycles (Figure 11). The seismic regions located close to the yellow curves in Figure 10 are thus "good" candidates for the locations where continuous monitoring of the ionospheric parameters during 2016-2020 needs to be carried out.

4. Conclusions

Experimental data and numerical simulations discussed in this paper convincingly demonstrated that earthquakes with a magnitude $M > 7$ can significantly modify parameters of the ionospheric plasma in the region mapped by the geomagnetic filed lines to the epicenter several days or hours before the commencement of the earthquake. The continuous monitoring with ground-based ionosondes of the parameters of the ionosphere inside the geomagnetic flux tube passing through the expected epicenter can therefore make possible the early detection of the forerunners of strong earthquakes. This earlier detection and the forecast of strong earthquakes are particularly important in regions containing large, densely populated urban areas (cities and capitals), power plants, military/industrial/oil/gas installations, etc.

Our study suggests that during the years 2016-2020, particular attention should be devoted to the seismic regions located near the ground footprints of the L = 2.0 magnetic shell. This is because strong earthquakes have a tendency to occur there predominantly in the declining phase of the 11-year solar cycle, and the declining phase of the current solar cycle will last until the year 2020.

The question of what might be a physical connection between the variability in the solar activity and the occurrence of strong earthquakes is not answered or addressed in this paper. Nevertheless, we conclude that monitoring of the ionospheric F region near the epicenters of strong earthquakes by itself is an inexpensive and quite valuable contribution to the development of a global, comprehensive understanding of earthquakes and their precursors. The importance of such understanding is emphasized in the studies [57, 58] focused on the precursors of strong earthquakes. Of course, the continuous monitoring of the ionospheric parameters above the regions of potential earthquake preparation should be considered as a long-term project, but it was noted in [59] that earthquake-prediction experiments "...will require run times of decades or longer. But we should begin a global program of comparative testing now, because it will help us build, brick by brick, a better system-level understanding of the earthquake predictability."

5. Acknowledgements

We are deeply grateful to Editor W. Ross Stone for attention to the article and fruitful comments on the text. We also thank the two anonymous reviewers for the analysis of the results and valuable comments, which undoubtedly contributed to improving the article.

6. References

1. K. Davies and D. Baker, "Ionospheric Effects Observed Around the Time of the Alaska Earthquake of March 28 1964," *Journal of Geophysical Research*, **70**, 9, 1965, pp. 2251-2253.

2. B. A. Bolt, "Seismic Air Waves from the Great 1964 Alaskan Earthquake," *Nature*, **202**, 1964, pp. 1094-1095.

3. R. S. Leonard and R. A. Barnes, "Observation of Ionospheric Disturbances Following the Alaska Earthquake," *Journal of Geophysical Research*, **70**, 1965, pp. 1250-1253.

4. J. Y. Liu, Y. B. Tsai, S. W. Chen, C. P. Lee, Y. C. Chen, H. Y. Yen, W. Y. Chang, and C. Liu, "Giant Ionospheric Disturbances Excited by the M9.3 Sumatra Earthquake of 26 December 2004," *Journal of Geophysical Research*, **33**, 2, January 2006, DOI: 10.1029/2005GL023963.

5. S. A, Pulinets and K. A. Boyarchuk, *Ionospheric Precursors of Earthquakes*, Berlin, Springer, 2004, p. 316.

6. M. B Gokhberg, I. L. Gulfeld, and V. I. Liperovsky, "Electromagnetic Precursors in the Earthquake System: Search Problem," *Bulletin Academy of Sciences of USSR*, 3, 1987, pp. 45-53 (in Russian).

7. T. Ondoh and M. Hayakawa, "Seismo Discharge Model of Anomalous Sporadic-E Ionization Before Great Earthquakes," in M. Hayakawa and O. A. Molchanov (eds.), *Seismo Electromagnetic Lithosphere-Atmosphere Coupling*, Tokyo, Terra Scientific Publishing Co., 2002, pp. 385-390.

8. A. J. Foppiano, E. M. Ovalle, K. Bataille, and M. Stepanova, "Ionospheric Evidence of the May 1960 Earthquake Over Concepciyn?" *Geofisica International*, **47**, 3, 2008, pp. 179-183.

9. J. Y. Liu, Y. I. Chen, S. A. Pulinets, Y. B. Tsai, and Y. J. Chuo, "Seismo-Ionospheric Signatures Prior to M≥6.0 Taiwan Earthquakes," *Geophysical Research Letters*, **27**, 19, 2000, pp. 3113-3116.

10. J. Y. Liu, Y. I. Chen, Y. J. Chuo, and C. S. Chen, "A Statistical Investigation of Pre-Earthquake Ionospheric Anomaly," *Journal of Geophysical Research*, **111**, 2006, A05304, doi:10.1029/2005JA011333.

11. V. H. Rios, V. P. Kim, and V. V. Hegai, "Abnormal Perturbations in the F2 Region Ionosphere Observed Prior to the Great San Juan Earthquake of 23 November 1977," *Advances Space Research*, **33**, 2004, pp. 323-327.

12. A. Trigunait, M. Parrot, S. Pulinets, and F. Li, "Variations of the Ionospheric Electron Density During the Bhuj Seismic Event," *Annales Geophysicae*, **22**, 2004, pp. 4123-4131.

13. R. S. Dabas, R. M. Das, K. Sharma, K. G. M. Pillai, "Ionospheric Precursors Observed Over Low Latitudes During Some of the Recent Major Earthquakes," *Journal of Atmospheric and Solar-Terrestrial Physics*, **69**, 2007, pp. 1813-1824.

14. B. Zhao, M. Wang, T. Yu, W. Wan, J. Lei, L. Liu, and B. Ning, "Is an Unusual Large Enhancement of Ionospheric Electron Density Linked with the 2008 Great Wenchuan Earthquake?" *Journal of Geophysical Research*, **113,** 2008, A11304, doi:10.1029/2008JA013613.

15. K.-I. Oyama, Y. Kakinami, J. Y. Liu, M. A. Abdu, and C. Z Cheng, "Latitudinal Distribution of Anomalous Ion Density as a Precursor of a Large Earthquake," *Journal of Geophysical Research*, **116**, 2011, A04319, doi:10.1029/2010JA015948.

16. D. K. Sharma, M. Israil, R. Chand, J. Rai, P. Subrahmanyam, and S. C. Garg, "Signature of Seismic Activities in the F2 Region Ionospheric Electron Temperature," *Journal of Atmospheric and Solar-Terrestrial Physics*, **68**, 2006, pp. 691-696.

17. J. Liu, Y. Chuo, S. Shan, C. Tsai, Y. Tsai, Y. Chen, S.A. Pulinets, and S. Yu, "Preearthquake Ionospheric Anomalies Registered by Continuous GPS TEC Measurements," *Annales Geophysicae*, **22**, 2004, pp. 1585-1593.

18. I. E. Zakharenkova, A. Krankowski, L. I. Shagimuratov, "Modification of the Low-Latitude Ionosphere Before the 26 December 2004 Indonesian Earthquake," *Natural Hazard Earth System Science*, **6,** 5, 2006, pp. 817-823, doi:10.5194/nhess-6-817-2006.

19. J. Y. Liu, Y. I. Chen, C. H. Chen, C. Y. Liu, C. Y. Chen, M. Nishihashi, J. Z. Li, Y. Q. Xia, K. I. Oyama, K. Hattori, and C. H. Lin, "Seismo-Ionospheric GPS Total Electron Content Anomalies Observed Before the 12 May 2008 Mw7.9 Wenchuan Earthquake," *Journal of Geophysical Research*, **114**, 2009, A04320, doi:10.1029/2008JA013698.

20. J. Y Liu, Y. I. Chen, C. H. Chen, and K. Hattori, "Temporal and Spatial Precursors in the Ionospheric Global Positioning System (GPS) Total Electron Content Observed Before the 26 December 2004 M9.3 Sumatra-Andaman Earthquake," *Journal of Geophysical Research*, **115**, 2010, A09312, doi:10.1029/2010JA015313.

21. J. Y. Liu, H. Le, Y. I. Chen, C.H. Chen, L.Liu, W. Wan, Y. Z. Su, Y. Y. Sun, C.H. Lin, and M. Q. Chen, "Observations and Simulations of Seismoionospheric GPS Total Electron Content Anomalies Before the 12 January 2010 M7 Haiti Earthquake," *Journal of Geophysical Research*, **116,** 2011, A04302, doi:10.1029/2010JA015704.

22. M. B. Gokhberg, N. I. Gershenzon, I. L. Gufel'd, A. V. Kustov, V. A. Liperovskiy, and S. S. Khusameddinov, "Possible Effects of the Action of Electric Fields of Seismic Origin on the Ionosphere," *Geomagnetism and Aeronomy*, **24**, 2, 1984, pp. 183-186.

23. S. V. Bilichenko, A. S. Inchin, A. V. Streltsov, G. A. Stanev, P. P. Puchaev, V. M. Chmyrev, E. F. Kim, and O. A. Pokhotelov, "ULF Pulsations of the Magnetic Field in the Ionosphere Associated with Earthquakes," *Reports Academy of Science USSR*, **311**, 1990, pp. 1077-1080 (in Russian).

24. S. K. Park, M. J. S. Johnston, T. R. Madden, F. D. Morgan, and H. F. Morrison, "Electromagnetic Precursors to Earthquakes in the ULF Band: A Review of Observations and Mechanisms," *Review Geophysics*, **31**, 2, 1993, pp. 117-132, doi:10.1029/93RG00820.

25. M. Parrot, J. Achache, J. J. Berthelier, E. Blanc, A. Deschamps, F. Lefeuvre, M. Menvielle, J. L. Plantet, P. Tarits, and J. P. Villain, "High-Frequency Seismo-Electromagnetic Effects," *Physics Earth Planet. Interior*, **77**, 1-2, 1993, pp. 65-83, doi:10.1016/0031-9201(93)90034-7.

26. M. Hayakawa (ed.), *Atmospheric and Ionospheric Electromagnetic Phenomena Associated with Earthquakes*, Tokyo, Terra Scientific Publishing Company, 1999, p. 996.

27. M. Hayakawa and O. A. Molchanov (eds.), *Seismo Electromagnetics: Lithosphere-Atmosphere-Ionosphere Coupling*, Tokyo, Terra Science Publishing Company, 2002, p. 478.

28. F. Nemec, O. Santolik, and M. Parrot, "Decrease of Intensity of ELF/VLF Waves Observed in the Upper Ionosphere Close to Earthquakes: A Statistical Study," *Journal of Geophysical Research*, **114,** 2009, A04303, doi:10.1029/2008JA0113972.

29. D. Piša, F. Nˇemec, O. Santolik, M. Parrot, and M. Rycroft, "Additional Attenuation of Natural VLF Electromagnetic Waves Observed by the DEMETER Spacecraft Resulting from Preseismic Activity," *Journal Geophysical Research*, **118,** 2013, pp. 5286-5295, doi:10.1002/jgra.50469.

30. M. Li and M. Parrot, "'Real Time Analysis of the Ion Density Measured by the Satellite DEMETER in Relation with the Seismic Activity," *Natural Hazards and Earth System Sciences*, **12**, September 2012, pp. 2957-2963.

31. M. Li and M. Parrot, "Statistical Analysis of an Ionospheric Parameter as a Base for Earthquake Prediction," *Journal of Geophysical Research*, **118**, 6, 2013, pp. 3731-3739.

32. M. Parrot and M. Li, "DEMETER Results Related to Seismic Activity," *Radio Science Bulletin*, **355**, December 2015, pp. 18-25.

33. H. Le, J. Y. Liu, and L. Liu, "A Statistical Analysis of Ionospheric Anomalies Before 736 M6.0+ Earthquakes During 2002-2010," *Journal of Geophysical Research*, **116**, 2011, A02303, doi:10.1029/2010JA015781.

34. S. A. Pulinets, P. Biagi, V. Tramutoli, A. D. Legen'ka, and V. Kh. Depuev, "Irpinia Earthquake 23 November 1980 – Lesson from Nature Reviled by Joint Data Analysis," *Annals of Geophysics*, **50**, 1, 2007, pp. 61-78.

35. S. A. Pulinets and A. D. Legen'ka, "Spatial-Temporal Characteristics of Large Scale Disturbances of Electron Density Observed in the Ionospheric *F*-Region Before Strong Earthquakes," *Cosmic Research*, **41,** 3, 2003, pp. 240-249.

36. R. G. Harrison, K. L. Aplin, and M. J. Rycroft, "Atmospheric Electricity Coupling Between Earthquake Regions and the Ionosphere," *Journal of Atmospheric and Solar-Terrestrial Physics*, **72,** 5-6, 2010, pp. 376-381.

37. V. M. Sorokin, V. M. Chmyrev, and A. K. Yaschenko, "Theoretical Model of DC Electric Field Formation in the Ionosphere Stimulated by Seismic Activity," *Journal of Atmospheric and Solar-Terrestrial Physics*, **67**, 2005, pp. 1259-1268.

38. A. A. Namgaladze, M. V. Klimenko, V. V. Klimenko, and I. E. Zakharenkova, "Physical Mechanism and Mathematical Modeling of Earthquake Ionospheric Precursors Registered in Total Electron Content," *Geomagnetism and Aeronomy*, **49**, 2, 2009, pp. 252-262, doi:10.1134/S0016793209020169.

39. A. Pulinets, "Physical Mechanism of the Vertical Electric Field Generation Over Active Tectonic Faults," *Advances in Space Research*, **44,** 2009, pp. 767-773.

40. M. J. Rycroft, and G. Harrison, "Electromagnetic Atmosphere-Plasma Coupling: The Global Atmospheric Electric Circuit," *Space Science Reviews*, **168,** 1-4, 2012, pp. 363-384.

41. C. L. Kuo, J. D. Huba, G. Joyce, and L. C. Lee, "Ionosphere Plasma Bubbles and Density Variations Induced by Pre-Earthquake Rock Currents and Associated Surface Charges," *Journal Geophysical Research*, **116**, 2011, A10317, http://dx.doi.org/10.1029/2011JA016628.

42. M. I. Karpov, O. V. Zolotov, and A. A. Namgaladze, "Modeling of the Ionosphere Response on the Earthquake Preparation," *Proceedings of the Moscow State Technical University*, **15**, 2, 2012, pp. 471-476 (in Russian).

43. R. G. Roble and I. Tzur, "The Global Atmospheric Electrical Circuit," in *Study in Geophysics - The Earth's Electrical Environment*, Washington, DC, National Academy Press, 1986, pp. 206-231.

44. R. G. Roble, "On Modeling Component Processes in the Earth's Global Electric Circuit," *Journal of Atmospheric and Terrestrial Physics*, **53**, 9, 1991, pp. 831-847.

45. E. R. Williams, "The Global Electric Circuit: A Review," Atmospheric Research. 13th International Conference on Atmospheric Electricity – ICAE 2007, **91**, 2-4, 2009, pp. 140-152.

46. E. A. Bering, A. A. Few, and J. R. Benbrook, "The Global Electric Circuit," *Physics Today*, October 1998, pp. 24-30.

47. M. J. Rycroft, S. Israelsson and C. Price, "The Global Atmospheric Electric Circuit, Solar Activity and Climate Change," *Journal of Atmospheric and Solar- Terrestrial Physics*, **62**, 2000, pp. 1563-1576.

48. M. J. Rycroft, A. Odzimek, N. F. Arnold, M. Fullekrug, A. Kulak and T. Neubert, "New Model Simulations of the Global Atmospheric Electric Circuit Driven by Thunderstorms and Electrified Shower Clouds: The Roles of Lightning and Sprites," *Journal of Atmospheric and Solar-Terrestrial Physics*, **69**, 2007, pp. 2485-2509.

49. F. T. Freund, I. G. Kulahci, G. Cyr, J. Ling, M. Winnick, J. Tregloan-Reed, and M. Freund, "Air Ionization at Rock Surfaces and Pre-Earthquake Signals," *Journal of Atmospheric and Solar-Terrestrial Physics*, **71**, 2009, pp. 1824-1834, doi:10.1016/j.jastp.2009.07.013.

50. D. Ouzounov, N. Bryant, T. Logan, S. Pulinets, and P. Taylor, "Satellite Thermal IR Phenomena Associated with Some of the Major Earthquakes in 1999-2003," *Phys. Chem. Earth*, **31**, 2006, pp. 154-163.

51. C. L. Kuo, L. C. Lee, and J. D. Huba, "An Improved Coupling Model for the Lithosphere-Atmosphere-Ionosphere System," *Journal of Geophysical Research*, **119**, 2014, 3189, doi:10.1002/2013JA019392.

52. S. Kon, M. Nishihashi, and K. Hattori, "Ionospheric Anomalies Possibly Associated with M≥6.0 Earthquakes in the Japan Area During 1998-2010: Case Studies and Statistical Study," *Journal of Asian Earth Sciences*, **41**, 2011, pp. 410-420, DOI:10.1016/j.jseaes.2010.10.005.

53. G. Khachikyan, A. Kim, A. Inchin, and A. Lozbin, "Seismo-Ionospheric Relationships: The Variations of Electron Temperature and Electron Density as Measured the Satellite DEMETER," *Reports of National Academy of Sciences of Kazakhstan*, **4**, 2015, pp. 71-78 (in Russian).

54. G. Khachikyan, A. Inchin, N. Zhakupov, N. Kadyrkhanova, and L. Kaliyeva, "Occurrence of Strong Earthquakes in Regions with Geomagnetic Shell *L*~2.0: Relation to 11 Year Solar Cycle," Proceedings of the 7th Kazakhstan-Chinese International Symposium on Earthquake Prediction Seismic Hazard and Seismic Risk Assessment in Central Asia, 2010, pp. 357-362.

55. R. A. Mewaldt, R. S. Selesnick, and J. R. Cummings, "Anomalous Cosmic Rays: The Principal Source of High Energy Heavy Ions in the Radiation Belts," 1996, http://authors.library.caltech.edu/46484/1/1996-04.pdf

56. J. F. Pacheco and L. R. Sykes, "Seismic Moment Catalog of Large Shallow Earthquakes, 1900 to 1989," *Bulletin Seismic Society America*, **82,** 1992, pp**.** 1306-1349.

57. S. Pulinets and D. Ouzounov, "Lithosphere-Atmosphere-Ionosphere Coupling (LAIC) Model – A Unified Concept for Earthquake Precursors Validation," *Journal Asian Earth Science*, **41**, 4-5, 2011, pp. 371-382, doi:10.1016/j.jseaes.2010.03.005.

58. D. Ouzounov, S. Pulinets, K. Hattori, M. Kafatos, and P. Taylor, "Atmospheric Signals Associated with Major Earthquakes. A Multi-Sensor Approach," in M. Hayakawa (ed.), *Frontier of Earthquake Short-Term Prediction Study*, Japan, 2011, pp. 510-531.

59. T. H. Jordan, "Earthquake Predictability, Brick by Brick," *Seismological Research Letters*, **77**, 3-6, 2006, doi:10.1785/gssrl.77.1.3.

50 Years of Arecibo Lunar Radar Mapping

Thomas W. Thompson,[1] Bruce A. Campbell,[2] and D. Benjamin J. Bussey[3]

[1]Jet Propulsion Laboratory
Pasadena, CA USA
E-mail: Thomas.W.Thompson@jpl.nasa.gov

[2]Center for Earth and Planetary Studies, Smithsonian Institution
Washington, DC USA
E-mail: campbellb@si.edu

[3]Applied Physics Laboratory, Johns Hopkins University
Laurel, MD USA
E-mail: Ben.Bussey@jhuapl.edu

Abstract

William E. Gordon conceived the giant radar/radio telescope at Arecibo, Puerto Rico (Figure 1) in 1958 as a backscatter radar system to measure the density and temperature of the ionosphere at altitudes of up to a few thousand kilometers [1, 2]. The backscattered ionospheric echo was calculated to be weak, requiring a large antenna with a diameter of 1000 ft (305 m) to measure it. From the beginning, Gordon (as noted in his in his 1958 URSI abstract on incoherent scattering [3]) realized that a radar system with an antenna that large could conduct radar studies of the moon and planets. With the recent celebration of the 50th anniversary of the Arecibo radio/radar telescope, it is appropriate to describe how radar mapping of the moon has evolved over the years: from the early monostatic 70-cm observations in the 1960s through the 1980s, to the 13-cm and 70-cm wavelength bistatic observation using the Robert C. Byrd Green Bank telescope in the 1990s to today, and then to the 13-cm wavelength bistatic observations conducted using the mini-RF radar instrument flown on the NASA/US Lunar Reconnaissance Orbiter spacecraft in the last few years.

1. Introduction/Background

The radar mapping of the moon that took place from the 1960s to the present using the Arecibo radio/radar telescope, like most scientific and engineering advances, had a number of important precursors. The first radar echoes from the moon were detected in 1946 when US Army Signal Corp personnel pointed their radar at the moon [4]. This was a huge media event in its day. About a month later, Zoltan Bay also detected lunar radar echoes using a Hungarian radar [5].

In the early 1960s, it was realized that the high-power transmitters and larger antennas of the day could be used to probe planetary surfaces. These methods were formulated when Gordon Pettengill, Tor Hagfors, John Evans, and others at the Massachusetts Institute of Technology (MIT) conducted a summer course on planetary radar. MIT personnel at that time used 7.84-m (784-cm) radars at El Campo, Texas, the 68-cm radar at Millstone Hill, Massachusetts, and the 3.6-cm radar at Pleasanton, California, to measure the scattering behavior of the moon [6]. In parallel, Richard Goldstein successfully detected anomalous scattering areas on Venus [7] using the then newly commissioned Deep Space Network antennas at Goldstone, California. This work demonstrated radar's ability to see through the thick clouds that obscure the Venusian surface.

An important precursor to the radar mapping of the moon, as well as of Venus, Mars, and the asteroids, was the development of the delay-Doppler technique. This was first demonstrated by lunar radar observations conducted at MIT's Millstone Hill radar (Westford, Massachusetts) [8]. This technique makes it possible to map radar reflectivity across the disk of moon, as shown in Figure 3. Radar echoes are located by their delay along the radar's line of sight and their Doppler shift due to the apparent rotation

Figure 1. The Arecibo radio/radar telescope. It was constructed in the early 1960s, dedicated in late 1963, and commissioned in 1964. The reflector surface diameter is 1000 feet (305 m). Note that the antenna beamwidth at 70 cm wavelength (430 MHz) is 10 arc-minutes, and 1.8 arc-minutes at 13 cm wavelength. The moon's angular width is 30 arc-minutes to 33 arc-minutes.

of the moon. When viewed from Earth, echoes with the same delay are rings concentric with the center of the lunar disk. Echoes with the same Doppler frequency are strips parallel with the moon's apparent axis of rotation. Location by delay and Doppler shifts are ambiguous, as two separate areas have the same properties. As noted below, narrow antenna beams that view only one these two areas can resolve this ambiguity. Once the echoes are located in the radar-centric x_d, y_d, z_d coordinate system, their location in selenographic coordinates (latitude and longitude) can be determined by a rotation about the origin of x_d, y_d, z_d coordinates, as described in Appendix 1.

This first delay-Doppler mapping of the moon showed that the crater Tycho [9] had much stronger echoes than other lunar areas. Tycho's stronger echoes are attributed to an abundance of wavelength-sized (centimeter- and meter-sized) rocks associated with this recent lunar impact. The observation that the young, large lunar impact craters had more centimeter- and meter-sized rocks was also shown by Saari and Shorthill [10], who observed the infrared cooling of the moon during a lunar eclipse. Warmer areas in these observations associated with large, young impact craters were consistent with the hypothesis of an increased abundance of rocks with sizes greater than about 5 cm, as rocks of these sizes still radiated heat while the nearby lunar (dusty) surface had cooled. All of this provided a basis for lunar radar observations at Arecibo that commenced in 1964, when the 1000-ft radio/radar telescope was being commissioned.

2. 1960s to 1980s

From 1964 through the 1980s, there was a progression of radar observations of the moon using the Arecibo radio/radar telescope, shown in Figure 1. The first radar echoes of the moon were detected by William Gordon and Merle LaLonde, using a horn feed at Arecibo that was installed on site to provide a means of validating the high-power 430-MHz (70 cm wavelength) transmitter before the main antenna/radar system (see Figure 4 of Mathews [11]). Soon

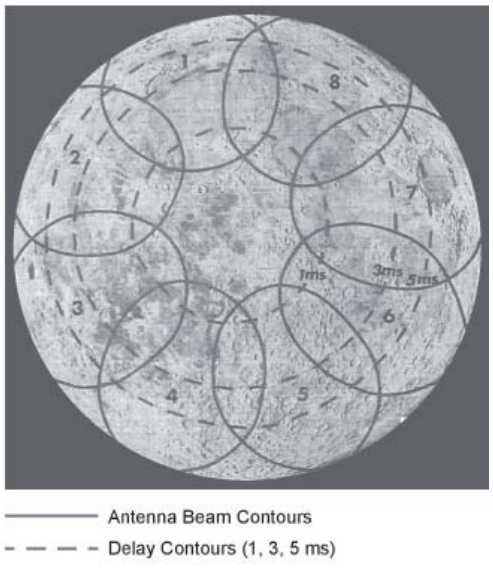

Figure 2a. The first lunar radar observations were conducted by pointing the 10-arc-minute antenna beam at eight positions around the limb of the 30 arc-minute lunar disc and recording echoes versus delay, as shown here [12].

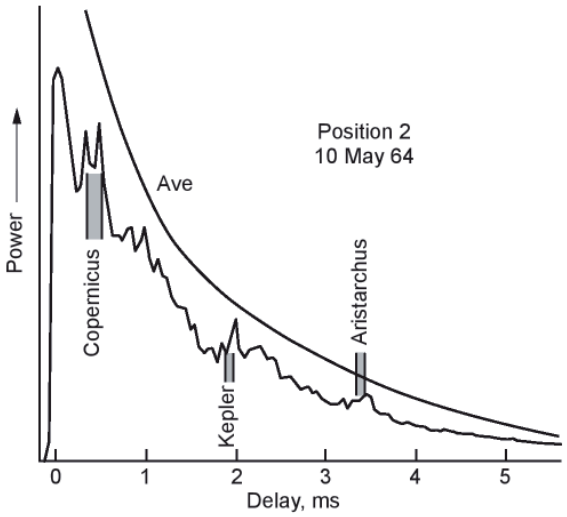

Figure 2b. Power as a function of delay for beam position 2 on Oceanus Procellarum with the antenna pointed 10 arc minutes from the center of the lunar disk for the opposite-sense-circular (OC) polarized component. Note the enhanced radar echoes associated with the large, young craters Copernicus, Kepler, and Aristarchus [12]

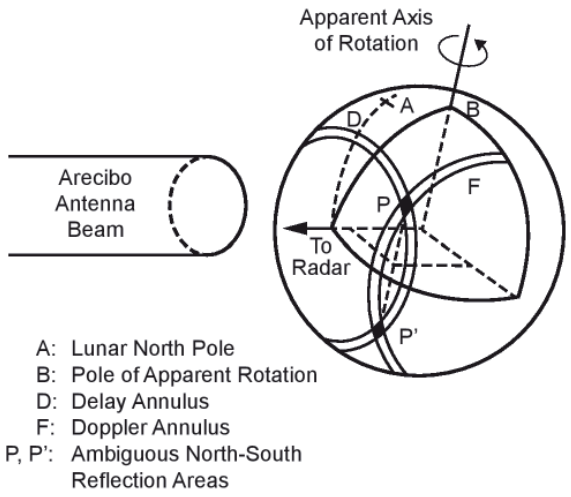

Figure 3. The geometry for delay-Doppler mapping of the moon with the 10 arc-minute Arecibo antenna beam at 430 MHz (70 cm wavelength). The intrinsic north-south ambiguity in delay-Doppler mapping was resolved by pointing the antenna at one of the ambiguous areas and having antenna sidelobes suppress echoes from the other ambiguous area. Here, x_0, y_0, and z_0 are a Cartesian coordinate system aligned with the radar observer, where the y_0 axis is aligned with an apparent axis of rotation, the z_0 axis is along the radar's line-of-sight, and the x_0 axis completes the triad.

thereafter, the first lunar radar observations were conducted in 1964 when the Arecibo radio/radar telescope was being commissioned [12]. These first observations were conducted by pointing the 10-arc-minute antenna beam at eight positions around the limb of the 30 arc-minute lunar disc and recording echoes versus delay, as shown in Figure 2a. The observations showed that large young craters (such as Copernicus, Tycho, Kepler, and Aristarchus) had enhanced backscatter, similar to the crater Tycho enhancement seen by Pettengill and Henry [9], as shown in Figure 2b. Later in 1964, preliminary delay-Doppler observations yielded maps with resolutions on the order of 20 km to 30 km, as shown in Figure 3b. These and other very early maps (Figure 4) were sufficient to verify the enhanced radar backscatter associated with the larger, young craters. In addition, these observations showed that the lunar highlands (the terrae) had stronger echoes than the lunar maria by a factor of two to four.

We note that the moon is a very cooperative body for radar imaging using delay-Doppler techniques. There are three primary factors:

1. The narrow Arecibo antenna beamwidths,

2. The relatively slow apparent rotation of the moon, and

3. The large angles in the plane of the sky between the actual and apparent axes of rotation.

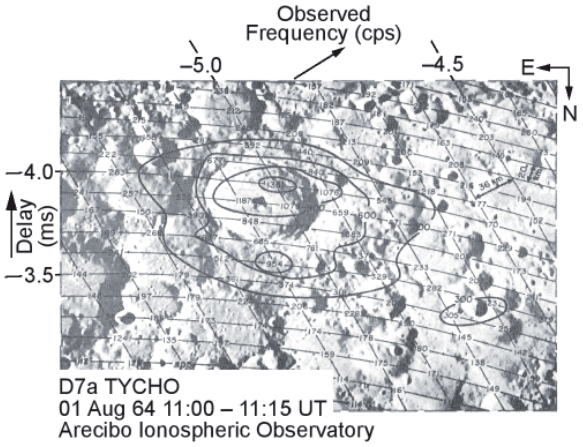

Figure 4. An example of a 1964 delay-Doppler mapping of the moon at 70 cm wavelength: a radar-scattering map of the crater Tycho and its environs. The power contours are for polarized, opposite-sense-circular (OC) radar echoes. The resolution was 20 km to 36 km [12].

These three factors enable efficient radar imaging of the moon with the Arecibo antenna. There is an intrinsic ambiguity in delay-Doppler observations, as there are two areas that appear at the same delay and Doppler frequency, as shown in Figure 3. This ambiguity is resolved by pointing the antenna beam at one of the two ambiguous areas. Echoes from the other ambiguous area are suppressed as they are within the antenna's sidelobes. The Arecibo antenna's beamwidths at 70-cm and 13-cm wavelengths are 10 arc-minutes and 2 arc-minutes, both smaller than the angular diameter of the moon (30 arc-minutes to 33 arc-minutes).

The second factor – the slow apparent rotation of the moon – as described in Appendix 1, produces about 10 Hz of limb-to-limb spread in Doppler frequencies at 430 MHz (70 cm wavelength). At 2380 MHz (13 cm wavelength) the spread in Doppler frequencies for echoes from areas illuminated by the antenna beam is 7.5 Hz. Pulse repetition rates of 10 Hz are thus enough to produce spectra that readily enable surface resolutions on the order of a few tens of kilometers with frequency resolutions of 0.01 Hz to 0.1 Hz. Such frequency resolutions can be achieved with time records (coherence intervals) of 10 seconds to 100 seconds in length. Equivalent range resolutions are accomplished by transmitting pulses of 10 microseconds to 100 microseconds.

The third factor is the fact that the moon's apparent axis of rotation in the sky can differ from the actual axis of rotation by angles as great as 45°. This enables radar imaging of the moon's equatorial regions. Figure 4 shows a radar image of crater Tycho obtained during the Arecibo commissioning in 1964.

From 1966 through 1969, the Apollo Program was well underway, and many lunar engineers and scientists

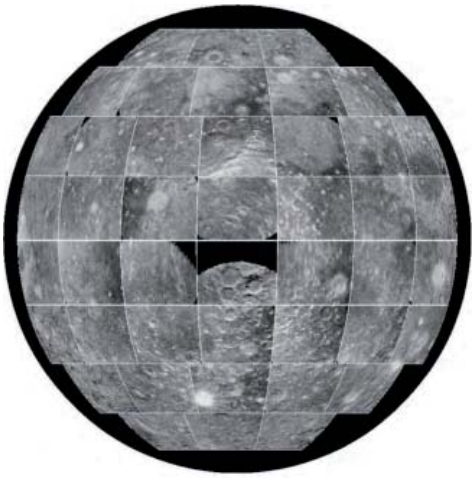

Figure 5a. 1966-1969 radar mapping of the moon: a lunar global radar map at 70 cm wavelength. The resolution was 5 km to 10 km. 42 separate observations were referenced to the Lunar Aeronautical Charts (LAC). These were the first global radar mapping results for the moon's near side [16]. This shows the opposite-sense-circular (OC) polarized component.

Figure 5b. As in Figure 5a, but for the same-sense-circular (SC) depolarized component.

were called upon to assist in landing-site selections. This led to the *Photographic Lunar Atlas* [13], used as base maps for the 1964 delay-Doppler maps, and to the 1:1,000,000 scale Lunar Aeronautical Charts (LAC) [14]. These Lunar Aeronautical Charts covered areas along the lunar equator with maps that covered 16° in latitude and 20° in longitude. Farther away from the equator, the latitude range remained 16°, but the longitude range was increased to 24°. Still farther from the equator, the longitude range was increased to 30°. As these map areas fit conveniently within the 10 arc-minute antenna beam at 430 MHz (70 cm wavelength), lunar radar observations in 1966 to 1969 concentrated on observation of each of the Lunar Aeronautical Chart areas. This resulted in the first global lunar radar map of the near side of the moon [15], shown in Figure 5.

Later, in the 1980s, it was realized that with improvements in computers and in data-storage capabilities, the global mapping of the late 1960s could be further improved. Rather than the 44 positions for the 1960s global lunar radar map tied to the Lunar Aeronautical Charts, 28 positions were used to map the moon's near-side hemisphere. Here, a coarse resolution "beam-swing' delay-Doppler mapping was performed to provide a background map. This in turn eliminated the map-to-map discontinuities in the 1960s' map. The resulting global radar map of the moon [16] is shown in Figure 6.

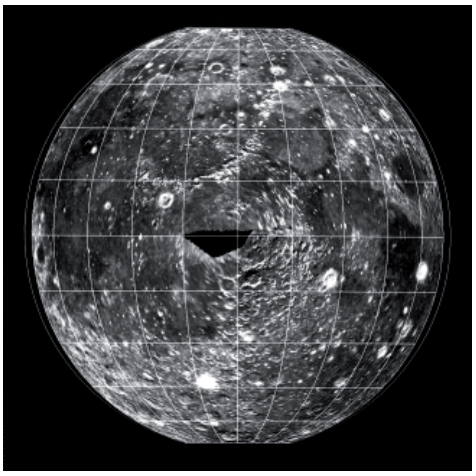

Figure 6a. A 1980s lunar global radar map at 70 cm wavelength. The resolution was 3 km to 5 km. 28 separate observations were used [16]. This shows the opposite-sense-circular (OC) polarized component.

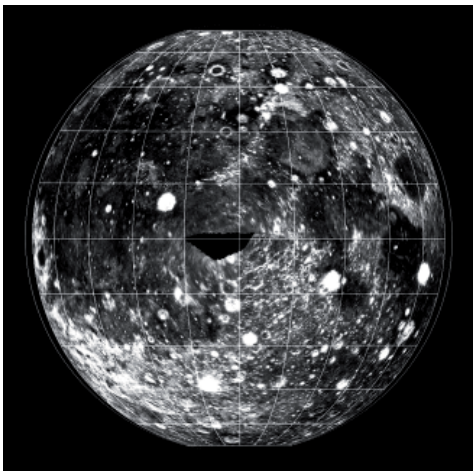

Figure 6b. As in Figure 6a, but for the same-sense-circular (SC) depolarized component.

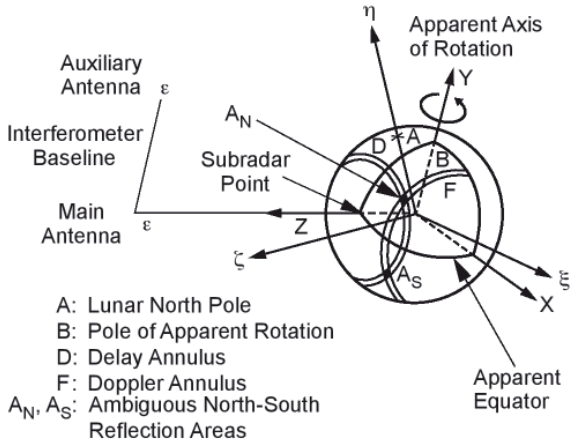

Figure 7a. The geometry of the lunar-surface radar reflections as observed by a two-element interferometer. The coordinates *X*, *Y*, and *Z* are radar-based, while ξ, η, and ζ are the standard selenographic direction cosines. Here, the intrinsic north-south delay-Doppler ambiguity was resolved via phase differences of the echoes observed by an interferometer.

In the late 1960s, another type of lunar radar observation was conducted. In this observation, lunar echoes from long-wavelength (7.5 m) transmissions were observed in a bistatic configuration using the main 1000 ft (305 m) Arecibo antenna and a nearby smaller auxiliary antenna. This 7.5 m transmitter system, which was coaxial with the 430 MHz feed (see Figure 5 of Mathews [11]), was installed in 1965 to offer a dual-frequency capability for ionospheric studies. It was never successfully used for incoherent-scatter measurements, possibly due to clutter issues. This low-frequency feed was conveniently attached to one of the carriage houses, and enabled tracking of the moon.

In order to obtain radar maps of the lunar surface at this wavelength, the separation of ambiguous delay-Doppler reflecting areas had to rely on a different technique. Alan Rodgers (MIT Lincoln Laboratory) had developed a bistatic radar-mapping method for Venus, where the phase differences between echoes from ambiguous reflecting areas observed by two nearby antennas could be used to separate their signals [17]. His mapping of radar echoes from Venus with this technique was the first for any planetary body.

For the mapping of the moon with this technique at 7.5 m wavelength, the optimum spacing between the main antenna and an auxiliary antenna placed this second antenna just inside the property owned by the Arecibo Observatory. The auxiliary Yagi antenna had a 40° beamwidth, so it could see lunar radar echoes for the ±20° of zenith coverage of the main antenna. This bistatic technique was used for two observations [18, 19]. Figure 7a is an overview of the radar configuration. Figure 7b shows the global radar image resulting from the second observation.

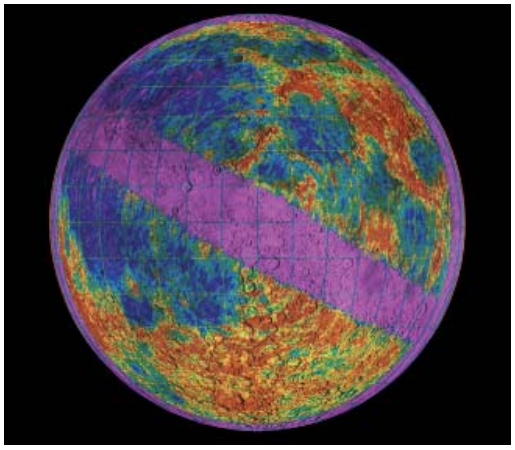

Figure 7b. A lunar global radar map at 40 MHz, 7.5 m wavelength [19].

It is useful here to summarize the improvements in the Arecibo radar system over the years, as these have led to a wide variety of lunar radar experiments. These were:

1963: 430 MHz system, pulsed transmitter, 2.5 MW peak, 150 kW maximum average power, which enabled the lunar radar mapping at 70 cm wavelength, described above.

1965: 40 MHz transmitter, pulsed or CW, 100 kW average power, 2 MW peak power. Although this transmitter was decommissioned in 1971, it enabled the lunar radar mapping at 7.5 m wavelength, described above.

1974: 2,380 MHz CW transmitter, 450 kW maximum power, installed as a part of a major upgrading of the Arecibo radio telescope/radar systems. This enabled the lunar radar mapping at 12.6 cm wavelength, described below.

1997: 2,380 MHz CW transmitter installed, 1.0 MW maximum power, an upgrade to the 1974, 450 kW transmitter that enabled improved lunar radar mapping at 12.6 cm wavelength, described below.

3. 1990s to Present: Arecibo–Green Bank Bistatic Observations

Lunar radar mapping through the late 1980s used well-demonstrated delay-Doppler techniques to achieve image spatial resolutions on the order of a few kilometers. The realization of finer resolutions over the full illuminated area on the moon required "focusing" of the echoes by adapting synthetic-aperture radar (SAR) techniques that account for both range migration and a very significant phase variation that occurs over integration periods longer than a few minutes. Nick Stacy [20, 21] demonstrated this using the 13 cm wavelength radar system in his PhD research at Arecibo.

Figure 8. The Robert C. Byrd Green Bank Radio Telescope is the world's largest fully steerable radio telescope, with an aperture diameter of 300 feet (92 m). It is located at the National Radio Astronomy Observatory (NRAO), Green Bank, West Virginia, USA. The antenna beamwidth at 70 cm is 33 arc-minutes, and 5 arc-minutes at 13 cm. For comparison, the moon's angular diameter is 30 arc-minutes to 33 arc-minutes.

The first bistatic observations of the moon at the 13.6 cm wavelength were conducted by Nick Stacy in 1990 and 1992 [20], using an auxiliary 30.5 m Los Caños antenna, 11 km to the north of the 305 m telescope. This auxiliary antenna was equipped with a dual-polarization maser receiver, and was used for both Venus (interferometry) and lunar radar mapping. These observations were also the first high-resolution, full-Stokes-parameter radar observations of the moon, and possibly of any other planetary surface.

Practical application for synoptic mapping needed a second receiving system to allow for dual-polarization measurements at both 13 cm and 70 cm wavelengths, since the Arecibo configuration did not support this type of observing. A bistatic configuration was implemented in 2003, using the Arecibo telescope for transmitting and the National Radio Astronomy Observatory's Green Bank telescope (Figure 8) in West Virginia for receiving lunar radar echoes (Figure 9).

Initial experiments at 430 MHz with an uncoded, 3 μs pulse and 17 minute coherence intervals showed that range- and Doppler-focusing could produce maps with 400 m to 600 m spatial resolution. This approach eventually yielded a map of most of the moon's near side [22]. Ongoing research uses the finest 1 μs time resolution of the 70 cm wavelength Arecibo transmitter with about 40 minute coherence intervals to make maps with 200 m spatial resolution, such as that of Mare Serenitatis shown in Figure 10 [23]. Observations at 13 cm wavelength can achieve spatial resolution as fine as 20 m per pixel, although the associated 57 minute coherence interval requires the use of auto-focusing methods to refine the ephemeris-based estimation of the relative motion of the sensor and selenographic points across the illuminated beam. Regional mapping at S band continues, using the Arecibo system

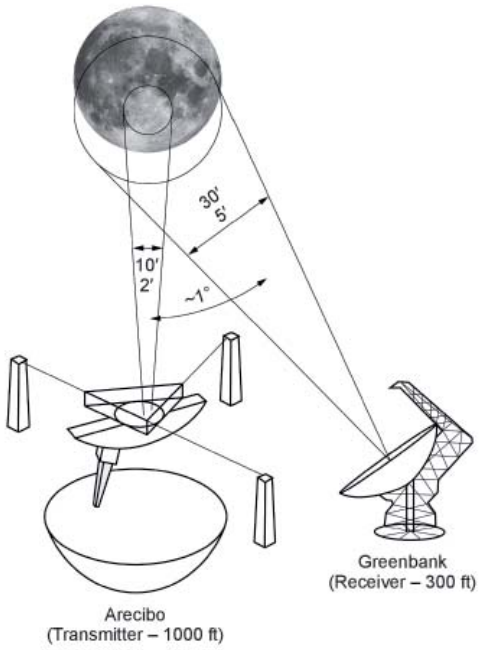

Figure 9. An overview of bistatic observations of the moon with the Arecibo (transmitter) and Green Bank (receiver) radio telescopes. Note that the Arecibo antenna's beamwidths of 10 arc-minutes at 430 MHz (70 cm wavelength) and 2 arc-minutes at 2380 MHz (13 cm wavelength) were sufficient to resolve the intrinsic north-south ambiguity in delay-Doppler mapping.

with a 0.2 μsec time resolution and a 29 minute integration period to yield four-look radar images with 80 m spatial resolution, such as that of Mare Crisium shown in Figure 11 [24]. Important scientific results of these efforts include delineation of impact-melt deposits from large craters up to the basin scale, mapping of ancient basalts now hidden by ejecta from the basins, refinement of mare stratigraphy and volcanic/tectonic history, as well as mapping of volcanic-ash deposits and rugged lava flows associated with some of the moon's most unusual geologic features.

4. Recent Lunar-Reconnaissance Orbiter Mini-RF Bistatic Observations

Recently, another type of lunar radar mapping has been achieved using spacecraft radars. In the late 2000s, NASA launched two lightweight synthetic-aperture radars (SARs) to the moon as part of the Mini-RF project. The first SAR flew on the Indian Space Research Organisation's (ISRO's) Chandrayaan-1 lunar orbiter, while the second operated on NASA's Lunar Reconnaissance Orbiter (LRO, Figure 12). Both instruments operated at 2380 MHz (12.6 cm wavelength), and the Lunar Reconnaissance Orbiter instrument also operated at 7140 MHz (4.2 cm wavelength). Collectively, they successfully mapped more than two thirds of the lunar surface, including the first SAR

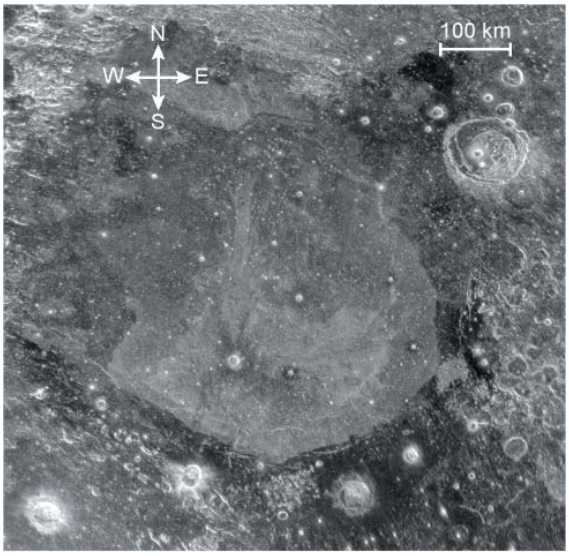

Figure 10. An Arecibo-Green Bank bistatic radar image of Mare Serenitatis at 70 cm wavelength. The radar polarization was in the same circular sense as that transmitted, so the echoes were sensitive to changes in the rock abundance and composition of the lunar regolith. Fine spatial patterns of volcanic flow complexes could be traced within the basin, due to the strong effect of lava titanium-content variations on radar-signal absorption [22].

mapping of the moon's far side, and complete mapping of the lunar poles (including the floors of the permanently shadowed polar craters that are not visible from Earth).

Arecibo provided two critical activities for these Mini-RF instruments. The first was for calibration, and the second was for bistatic radar measurements [25]. Arecibo

Figure 12. The Lunar Reconnaissance Orbiter (LRO), a NASA robotic spacecraft, was launched in June 2009. It is currently orbiting the moon in an elliptical 30 km by 160 km (19 miles by 100 miles) polar orbit. LRO's Miniature Radio Frequency (Mini-RF) radar instrument demonstrated new lightweight synthetic-aperture radar techniques at the moon. Although the Mini-RF transmitter failed in January 2011, it was possible to conduct bistatic lunar radar observations using the Mini-RF receiver for observing lunar radar echoes from the Arecibo transmissions.

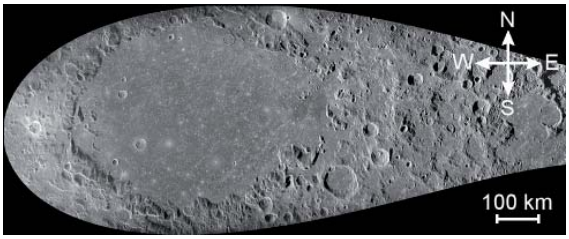

Figure 11. An Arecibo-Green Bank bistatic radar image at S band (12.6 cm wavelength) of the 550 km diameter Mare Crisium on the moon's eastern near side [23]. The received radar polarization was in the opposite sense of circular polarization to that transmitted, so the echoes were highly sensitive to local slopes oriented toward the sensor. Radar shadows, cast by the lunar terrain, became longer toward the edge of the visible disk at right.

provided the signal for the Mini-RF receiver calibrations. For this activity, Arecibo transmitted an S-band signal of known circular polarization towards the moon. At the same time, the Mini-RF antenna was pointed directly towards the Arecibo radar. The Lunar Reconnaissance Orbiter then executed maneuvers to scan the Mini-RF antenna-beam footprint across the line of sight along the principal planes of the pattern as measured on Earth. This required two scans: a 24° scan in elevation, and a second 12° scan in azimuth (12° and 6° either side of boresight, respectively), providing data points at 0.5° increments. Arecibo was not used for

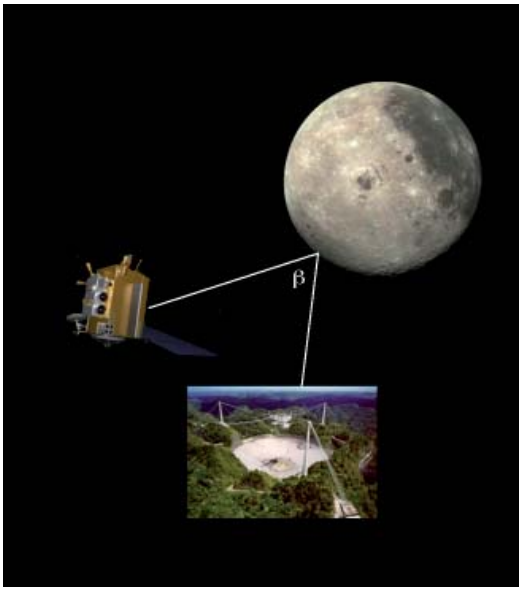

Figure 13. An overview of S-band (13 cm wavelength) Arecibo-LRO Mini-RF bistatic radar mapping of the moon. These bistatic lunar radar observations were conducted by transmitting from Arecibo to areas on the moon that were within the LRO Mini-RF beamwidth as the LRO spacecraft orbited the moon. The bistatic angle, β, is the angle between the lines of sight of the transmitted and received signals.

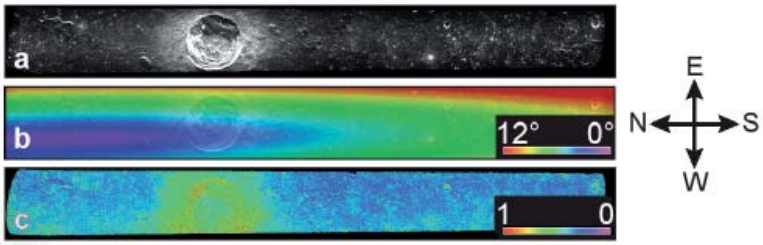

Figure 14. Arecibo-LRO Mini-RF bistatic 13 cm wavelength observations of crater Kepler, a 32 km diameter Copernican crater in Oceanus Procellarum: (a) The Stokes parameter S1, total power; (b) bistatic angle; (c) circular polarization ratio, CPR.

the Mini-RF transmitting calibration. The Greenbank radio telescope was instead used, as it could directly receive horizontal and vertical polarizations, whereas Arecibo received only circular polarizations.

The second activity was a bistatic radar mapping of the lunar surface. Here, the bistatic angle, β, is the angle between the lines of sight of the transmitted and received signals (see Figure 13). When the same antenna is used for both transmitting and receiving, β is zero. For bistatic observations where both antennas are on the Earth (e.g., Arecibo-Green Bank), β is very small, $\sim 0.35°$. By using Arecibo as the transmitter, and Mini-RF on the Lunar Reconnaissance Orbiter in lunar orbit as the receiver, the first-ever planetary bistatic-angle images were obtained. Measuring how the circular polarization ratio (CPR) varied as a function of β provided a unique method to discriminate between rocks and buried ice deposits. Figure 14 shows an Arecibo-Lunar Reconnaissance Orbiter bistatic radar image of crater Kepler and surrounding Oceanus Procellarum.

5. Salient Global Features of Lunar Radar Scattering

To understand these Arecibo lunar radar observations, we examine the average backscatter behavior of the moon as described by the average radar cross section per unit surface area, a dimensionless quantity that varies with the angle of incidence, as shown in Figure 15. Here, the angle of incidence of 0° is at the center of the lunar disk, and 90° is at the limb as viewed from Earth. Hagfors [26] tabulated these radar cross section values for wavelengths of 3.8 cm, 23 cm, and 68 cm, based on the earlier measurements of Evans and Pettengill [6]. These radar cross sections were obtained using the usual Earth-based radar configuration, where circularly polarized waves were transmitted and received to obviate the adverse effects of Faraday rotation of linearly polarized waves in the Earth's ionosphere.

The values given by Hagfors [26] were for opposite-sense circular (OC) echoes, the polarization for mirror reflections from large, flat surfaces that are oriented perpendicular to the radar's line-of-sight. Average radar echoes in the same-sense circular (SC) polarization have been shown to be proportional to the cosine of the angle of incidence (θ), with values such that the ratio of stronger opposite-sense-circular to weaker same-sense-circular echoes is two at the limb, as observed in the 1960s lunar radar experiments performed by the Massachusetts Institute of Technology [6], as well as at 13 cm wavelength by Campbell [27]. Observed average opposite-sense-circular, polarized echoes have an angular dependence where the echoes fall precipitously from angles of incidence of 0° to about 20° to 30°, then gradually diminish to 70°, and then fall precipitously again from 70° to 90° at the limb. Observed same-sense-circular, depolarized echoes diminish gradually, with a cosine-like dependence, from angles of incidence of 0° for the center of the disk to 90° at the limb.

Evans and Hagfors [28] showed that the lunar radar echoes can be interpreted as consisting of specular and diffuse components, as shown in Figure 15. The specular component results from mirror-like echoes from large (10 radar wavelengths, or more) surfaces, which are flat to one-tenth of the radar wavelength and oriented perpendicular to the radar's line-of-sight. As the lunar surface is gently undulating with root mean square (rms) slopes on the order of 2° to 4° in the maria and 6° to 8° in the terra [29], the specular scattering from the surface-regolith interface contribute only to the opposite-sense-circular echoes with strengths that decrease sharply with angle of incidence. For angles of incidence beyond about 35°, the opposite-sense-circular echoes have a $\cos^{1.5}(\theta)$ dependence. Thompson et al. [30] showed that the subsurface layers of crater ejecta observed in Apollo core-tube data could create average opposite-sense-circular cross sections with this $\cos^{1.5}(\theta)$ dependence.

The diffuse component is attributed to scattering from wavelength-sized (one-tenth to 10 wavelengths) rocks, either on the surface or subsurface up to the radar's penetration depth, which is on the order of 10 wavelengths in the maria and up to 40 wavelengths in terra [31]. We also note that as slopes modulate lunar-radar echoes – so that areas tilted toward the radar have stronger echoes and areas tilted away from the radar have weaker echoes – the radar images of the moon appear similar to visual photographs of sunlit terrains.

Other salient global features of lunar radar scattering at 430 MHz (70 cm wavelength) are shown in Figures 5, 7, and 10. The strongest same-sense-circular (SC), depolarized, echoes are associated with the large young craters such as Aristarchus, Copernicus, Kepler, Langrenus, Theophilus, and Tycho, where echo strengths are on average an order-of-magnitude stronger than their environs. Opposite-sense-circular (OC) polarized echoes for these large young craters

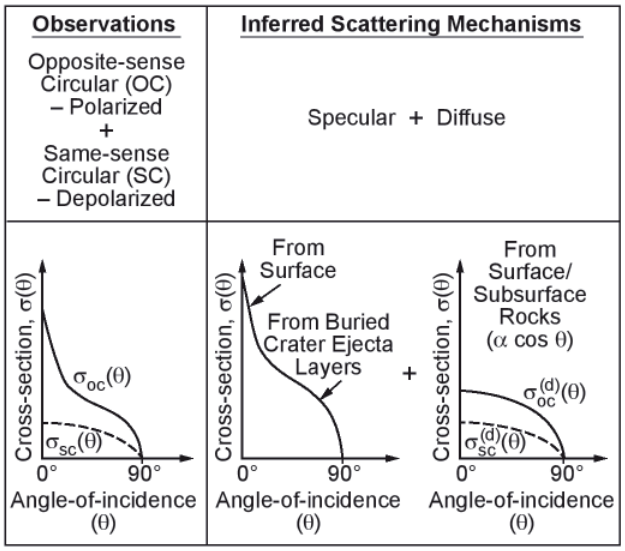

Figure 15. The interpretation of lunar radar backscatter as the sum of inferred specular and diffuse echoes, as hypothesized by Evans and Hagfors [28]. The specular component is associated with the echoes for large smooth (10 radar wavelengths or more) areas that are flat to one-tenth of the radar wavelength, and are oriented perpendicular to the radar's line-of-sight. The diffuse component is associated with the scattering from wavelength-sized (one-tenth to 10 wavelengths) rocks, either on the surface or subsurface up to the radar's penetration depth (on the order of 10 wavelengths in the maria, and up to 40 wavelengths in terra). Thompson et al. [30] showed that specular scattering from subsurface layers of crater ejecta can generate high-angle opposite-sense-circular (OC) echoes that vary with the angle of incidence, θ, as $\cos^{1.5}(\theta)$.

vary, depending upon their location with respect to the center of the lunar disk. For Copernicus, which is observed at low angles of incidence near the center of the disk, polarized echoes are only three times stronger than its environs. Aristarchus and Langrenus, which are nearer the lunar limb, have opposite-sense-circular echo enhancements slightly smaller than the same-sense-circular echo enhancements.

Echo enhancements for other craters depend upon their ages, with the young Copernican and middle-aged Eratosthenian craters having notable echo enhancements, while older Nectarian craters have no echo enhancements. This is attributed to meteoritic gardening of the lunar surface, a process that wears away at the excess wavelength-sized rock populations associated with the younger craters [32, 33]. These salient features of 430 MHz (70 cm wavelength) lunar radar echoes are also seen in the near-global 40 MHz, (7.5 m wavelength) image shown in Figure 6b, which shows the mare-terra differences, as well as an echo enhancement for crater Tycho. Similar radar-echo differences for these younger lunar craters were observed in the 2380 MHz frequency (13 cm wavelength) Arecibo-Green Bank and Arecibo-Lunar Reconnaissance Orbiter Mini-RF bistatic experiments.

The terra backscatter same-sense circular depolarized echoes are also two to four times stronger than mare echoes. This is attributed to higher electrical losses in the first few meters of the lunar maria, resulting from higher concentrations of iron and titanium [31]. This can be seen in Figure 2b, where the echoes for the beam position on Oceanus Procellarum are less than the average for the eight beam positions around the disk of the moon. Similar mare-terra radar echo differences were observed in Arecibo-Green Bank and Arecibo-Lunar Reconnaissance Orbiter Mini-RF bistatic experiments at 2380 MHz frequency (13 cm wavelength).

6. Scientific Results and Annotated Bibliography

The scientific legacy of the Arecibo lunar radar observations is illustrated here by citing a number of journal articles based on Arecibo lunar radar measurements. These articles are:

B. A. Campbell, "Planetary Geology with Imaging Radar: Insights from Earth-based Lunar Studies, 2001-2015," *Publications of the Astronomical Society of the Pacific*, **128**, 2016, doi:10.1088/1538-3873/128/964/062001.

This paper traced these developments through a case study of lunar observations over the past 15 years, and their implications for ongoing and future solar-system radar studies. During the period, advances in computing power and imaging techniques also allowed Earth-based radar experiments to acquire data at the highest spatial resolutions permitted by their transmitter systems. The interpretation of radar echoes from the moon and planets has dramatically changed. These changes include development of polarimetric scattering models developed through lunar radar observations, terrestrial field measurements, and airborne radar studies.

B. A. Campbell, B. R. Hawke, and T. W. Thompson, "Regolith Composition and Structure in the Lunar Maria: Results of Long Wavelength Radar Studies," *Journal of Geophysical Research*, **102**, E8, 1997, pp. 19307-19320.

This article showed that the majority of the radar scatter from the lunar maria comes from Mie scattering by rocks buried in the regolith, and that scattering from a buried substrate does not greatly affect radar echo strengths.

B. A. Campbell, "High Circular Polarization Ratios in Radar Scattering from Geologic Targets," *Journal of Geophysical Research*, **117**, E06008, 2012, doi:10.1029/2012JE004061.

This article examined the occurrence of circular-polarization ratios (CPRs) greater than unity in terrestrial and planetary observations as a guide to associated surface morphologies. Lunar-crater deposits have circular-

polarization ratios of two to three, similar to those for Arizona's SP crater flows. These higher circular-polarization ratio values can be modeled by a dihedral-scattering geometry or a random dipole model.

B. A. Campbell, L. M. Carter, D. B. Campbell, M. C. Nolan, J. F. Chandler, R. R. Ghent, B. R. Hawke, R. F. Anderson, and K. S. Wells, "Earth-Based 12.6-cm Wavelength Radar Mapping of the Moon: New Views of Impact Melt Distribution and Mare Physical Properties," *Icarus*, **208**, 2, 2010, doi:10.1016/j. icarus.2010.03.011.

This article showed that radar backscatter data for the moon provide information on regolith dielectric and physical properties, with particular sensitivity to ilmenite content and surface or buried rocks with diameters of about one-tenth the radar wavelength and larger. Average 12.6-cm circular polarization ratio (CPR) values for low-to-moderate-TiO_2 mare basalt deposits were similar to those of rough terrestrial lava flows. This was attributed to abundant centimeter-sized rocks from small impacts, and to a significant component of subsurface volume scattering. Deposits of similar morphology and/or radar brightness were noted for craters such as Pythagoras, Rutherford, Theophilus, and Aristillus.

D. B. Campbell, B. A. Campbell, L. M. Carter, J-L Margot, and N. J. S. Stacy, "No Evidence for Thick Deposits of Ice at the Lunar South Pole," *Nature,* **443**, 7113, 2006, pp. 835-837; and

B. A. Campbell, and D. B. Campbell, "Regolith Properties in the South Polar Region of the Moon from 70-cm Radar Polarimetry," *Icarus*, **180**, 1, 2006, pp. 1-7.

These two articles concluded that if the hydrogen enhancement observed by the Lunar Prospector orbiter neutron spectrometer indicated the presence of water ice, then the lunar radar data were consistent with the ice being present only as disseminated grains in the lunar regolith. The interior wall of Shackleton crater, permanently shadowed from the sun but visible from Earth, was not significantly different in 70 cm scattering properties from sunlit areas of craters with similar morphologies.

L. M. Carter, B. A. Campbell, B. R. Hawke, D. B. Campbell and M. C. Nolan, "Radar Remote Sensing of Nearside Lunar Pyroclastic Deposits," *Journal of Geophysical Research*, **114**, E11004, 2009, doi:10.1029/2009JE003406.

This article showed that polarimetric radar observations can be used to address the distribution, depth, and embedded rock abundance of nearside lunar pyroclastic deposits. Radar backscatter and CPR maps can identify fine-grained mantling deposits in cases where optical and near-infrared data are ambiguous about the presence of pyroclastics.

R. R. Ghent, D. W. Leverington, B. A. Campbell, B. Ray Hawke, and D. B. Campbell, "Earth-Based Observations of Radar-Dark Crater Haloes on the Moon: Implications for Regolith Properties," *Journal of Geophysical Research*, **110**, E2, 2005, doi:10,1029/2204JE002366.

This article concluded that the common radar-dark haloes surrounding many lunar craters resulted from a block-poor ejecta, where the rock deficiencies disappeared over time with meteoritic bombardment. They also noted that additional high resolution could refine the lunar geologic timescale.

T. W. Thompson, B. A. Campbell, R. R. Ghent, B. R. Hawke, and D. W. Leverington, "Radar Probing of Planetary Regoliths: An Example from the Northern Rim of the Imbrium Basin," *Journal of Geophysical Research*, **111**, E6, 2006, E606S14.

This article concluded that that the extensive radar-dark area associated with the Montes Jura region in the vicinity of the crater Plato on the northern rim of the Imbrium Basin was due to overlapping, rock-poor ejecta deposits from the Iridum and Plato craters. Comparison of the radial extent of low-radar-return crater haloes with a model for ejecta thickness showed that these rock-poor layers detected by 70 cm radar were on the order of 10 m and thicker.

T. W. Thompson, B. A. Campbell, R. R. Ghent, B. R. Hawke, "Rugged Crater Ejecta as a Guide to Megaregolith Thickness in the Southern Nearside of the Moon," *Geology*, **37**, 7, 2009, pp. 655-658.

This article described how the size-frequency distributions of small (less than 10 km-sized) craters with radar-bright floors and ejecta were consistent with the hypothesis that the southern highlands of the moon were comprised of kilometer-thick ejecta layers that were thicker than elsewhere on the moon by about a kilometer, a difference attributed to abundant South Pole-Aitken Basin ejecta across the southern lunar highlands.

T. W. Thompson, H. Masursky, R. W. Shorthill, G. L. Tyler, and S. H. Zisk, "A Comparison of Infrared, Radar, and Geologic Mapping of Lunar Craters," *The Moon*, **10**, 1974, pp. 87-117; and

T. W. Thompson, J. A. Cutts, R. W. Shorthill, and S. H. Zisk, "Infrared and Radar Signatures of Lunar Craters: Implications for Crater Evolution," in *Conference on the Lunar Highlands Crust*, J. J. Papike and R. B. Merrill (eds.), New York, Pergamon Press, 1980, pp. 483-499.

These two articles described how the erosion and gardening of centimeter- and meter-sized blocks by meteoritic impacts will be evident in the infrared and radar signatures of craters and their ejecta. The youngest

craters have enhanced infrared eclipse temperatures and radar echoes. As these craters age, the enhancements diminish and disappear. The infrared and short (4 cm) radar enhancements disappear first, followed by long wavelength (70 cm) radar enhancement.

7. Concluding Remarks

Radar mapping/imaging of the moon has progressed through a series of resolution improvements over the years, as shown in Table 1. The best resolutions at 70 cm wavelength are now a hundred times better than those of the first 1964 observations, and the best resolutions at 13 cm wavelength are a thousand times better.

In broader terms, planetary radar studies pioneered in the 1960s with our nearest celestial neighbor, the moon, have evolved significantly over the intervening decades. Planetary radar studies have become a very effective means of providing a wealth of data on the surface geology of the moon, as well as of Venus, Mars, and the asteroids. Both Earth-based and space-borne radar studies of Venus, Mars, and the asteroids have further demonstrated the great potential of the planetary radar studies.

8. Acknowledgment

The Associate Editor thanks D. B. Campbell and S. Kesaraju for their valuable and expert assistance in reviewing this article.

9. Appendix 1

Here, we provide a description of one of the key elements in delay-Doppler mapping of the moon and other planetary bodies. This is the limb-to-limb difference in Doppler frequencies as observed at the radar. It is convenient to use a radar-observer Cartesian coordinate system, shown in Figure 3, where the y axis is aligned with an apparent axis of rotation, the z axis is along the radar's line-of-sight, and the x axis completes the triad. The z axis intersects the moon's surface at the sub-radar point, the point that appears to the radar to be at the center of the lunar disk. This sub-radar point is described by a longitude, l', and a latitude, b', quantities that vary slowly with time. The moon's natural librations generate a difference of about 7° in l' and about 5° in b' over the moon's 27 day orbital period. In addition, the motion of the radar on the rotating Earth generates differences of about 2° in 12 hours. The locations of l' and b' move across the surface with velocities of the order of 2 m/s.

The formulae that describe this, as given in Thompson [10] and shown in Figure 3, are:

$$\omega_a = \sqrt{\omega_{xd}^2 + \omega_{yd}^2}\,, \tag{1}$$

$$\omega_{xd} = \frac{\mathrm{d}b'}{\mathrm{d}t}, \tag{2}$$

$$\omega_{yd} = \cos(b')\frac{\mathrm{d}l'}{\mathrm{d}t}, \tag{3}$$

$$\mathrm{d}a = \arctan\left(\frac{\omega_{xd}}{\omega_{yd}}\right), \tag{4}$$

where ω_a is the total apparent rotation rate of the moon, ω_{xd} is the apparent rotation about the radar-observer x axis, ω_{yd} is the apparent rotation about the radar-observer y axis, and $\mathrm{d}a$ is the angle between the moon's apparent and true axes of rotation as observed at the radar.

The apparent spin of the moon creates a velocity difference between the approaching and receding limbs of the moon. This in turn creates a frequency spread that is characterized by the limb-to-limb Doppler shift, given by

$$f_{ll} = 2\Delta v/\lambda = 4\omega_a R/\lambda\,, \tag{5}$$

where f_{ll} is the limb-to-limb Doppler shift between the approaching and receding limbs, Δv is the velocity difference between the approaching and receding limbs of the moon, λ is the radar wavelength, ω_a is the apparent angular spin rate of the moon, and R is the radius of the moon (1738 km).

Once the apparent angular spin rate has been determined, the radar-echo delay and Doppler frequency can be located in the x_d, y_d, z_d coordinate system by

$$x_d = 2f/f_{ll}\,, \tag{6}$$

$$y_d = \pm\sqrt{1 - x_d^2 - z_d^2}\,, \tag{7}$$

$$z_d = 1 - (d/11{,}595)\,, \tag{8}$$

where f is the offset in Doppler frequency from that of the center of the moon, and d is the delay beyond the first echo from the moon in microseconds. Note that x_d is positive toward moon's east limb, and negative toward its west limb. Also, y_d is positive toward the north and negative toward the south. The x_d, y_d, z_d coordinate system is normalized so that the lunar radius equals unity. Once the echoes are located in the x_d, y_d, z_d coordinate system, their location in selenographic coordinates (latitude and longitude) can be determined as described by Thompson [10].

10. Acknowledgements

The authors, as well as all of the users of the Arecibo radar/radio telescope, are deeply indebted to William E. Gordon for his ingenuity and steadfast perseverance that led to the construction of this world-class facility. The authors are also indebted to Gordon Pettengill and Donald Campbell, who pioneered radar-astronomy studies with this facility. The accomplishments since the 1960s reported here were also enabled by the dedication and perseverance of the technical staff of the Arecibo and Green Bank Observatories. The dedication and perseverance of the technical staff of the Lunar Reconnaissance Orbiter Mission and Lunar Reconnaissance Orbiter Mini-RF Instrument made the recent novel Arecibo-Lunar Reconnaissance Orbiter bistatic observations possible. NASA support from the mid-1960s to the present enabled all of the radar observations described here. Two anonymous reviewers are acknowledged for their insightful comments and suggestions. Our colleagues, Eugene Ustinov as well as JPL documentarians Roger Carlson and Mary Young provided invaluable help in preparing this paper.

Preparation of this document was supported at the Jet Propulsion Laboratory, California Institute of Technology, under a contract with the National Aeronautics and Space Administration.

11. References

1. W. E. Gordon, "Incoherent Scattering of Radio Waves by Free Electrons with Applications to Space Exploration by Radar," *Proceedings of the Institute of Radio Engineers*, **46**, 1958, pp. 1824-1829.

2. M. H. Cohen, "Genesis of the 1000-Foot Arecibo Dish," *Journal of Astronomical History and Heritage*, **12**, 2, 2009, pp. 141-152.

3. D. Mathews, "Fifty Years of Radio Science at Arecibo Observatory: A Brief Overview," *URSI Radio Science Bulletin*, **346,** 2013, pp. 12-16.

4. J. H. Dewitt, Jr., and E. K. Stodola, "Detection of Radio Signals Reflected from the Moon," *Proceedings of the Institute of Radio Engineers*, **37**, 3, 1949, pp. 229-242, doi:10.1109/JRPROC.1949.231276.

5. Kovacs, Laszlo, "Zoltan Bay and the First Moon-Radar Experiment in Europe (Hungary, 1946)," *Science and Education*, 7, 3, pp. 313-316.

6. J. V. Evans and G. H. Pettengill, "The Scattering Behavior of the Moon at Wavelengths of 3.6, 68 and 784 Centimeters," *Journal of Geophysical Research*, **68**, 2, 1963, pp. 423-447, doi:10.1029/JZ068i002p00423.

7. R. M. Goldstein, *Radar Exploration of Venus*, PhD Thesis, California Institute of Technology, Pasadena, California, 1962.

8. P. E. Green, Jr., "Radar Astronomy Symposium Report," R. Leadabrand (ed.), *Journal of Geophysical Research,* **65**, 1960, pp. 1108-1115.

9. G. H. Pettengill and J. C. Henry, "Enhancement of Radar Reflectivity Associated with Lunar Crater Tycho," *Journal of Geophysical Research*, **67**, 12, 1962, pp. 4881-4885.

10. J. M. Saarri and R. W. Shorthill, "Isotherms of Crater Regions on the Illuminated and Eclipsed Moon," *Icarus*, **2**, 1963, pp. 115-1363.

11. J. D. Mathews, "A Short History of the Geophysical Radar at Arecibo Observatory," *History of Geo- and Space Sciences,* **4**, 1, 2013, pp. 9-33, doi:10.5194/hgss-4-19-2013.

12. T. W. Thompson, *A Study of Radar-Scattering Behavior of Lunar Craters at 70 cm*, PhD Thesis, Research Report RS 64, Center for Radiophysics and Space Research, Cornell University, Ithaca, New York, 1965.

13. G. P. Kuiper, *Photographic Lunar Atlas*, Chicago, University of Chicago Press, 1960.

14. L. A. Schimerman (ed.), *The Lunar Cartographic Dossier*, NASA-CR 1464000, Defense Mapping Agency, Aerospace Center, St. Louis, MO, 1973; available at Lunar and Planetary Institute LAC Web site http://www.lpi.usra.edu/resources/mapcatalog/LAC/.

15. T. W. Thompson, "Atlas of Lunar Radar Maps at 70 cm Wavelength," *The Moon*, **10**, 1974, pp. 51-85.

16. T. W. Thompson, "High-Resolution Lunar Radar Map at 70 cm Wavelength," *Earth, Moon and Planets*, **37**, 1987, pp. 59-70.

17. A. E. E. Rodgers and R. P. Ingalls, "Radar Mapping of Venus with Interferometric Resolution of the Range-Doppler Ambiguity," *Radio Science*, **5**, 1970, pp. 425-433.

18. T. W. Thompson, "Map of Lunar Reflectivity at 7.5-Meter Wavelength," *Icarus*, **13**, 3, 1970, pp. 365-370.

19. T. W. Thompson, "High-Resolution Lunar Radar Map at 7.5 Meter Wavelength," *Icarus*, **36**, 1978, pp. 174-188.

20. N. Stacy, "High Resolution Synthetic Aperture Radar Observations of the Moon," PhD Thesis, Cornell University, 1993.

21. J. L. H. Webb, D. C. Munson, and N. J. S. Stacy, "High-Resolution Planetary Imaging via Spotlight-Mode Synthetic Aperture Radar," *IEEE Transactions on Image Processing*, **7**, 1998, pp. 1571-1582.

22. A. Campbell, D. B. Campbell, J. L. Margot, R. R. Ghent, M. Nolan, J. Chandler, L. M. Carter, and N. J. S. Stacy, "Focused 70-cm Radar Mapping of the Moon," *IEEE Transactions on Geoscience and Remote Sensing*, **45**, 12, 2007, pp. 4032-4042, doi:10.1109/TGRS.2007.906582.

23. B. A. Campbell, B. R. Hawke, G. A. Morgan, L. M. Carter, D. B. Campbell, and M. Nolan, "Improved Discrimination of Volcanic Complexes, Tectonic Features, and Regolith Properties in Mare Serenitatis from Earth-based Radar Mapping," *Journal of Geophysical Research*, **119**, 2014, doi:10.1002/2013JE004486.

24. B. A. Campbell, L. M. Carter, D. B. Campbell, M. Nolan, J. Chandler, R. R. Ghent, B. R. Hawke, R. F. Anderson, and K. Wells, "Earth-based 12.6-cm Wavelength Radar Mapping of the Moon: New Views of Impact Melt Distribution and Mare Physical Properties," *Icarus*, **208**, 2, 2010, pp. 565-573, doi:10.1016/j.icarus.2010.03.011.

25. G. W. Patterson, et al. "Mini-RF on LRO and Arecibo Observatory Bistatic Radar Observations of the Moon," 46th Lunar and Planetary Science Conference, 2888, 2015.

26. T. Hagfors, "Remote Probing of the Moon By Infrared and Microwave Emissions and By Radar," *Radio Science*, **5**, 2, 1970, pp. 189-227. doi:10.1029/RS005i002p00189.

27. B. A. Campbell, "High Circular Polarization Ratios in Radar Scattering from Geologic Targets," *Journal of Geophysical Research*, **117**, 2012, E06008, doi:10.1029/2012JE004061.

28. J. V. Evans, and T. Hagfors, "On the Interpretation of Radar Reflections From the Moon," *Icarus*, **3**, 2, 1964, pp. 151-160, doi:10.1016/0019-1035(64)90056-9.

29. G. L. Tyler, and H. T. Howard, "Dual-Frequency Bistatic-Radar Investigations of the Moon with Apollos 14 and 15," *J. Geophys. Res.,* **78**, 23, 1973, pp. 4852-4874, doi:10.1029/JB078i023p04852.

30. T. W. Thompson, E. A. Ustinov, and E. Heggy, "Modeling Radar Scattering From Icy Lunar Regoliths at 13 cm and 4 cm Wavelengths," *Journal of Geophysical Research,* **116**, 2011, E01006, doi:10.1029/2009JE003368.

31. B. A. Campbell, and B. R. Hawke, "Radar Mapping of Lunar Cryptomaria East of Orientale Basin," *Journal of Geophysical Research*, **110**, 2005, E09002, doi:10.1029/2005JE002425.

32. T. W. Thompson, H. Masursky, R. W. Shorthill, G. L. Tyler, and S. H. Zisk, "A Comparison of Infrared, Radar, and Geologic Mapping of Lunar Craters," *The Moon*, **10**, 1, 1974, pp. 87-117.

33. T. W. Thompson, J. A. Cutts, R. W. Shorthill, and S. H. Zisk, "Infrared and Radar Signatures of Lunar Craters: Implications for Crater Evolution," in J. J. Papike and R. B. Merrill (eds.), *Conference on the Lunar Highlands Crust*, New York, Pergamon Press, 1980, pp. 483-499.

Special Section: Joint URSI BeNeLux - IEEE AP-S - NARF Symposium

On Monday, December 7, 2015, a joint URSI Benelux, IEEE BeNeLux Chapter on Antennas and Propagation and Netherlands Antenna Research Forum symposium was organized at the University of Twente in The Netherlands. The theme of the event was "Smart Antennas and Propagation."

Over 70 people attended the symposium, which gave an excellent overview of antenna-related activities in the BeNeLux (Belgium, the Netherlands, and Luxembourg).

Young scientists presented their research during a poster session. The three winning posters were (1) Elles Raaijmakers of the Technical University of Eindhoven and the Erasmus Medical Center in Rotterdam (coauthors R. M. C. Mestrom and M. M. Paulides), "Development of a Murine Head & Neck Hyperthermia Applicator;" (Figure 1) (2) Gert-Jan Stockman of Ghent University (coauthors Dries Vande Ginste and Hendrik Rogier), "Efficient Modeling of the Wireless Power Transfer Efficiency for Varying Positions and Orientations Between Transmitter and Receiver;" and (3) Jurgen Vanhamel of the Belgian Institute for Space Aeronomy (coauthors S. Berkenbosch, E. Dekemper, D. Fussen, P. Leroux, E. Neefs, and E. Van Lil), "**Implementation of Different RF-Chains to Drive Acousto-Optical Tunable Filters in the Framework of an ESA Space Mission**."

The work of Jurgen Vanhamel is published in this issue of the *Radio Science Bulletin*.

Next year's URSI BeNeLux Forum will be organized by the Belgium URSI Committee. It will be held in the Fall of 2016 in Brussels, at the Royal Military School.

Figure 1. The first place Young Scientist paper prize (l-r): Ramiro Serra, Secretary of the Netherlands URSI committee; Elles Raaijmakers, winner of the prize; Mark Bentum, Chair of the Netherlands URSI committee.

Implementation of Different RF-Chains to Drive Acousto-Optical Tunable Filters in the Framework of an ESA Space Mission

J. Vanhamel[1], S. Berkenbosch[1], E. Dekemper[2], D. Fussen[2], P. Leroux[3], E. Neefs[1], and E. Van Lil[4]

[1]Engineering Department
Royal Belgian Institute for Space Aeronomy Ringlaan 3, 1180 Brussels, Belgium
E-mail: jurgen.vanhamel@aeronomie.be

[2]Department of Solar Radiation in Atmospheres Royal Belgian Institute for Space Aeronomy
Ringlaan 3, 1180 Brussels, Belgium

[3]KU Leuven, Department of Electrical Engineering ESAT, Advanced Integrated Sensing Lab (AdvISe)
Kleinhoefstraat 4, 2440 Geel, Belgium

[4]KU Leuven, Department of Electrical Engineering ESAT – TELEMIC, Telecommunications and Microwaves
Kasteelpark Arenberg 10, bus 244, 3001 Leuven, Belgium
E-mail: streltsa@erau.edu

Abstract

The work reported in this paper addresses different solutions to the problem of building a space-qualified RF chain for an acousto-optical tunable filter. This research was undertaken as part of the development of the ALTIUS space mission (atmospheric limb tracker for the investigation of the upcoming stratosphere), which aims at the measurement of atmospheric trace species (ozone, nitrogen dioxide, methane, water vapor,...) concentration profiles with a high spatial resolution.

1. Introduction

Wide-aperture acousto-optical tunable filters (AOTF) appeared in the 1970s [1] and found applications in various areas, such as agriculture (crop-stress monitoring), the food industry (product quality), biology (fluorescence spectroscopy), etc. Their main advantages are robustness, compactness, low power consumption, high filtering efficiency, ability to be tuned, potentially high spectral resolution (< 1 nm), and good image quality. In general, they offer interesting features for meeting the needs in hyperspectral-imaging applications.

The physical process behind the wide-aperture acousto-optical tunable filter is the interaction of light and sound inside a birefringent crystal. For a given acoustic frequency, only photons of a particular energy (i.e., wavelength) will couple with the acoustic wave, and then leave the crystal in a slightly different direction than the rest of the light. By focusing the diverted beam onto a detector, one effectively performs a spectral image of the scene. Selecting another window of the light spectrum only requires the tuning of the sound frequency. A piezoelectric transducer bonded to the crystal is responsible for converting the electrical RF signal into an acoustic wave.

As most acousto-optical tunable filters operating in the visible and near-infrared domains are driven with frequencies ranging from a few MHz to several hundreds of MHz, they do not necessitate particular electronics equipment. This statement does not hold when it comes to operating acousto-optical tunable filters in a space environment: the RF-driving chain must be made from the limited catalogue of space-qualified parts. The problem gets even larger when frequencies of several tens of MHz or higher must be generated.

The work reported in this paper addresses different solutions to the problem of building a space-qualified RF-

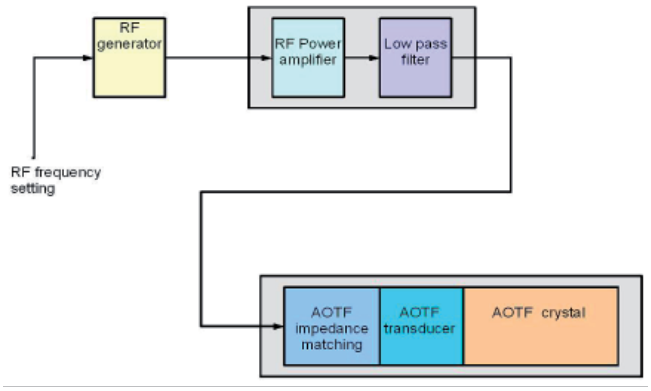

Figure 1. The channel RF-chain concept.

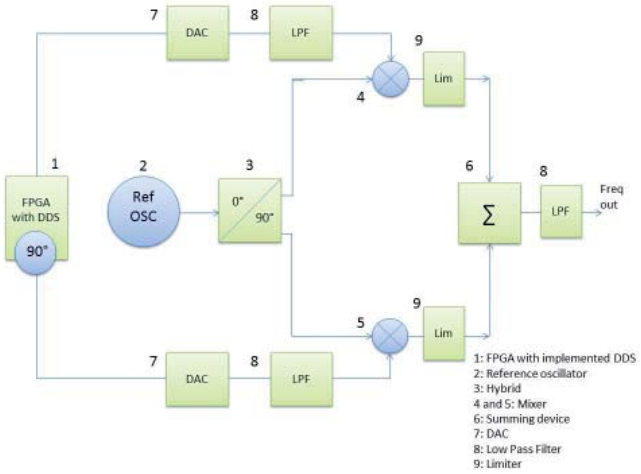

Figure 2. The Hilbert-transform solution setup.

chain for an acousto-optical tunable filter. This research was undertaken as part of the development of the ALTIUS space mission (atmospheric limb tracker for the investigation of the upcoming stratosphere), which aims at the measurement of atmospheric trace species (ozone, nitrogen dioxide, methane, water vapor,...) concentration profiles with a high spatial resolution [2, 3]. The measurement concept relies on the acquisition of spectral images of the bright atmospheric limb at well-chosen wavelengths. The imager concept allows avoiding the need for scanning the atmosphere, as was done by previous remote-sensing missions. The instrument will be mounted onboard a PROBA satellite (Project for On-Board Autonomy) [4-6]. The PROBA-satellite is a platform containing all the essential subsystems, such as a GPS, an attitude and orbit control system, etc., to facilitate the payload, which is placed on top of the platform. The complete project (platform and payload) is being developed under the supervision of ESA (European Space Agency), and with funding from the Belgian Science Policy Office (BELSPO).

The original ALTIUS concept made use of three independent spectral imagers (channels), each of them relying on an acousto-optical tunable filter capable of isolating narrow pass-bands across the channel's spectral range (ultraviolet, UV, from 250 nm to 400 nm; visible, from 440 nm to 800 nm; near-infrared, NIR, from 900 nm to 1800 nm). For the visible and NIR channels, the two acousto-optical tunable filters will be made of a paratellurite crystal. For the UV channel, the acousto-optical tunable filter would have been made from a KDP crystal (potassium dihydrogen phosphate). Unfortunately, the latter did not reach the necessary level of maturity for a space mission, and the KDP-based acousto-optical tunable filter was replaced by a stack of Fabry-Pérot interferometers (FPI). Nevertheless, for technological interest, the acousto-optical tunable filter approach will also be developed and matured for the UV-channel up to flight level.

The focus of this paper was to design, for each of the different channels, a dedicated RF-chain containing an RF generator and an RF amplifier (see Figure 1). The output of the RF amplifier was tunable to a specific frequency and a specific power level, and was injected into the acousto-optical tunable filter's transducer via an impedance-matching network.

Different architectures [7-11] are possible to generate the frequency range needed for the different wavelength domains. While the Hilbert-transform solution will be only summarized here and not further investigated, this paper focuses on the phase-locked loop (PLL) solution. Phased-locked loop solutions were bread-boarded for the three wavelength domains. A detailed study was done on the achievable power levels in the infrared, visible, and the ultraviolet.

Table 1. The available preliminary design requirements.

Requirement	Value
Unwanted spectral components in RF output	< –30 dBc
UV channel frequency range	130 - 260 MHz
Visible channel frequency range	60 - 120 MHz
NIR channel frequency range	30 - 60 MHz
Nominal load	50 Ohms
RF generator dc power consumption	< 2 W
RF generator output power level	> 0 dBm

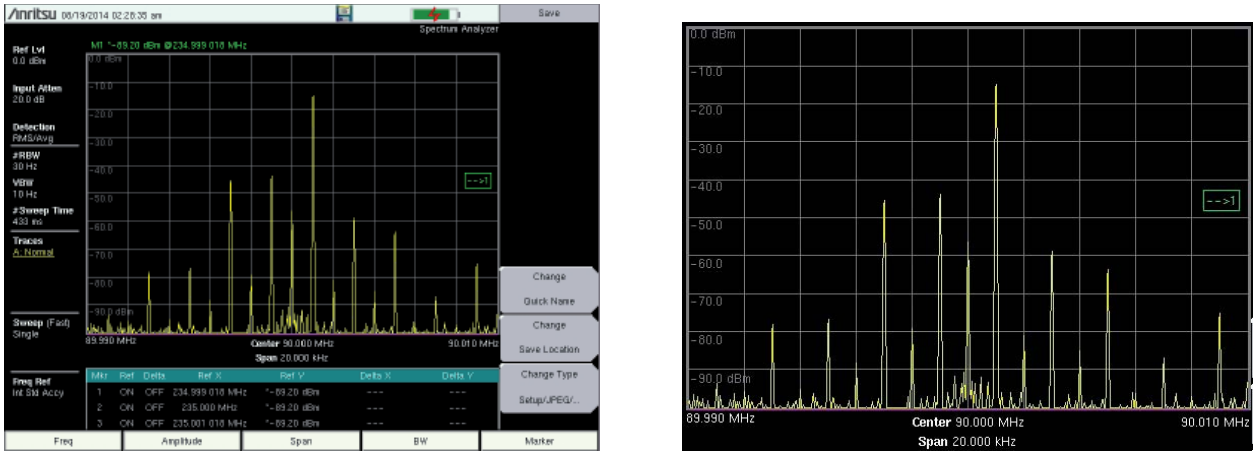

Figure 3. The spectral output for the visible channel.

2. RF Generator Architectures

Both the RF generator and the RF amplifier will have specific requirements for electrical performance, sensitivity, frequency range, and resolution. Their development will focus on survivability in space and compliance with the selected spacecraft. For this, a well-defined package of environmental tests has to be carried out, such as thermal-vacuum, radiation, vibration, shock, and EMC (electromagnetic compatibility). The test levels were derived from the scientific requirements for the instrument. Because the project is currently in a preliminary design phase, some requirements still need to be defined. For instance, the choice of the launcher will determine several environmental parameters. This paper will focus on fulfilling of the requirements listed in Table 1.

All the other requirements will be determined in a later stage. To fulfill the environmental requirements, the electronic components need to be selected and built in accordance with "space-qualified" standards. Because of the space environment wherein this instrument has to perform, the availability of electronic components is limited to those screened and qualified for space applications. ESA also restricts the use of components to those present in their preferred parts list. This restricts the possibilities for generating an RF signal based on a high-tech up-to-date solution. Solutions containing commercial electronics also cannot be retained.

For the design of a space-qualified acousto-optical tunable-filter RF generator, different approaches were investigated [7-11]. Taking into account the space environment, and the limitations of restricted power, voltage levels, mass, and volume, two solutions were considered, namely the Hilbert transform [8, 9] and the phased-locked-loop approach [10, 11]. Today, the latter solution is preferred, and hence was further investigated in this paper. This is because it has better spectral purity, lower complexity, lower power consumption, and a higher output-power level. A scientific space project under the supervision of ESA in a preliminary design phase needs to have a main and a spare solution. This is why the Hilbert transform was kept as a backup. The setup is explained in Figure 2.

The key elements in the Hilbert-transform solution are a fixed oscillator and an FPGA (field-programmable gate array) from Actel-Microsemi (RTAX2000S-CQ352V) [12]. In the FPGA, a firmware DDS (direct digital synthesizer) was implemented that created two 90°-shifted digital waveforms. The output of the FPGA was presented to two DACs (digital-to-analog converters) [13] that converted the output into analog sine waves. The signals in both chains are then filtered by an LPF (low-pass filter) and applied to two mixers. The output of a reference oscillator was shifted by 0° and 90°. Each output was combined in a mixer stage and filtered (low-pass filter). Both chains were summed in a summing device. This sine wave was filtered before entered the RF amplifier. Several breadboards were built and tested for the different channels. Looking at the spectral output – for example, of the visible channel – it

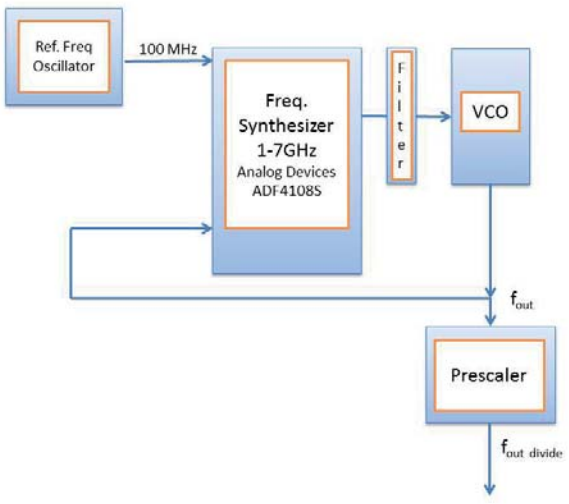

Figure 4. The phase-locked-loop solution setup.

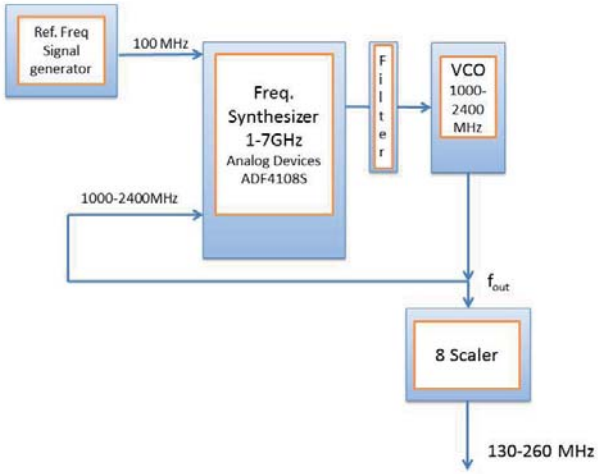

Figure 5. The UV-channel setup.

could be seen that many harmonics and spurs were created, depending on the frequency used (Figure 3). The production of the harmonics and spurs was caused by several mixing stages in the setup, as well as the summing at the end of the chain. The level of the spurs and harmonics was still below the requirement of −30 dBc.

Although all requirements concerning harmonic suppression and output level were fulfilled, and although all proposed components existed in a space-qualified version, the solution exceeded the available electrical-power budget. The higher mass, volume, and complexity also made it less attractive compared to the phased-locked-loop solution. The reason was that the Hilbert transform used an FPGA (1 W) and two mixer stages. These mixers were passive devices, which meant that the input power had to be high (around +7 dBm). For the Hilbert transform, two extra DACs would have been needed, which implied an additional 2 × 660 mW. Together with the lower output level of the RF generator (compare Figure 3 with Figures 6, 9, and 12), this would have resulted in twice the needed dc power compared to the phased-locked-loop solution.

The phased-locked-loop design (Figure 4) used an ADF4108S space-qualified frequency synthesizer from Analog Devices [14], a voltage-controlled oscillator (VCO), an active-loop filter, and a space-qualified prescaler from Peregrine Semiconductor. The power consumption of this setup was limited compared to the Hilbert-transform solution. The ADF4108S consumed around 100 mW, the VCO consumed around 200 mW, and the prescaler consumed around 40 mW. An FPGA was also needed to steer the RF chain, which introduced an extra power consumption of 1 W. While the power consumption for the Hilbert-transform solution was estimated to be 3 W, the estimated power consumption of the phased-locked-loop solution was 1.5 W. Depending on the channel setup, and taking into account some margins, the total power varied from one channel to another: UV: ±1400 mW; visible: ±1450 mW; and NIR: ±1450 mW. An additional advantage of the phased-locked loop was the increased output level of the signal.

In the next paragraphs, the detailed phased-locked-loop design for the different channels is described, and the test results obtained on the breadboards are explained.

3. Test Results

3.1 The UV Channel

For the UV channel (Figure 5), the ADF4108S from Analog Devices was used together with an in-house custom-designed active-loop filter. In the phased-locked-loop a VCO (Mini-Circuits ZX95-2500W+) [15] was used, which was controlled between 1 GHz and 2.4 GHz, followed by a divide-by-eight prescaler from Peregrine Semiconductor [16].

This phased-locked-loop combination allowed spanning the required output-frequency range for the UV channel (130 MHz to 260 MHz). Tests showed that the generated spectrum was compliant with the requirements: no excessive harmonics or spurs existed in the spectrum

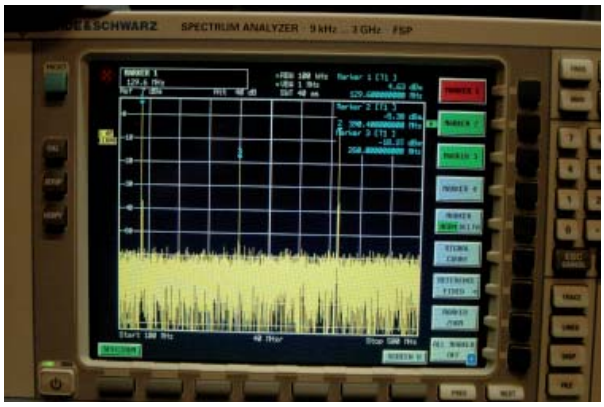

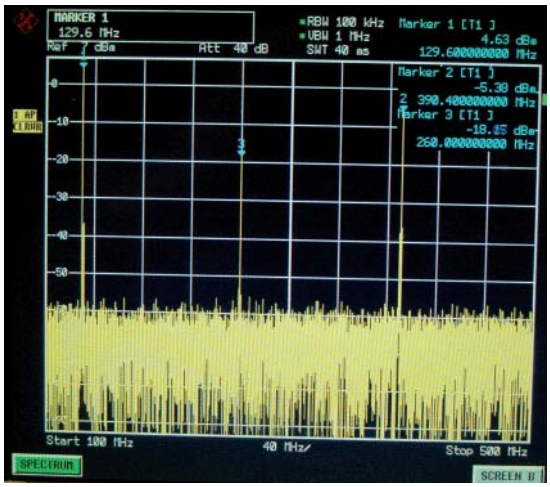

Figure 6. The output signal at 129.6 MHz after the divide-by-eight prescaler.

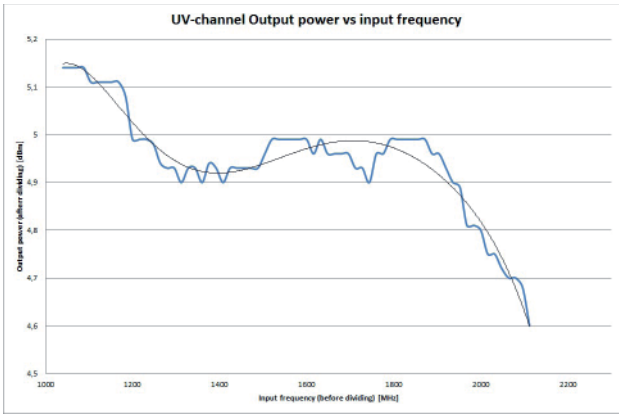

Figure 7. The output power level of the UV channel.

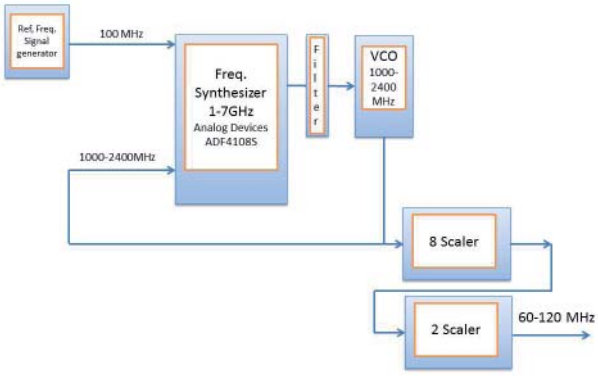

Figure 8. The visible-channel setup.

(Figure 6), the second harmonic was less than −22 dBc, and the third harmonic was −10 dBc. The use of an additional passive third-order bandpass hourglass filter that had a bandwidth of 130 MHz and a center frequency of 195 MHz suppressed these higher harmonics. As a consequence, the power level of the output signal was attenuated by 10 dB because of this filter.

Additionally, tests were carried out to check the output level of the RF generator (Figure 5). Different input frequencies were programmed into the ADF4108, delivering output frequencies in the desired range. The VCO's output level varied with the output frequency. The lowest output level was around −1.4 dBm, and the highest output was around +4.3 dBm. These numbers were based on the datasheets of the VCO used. A fit with a sixth-order polynomial indicated the trend of the setup's output-power curve (Figure 7). The drift of the output-power level was quite limited in the frequency range. At the low end, the output power was around 5.1 dBm, and at the higher end, the power was around 4.6 dBm, resulting in a spread of around 0.5 dB.

3.2 The Visible Channel

The same ADF4108, Mini-Circuits VCO, and custom-made loop filter were used for the RF generator of the visible channel (Figure 8). However, a different divider combination was used with divide-by-eight and divide-by-two prescalers [17] to match the required frequency range (60 MHz to 120 MHz), because no space-qualified divide-by-16 prescaler was available on the market today.

As for the RF generator in the UV channel, the VCO output could also be controlled in the range of 1 GHz to 2.4 GHz. At the lower end of the required range (with the synthesizer frequency set to 1 GHz), an output frequency of 62.6 MHz was obtained after the prescalers with harmonics located at 187.9 MHz (−9.7 dBc) and 313.2 MHz (−14.5 dBc) (Figure 9). Again, no excessive harmonics or spurs existed in the spectrum. The requirement of −30 dBc could easily be met by implementing a passive third-order bandpass hourglass filter. The upper end of the required output frequency range could be reached with a synthesizer

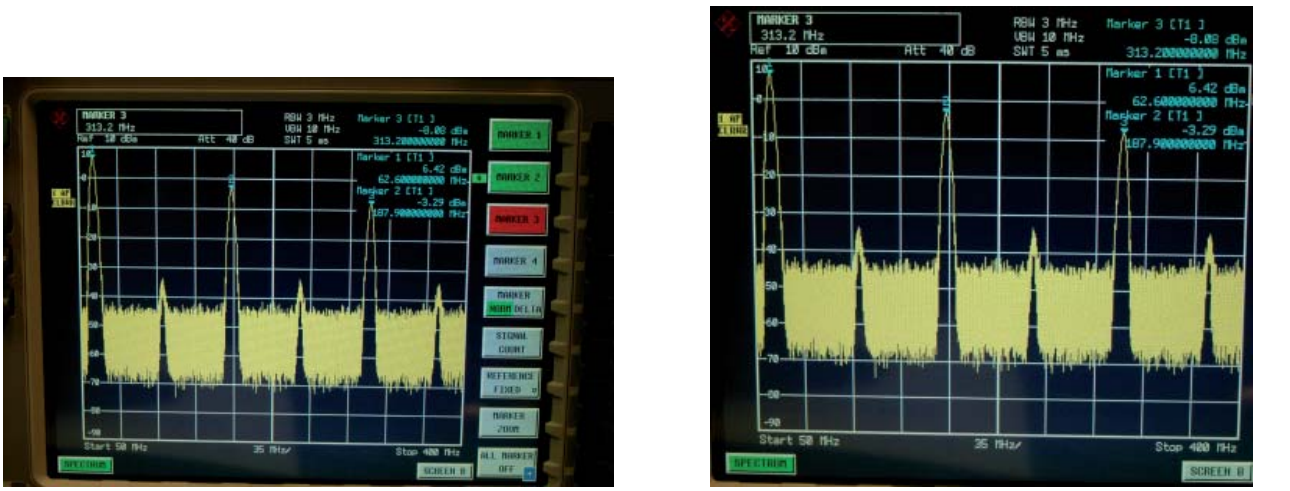

Figure 9. The output signal at 62.5 MHz after the divide-by-eight and divide-by-two prescalers.

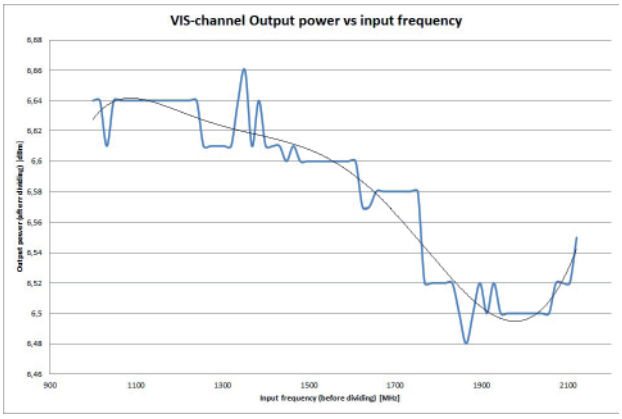

Figure 10. The output power level of the visible channel.

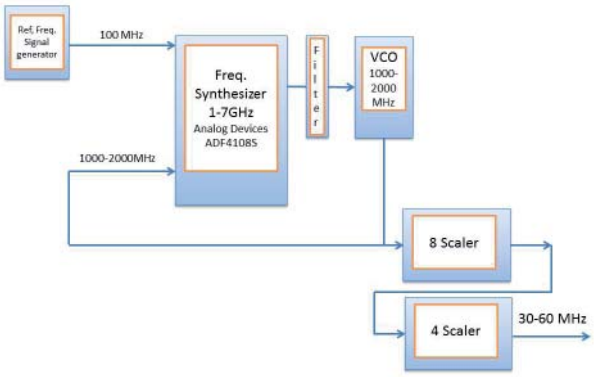

Figure 11. The NIR-channel setup.

frequency of 1.92 GHz, after scaling leading to an output frequency of 120 MHz. Additional filtering, similar to that used in the UV channel, removed the harmonics from the output.

Similarly to the UV channel, the stability of the output level was verified (Figure 10). At the low end of the frequency range, the output power was around 6.7 dBm, and it was around 6.5 dBm at the higher end, giving a spread of about 0.15 dB. Based on these numbers, it could be concluded that the stability of the RF generator was proven.

3.3 The NIR Channel

The phased-locked-loop solution for the NIR channel was very similar to the two previous designs (Figure 11). The same components were used. The VCO was used in a slightly reduced frequency range, while the end stage was composed of a divide-by-eight followed by a divide-by-four prescaler [18]. No space-qualified divide-by-32 prescaler exists on the market today. With this setup, an output frequency range between 30 MHz and 60 MHz was obtained.

The output of the VCO was controlled between 1 GHz and 2 GHz. At a synthesizer frequency of 1.23 GHz, an output frequency of 38.439 MHz was obtained after the prescaler stage, with harmonics at 115.32 MHz (–9.8 dBc) and 192.54 MHz (–14.1 dBc) (Figure 12), well below the expected –30 dBc if a passive third-order bandpass hourglass filter was used.

Figure 13 shows the deviation of the output power for the measurements performed. At the low end of the frequency range, the output power was around 6.0 dBm. At the high end, it was around 5.8 dBm, yielding a spread of about 0.2 dB.

4. Conclusions and Future Work

This study was part of the development of the driving electronics of a spaceborne remote-sensing instrument (ALTIUS), which used acousto-optical tunable filters to take spectral images of the bright atmospheric limb in order to retrieve the concentration profiles of key trace species. Although building RF-chains for driving acousto-optical tunable filters on the ground is a common task, it required

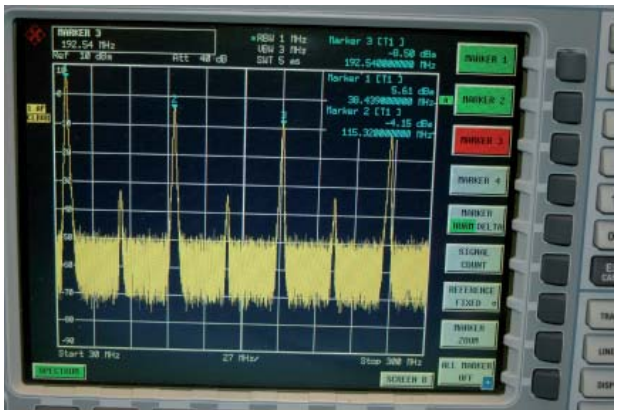

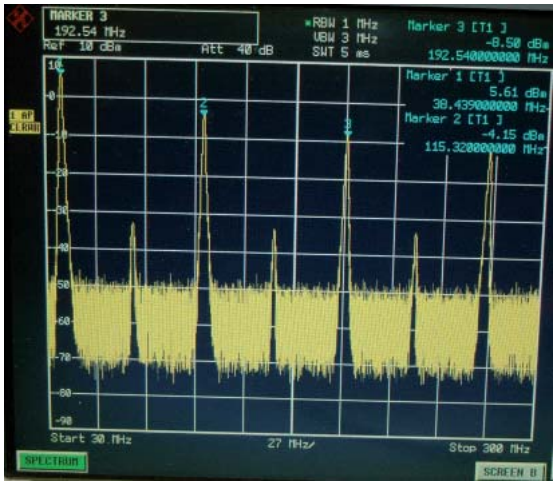

Figure 12. The output signal at 38.439 MHz after the divide-by-eight and divide-by-four prescalers.

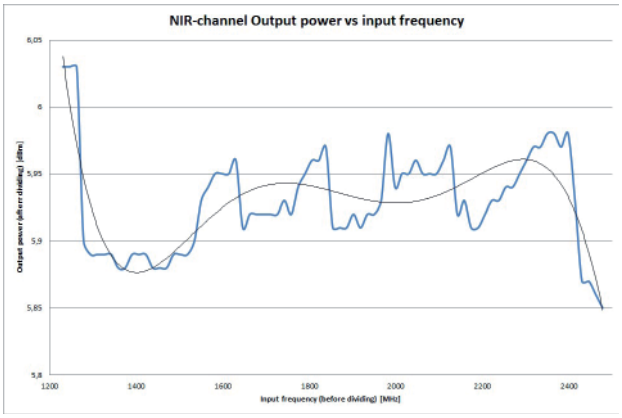

Figure 13. The output power level of the NIR channel.

specific developments in the framework of a space instrument, as it had to undergo space-qualification procedures. Two driving concepts were designed and bread-boarded.

As a conclusion of this work, it was clear that for the generation of the RF signals driving the three acousto-optical tunable filters originally proposed in the ALTIUS concept, a phased-locked-loop solution was preferred over a Hilbert-transform solution. A phased-locked-loop setup offered less complexity (fewer parts needed), and hence a reduced printed-circuit-board area, reduced mass, and better resistance to mechanical stresses. The implementation of the design into a flight-compatible form, rather than a breadboard, and with realistic harnessing and connectors is ongoing.

The achieved output levels for the phased-locked-loop solution showed acceptable output-level stabilities in the applied frequency range of 0.2 dB in the NIR and visible channels, and 0.5 dB in the UV channel. Both values were in line with the input specifications of the RF amplifiers. It was shown that the use of a combination of prescalers (visible and NIR channels) in the last stage instead of a single prescaler had no negative impact on the stability.

Future work will consist of assessing the stability of the output signal, including the thermally induced jitter. It is known that the performance of analog VCO circuits has to be strictly monitored (and sometimes even controlled) in environments with thermal variations. Further investigation will clarify these items.

5. Acknowledgments

The ALTIUS project is supported by the Belgian Federal Science Policy Office (BELSPO), and funded through ESA-PRODEX contract PEA4200090274.

6. References

1. I. C. Change, "Noncollinear Acousto-Optic Filter with Large Angular Aperture," *Applied Physics Letters*, **25**, 1974, pp. 370-372.

2. E. Dekemper, D. Fussen, B. Van Opstal, J. Vanhamel, D. Pieroux, F. Vanhellemont, N. Mateshvili, G. Franssens, V. Voloshinov, C. Janssen, and H. Elandaloussi, "ALTIUS: A Spaceborne AOTF-Based UV-VIS-NIR Hyperspectral Imager for Atmospheric Remote Sensing," *Proceedings of SPIE*, **9241-92410L**, 1-10, 2014.

3. E. Dekemper, D. Fussen, F. Vanhellemont, D. Pieroux, N. Mateshvili, G. Franssens, Q. Errera, J. Vanhamel, E. Neefs, L. De Vos, and L. Aballea, "ALTIUS, A Future Small Mission for O_3 and Other Atmospheric Trace Species Concentration Profiles Retrieval," *Geophysical Research Abstracts*, **18**, EGU2016-17653, 2016.

4. K. Gantois, S. Santandrea, F. Teston, K. Strauch, J. Zender, E. Tilmans, and D. Gerrits, "ESA's Second In-Orbit Technology Demonstration Mission: Proba-2," *ESA Bulletin-European Space Agency*, **144**, November 2010, pp. 22-33.

5. M. J. Barnsley, J. J. Settle, M. A. Cutter, D. R. Lobb, and F. Teston, "The PROBA/CHRIS Mission: A Low-Cost Smallsat for Hyperspectral Multiangle Observations of the Earth Surface and Atmosphere," *IEEE Transactions on Geoscience and Remote Sensing*, **42**, 7, July 2004, pp. 1512-1520.

6. F. Teston, P. Vuilleumier, D. Hardy, E. Tilmans, and K. Gantois, "Proba Proves the Technology," *ESA Bulletin-European Space Agency*, **129**, February 2007, pp. 47-53.

7. J. Vanhamel, D. Fussen, E. Dekemper, E . Neefs, B. Vanopstal, D. Pieroux, J. Maes, E. Van Lil, and P. Leroux, "RF-Driving of Acoustic-Optical Tunable Filters; Design, Realization and Qualification of Analog and Digital Modules for ESA," *Microelectronics Reliability*, **55**, 2015, pp. 2103-2107.

8. P. Das, D. Shklarsky and L. B. Milstein, "SAW Implemented Real-Time Hilbert Transform and its Application in SSB," IEEE Ultrasonics Symposium, 1979, pp. 752-756

9. L. Moura and P. Monteiro. "Design Method for FIR-Based Hilbert Transform Filters Suitable for Broadband AM-SSB," *Electronics Letters*, **38**, 12, June 6, 2002, pp. 605-606.

10. I. A. Young, J. K. Greason, and K. L. Wong, "A PLL Clock Generator with 5 to 110 MHz of Lock Range for Microprocessors," *IEEE Journal of Solid State Circuits*, 1992, pp. 1599-1607.

11. R.E. Best, *Phase-Locked Loops, Sixth Edition*, New York, McGraw-Hill, USA, 2007.

12. The Actel RTAX FPGA, RTAX2000S-CQ352V (V-flow) www.microsemi.com/products/fpga-soc/radtolerant-fpgas/rtax-s-sl

13. Texas Instruments Digital to Analog Converter DAC5675 A-SP, www.ti.com/product/dac5675a

14. Information and datasheet for the Analog Devices frequency synthesizer (1-7 GHz) ADF4180S, www.analog.com/en/products/application-specific/militaryaerospace/aerospace/adf4108s.html

15. Information and datasheet for the VCO of Mini-Circuits (ZX95-2500W+), http://194.75.38.69/pdfs/ZX95-2500W+.pdf

16. Information and datasheet for the Peregrine 8 prescaler PE9303, www.psemi.com/products/prescalers/pe9303

17. Information and datasheet for the Peregrine 2 prescaler PE9311, www.psemi.com/products/prescalers/pe9311

18. Information and datasheet for the Peregrine 4 prescaler PE9312, www.psemi.com/products/prescalers/pe9312

RADIO SCIENCE FOR HUMANITY

PRELIMINARY CALL FOR PAPERS

The URSI-France 2017 Workshop, under the sponsorship of the French Academy of Sciences, will be dedicated to **"Radio Science for Humanity".** The workshop will be held at Campus SophiaTech located in Sophia Antipolis, South of France, on February 1-3, 2017. **JS'17** is co-organised by Institute Mines Telecom - Telecom ParisTech and Université Nice Sophia Antipolis. On Thursday, February 2, at 5 pm, the **General Assembly of URSI-France** will hold their annual meeting.

Electromagnetism, telecommunications, electronics and photonics are an essential backbone of our modern society. The development of these activities benefits humanity in a wide range of issues, from extreme situations to simple comfort in our everyday lives. In this rapidly evolving field, we will focus in the workshop on both fundamental and conceptual aspects as well as technological developments and resulting applications.

A wide spectrum of areas will be covered, including waves and electromagnetic fields, both from the point of view of metrology and theory, spread, modelling, etc., and communications systems together with their applications. We will also address environmental electromagnetic propagation, both global (surface and subsurface), ionospheric or through matter in particular plasma and radio astronomy. Electromagnetism in biology and medicine will also be included.

The workshop will be organized around **oral and poster sessions**. Most sessions will be introduced by **invited lecturers** presenting the state of the art and/or recent developments, followed by **regular communications**, which will be selected by the Scientific Committee. The program will be organised around the following (non exhaustive) list of topics. The working languages will be French and English.

Topics:

- **Radio science and risk, disaster management, space weather**
- **Earth observation by remote sensing and essential climate variables monitoring**
- **Advanced radars for societal needs**
- **Computational sciences, exact methods, complexity management**
- **Design and modelling of antennas, systems of detection and imaging, antenna systems**
- **Communication systems: 5G, software defined radio, Internet of Things**
- **Metrologies and electromagnetism**
- **Electromagnetism in biology and medicine**

DATES TO REMEMBER

June 20, 2016:	Preliminary call for papers
July 20, 2016:	Opening of the website for abstracts
October 16, 2016:	**Deadline for submission of abstracts**
October 31, 2016:	Scientific committee notification to authors
December 20, 2016:	**Deadline for full text submissions**
January 9, 2017:	Notification of the final acceptance of the full paper
February 1-3, 2017:	**JS'17 workshop**
February 3, 2017:	List of the selected papers invited for journal publication

All information relating to the workshop can be found on the URSI-France website: **http://ursi-france.mines-telecom.fr**

In Memoriam: Per-Simon Kildal

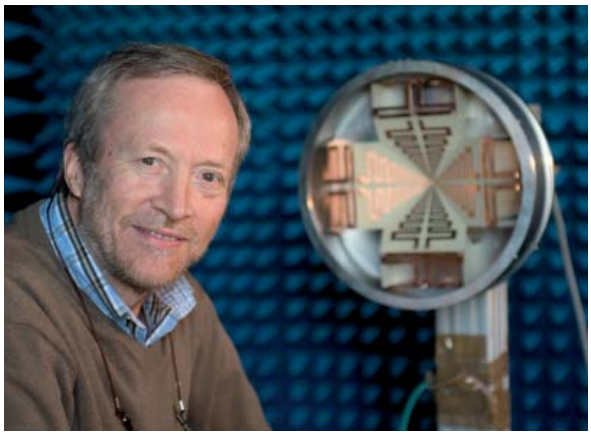

Prof. Per-Simon Kildal tragically passed away on April 21, 2016, after a very short period of illness. He was born on July 4, 1951. He was employed and became Professor at Chalmers University of Technology in 1989. Before that, he held several positions as a researcher at the Norwegian University of Technology (now Norwegian University of Science and Technology), ELAB, and SINTEF, all in Trondheim, Norway. He obtained his MSEE, PhD, and doctor technicae (an old-style doctoral degree) at the Norwegian University of Technology in 1975, 1982, and 1990, respectively. He became a Fellow of the IEEE in 1995.

Prof. Per-Simon Kildal was an outstanding antenna specialist. He was the author or coauthor of over 700 papers in journals and conferences concerning antenna theory, analysis, design, applications, and measurement techniques. He was one of the most-productive authors at Chalmers, and had been cited almost 9000 times. His most-cited paper, entitled "Artificially Soft and Hard Surfaces in Electromagnetics," was published in *IEEE Transactions on Antennas and Propagation* in 1990, and was cited more than 400 times. Prof. Kildal held many granted patents for reverberation chambers, reflector antennas, dipole antennas, metamaterial applications, and, most recently, GAP™ waveguide technologies.

Prof. Kildal had an extremely high international reputation in electromagnetics, antenna theory, and wave propagation. The quality and quantity of his research placed him in the top 1% of researchers in these areas worldwide. His work had a major impact in the field of applied electromagnetics for antennas and propagation research, development, and production. Prof. Kildal had an uncanny ability to grasp new concepts, "to see the big picture and hear the grass growing," while comfortably managing with the mathematical details. It is very rare to encounter a scientist who is equally versatile and highly successful in theory, hardware, and application. It was this versatility, coupled with hard work and a fertile imagination, which contributed to Prof. Kildal's success and international reputation.

Prof. Kildal was awarded several prestigious international prizes, most notably the "Distinguished Achievement Award" of the IEEE Antennas and Propagation Society. He was invited to give keynote talks at conferences all around the world on numerous occasions, and was appointed an IEEE Distinguished Lecturer for two periods. Prof. Kildal was the recipient of a prestigious individual European Research Council Advanced Grant in 2013.

Per-Simon made important contributions to radio-astronomy instrumentation, in particular via his work in helping design the Gregorian secondary optics installed on the 305 m diameter radio telescope in Arecibo, as part of its major upgrade in 1997. His work significantly improved the performance of the Arecibo dish, which is to date the largest and most-sensitive radio telescope in the world. Additionally, the Eleven-antenna ultra-wideband feed, a patented invention of Prof. Kildal, is under consideration for use on the Square Kilometre Array (SKA), which is the next huge step in centimeter- and meter-wave radio astronomy. The Eleven-feed is also being used in geodetic very-long-baseline interferometry, in order to realize the new specifications for broadband observing that will allow sub-millimeter-accuracy position determination over global baselines. Prof. Kildal invented industrialized antennas used in successful products such as Ericsson's MINILINK.

Prof. Kildal was the founder of Bluetest AB and Gapwaves AB. Bluetest AB provides new over-the-air (OTA) measurement technology for wireless devices with multiple-input multiple-output (MIMO) antenna systems. Their well-proven reverberation-chamber test systems are a result of Per-Simon's research at Chalmers, and these are now used by many companies and operators all around the world. The innovative measurement technology of Bluetest has now been adopted in international standards. Gapwaves AB aims at commercializing the GAP™ waveguide technology as the leading technology platform for millimeter-wave and terahertz applications. The focus is on developing a mass-production method for the manufacturing of GAP- waveguide-based antennas. The GAP technology is a result and further development of Prof. Kildal's pioneering work on soft and hard surfaces.

Per-Simon taught antenna engineering based on his antenna textbook, which recently came out in a new release. He supervised and led 24 students to a PhD and nine to a Licentiate degree. He was very active in the antenna systems community, such as in COST (the European Cooperation in Science and Technology) actions, EuCAP (the European Conference on Antennas and Propagation), EurAAP (the European Association on Antennas and Propagation), the IEEE (Institute of Electrical and Electronics Engineers), to mention the most important activities. He was the conference Chair of EuCAP 2013, which was organized in Gothenburg, and was a great success. He was also a popular and appreciated lecturer at antenna courses organized by ESoA (the European School of Antennas) and others.

Per-Simon had great success with his research and was a very active researcher until he passed away. He initiated and was the main driver of the application for the Chalmers Antenna Systems Excellence Center (Chase), which started in 2007 with funding from Vinnova, participating companies, and Chalmers. Chase has been a very big success, with excellent evaluations by international experts, and has contributed to the success of the participating companies. During the last few years, Per-Simon was more active than ever. He was the main writer of three proposals for large research initiatives on OTA and GAP technologies. He was also in the process of writing a fourth proposal for an Industrial Research Center (IRC) during the last months before his tragic death. This proposal will be continued by his colleagues in the division of antenna systems, and they will continue in Per-Simon's footsteps.

Per-Simon was able to do what he loved to do until the very end. He participated in the EuCAP 2016 conference in Davos, where he had a rupture of the aorta, and went to the hospital where he had two surgeries. Unfortunately, he did not survive the surgeries. He was in coma for one week after the surgeries, and then passed away on April 21, 2016. The day before the conference, he was skiing in the Alps with one of his daughters and a few more friends. Skiing was among his favorite interests outside of work. He spent the Easter break with his family and friends in the Norwegian mountains almost every year. During the last few years, he took his research group for a much-appreciated long skiing weekend, also to the Norwegian mountains. He was always joking that participation in the skiing weekend was a requirement to get a PhD in the antenna group.

The death of Per-Simon is a very tragic loss for his family, the scientific community, Chalmers, and his colleagues in the Department of Signals and Systems. Per-Simon is survived by his wife, two daughters, and a brother. We will all miss him very much.

Arne Svensson, Head of Department, Signals and Systems, Chalmers University of Technology
Jan Carlsson, SP Technical Research Institute
John Conway, Director of Onsala Space Observatory
Marianna Ivashina, Associate Professor
Jian Yang, Associate Professor
Rob Maaskant, Associate Professor
Ashraf Uz Zaman, Assistant Professor
Andres Alayon Glazunov, Assistant Professor, Antenna Systems Division, Chalmers University of Technology

In Memoriam: Richard Davis

Very sadly, we must announce that Prof. Richard Davis OBE passed away on Monday, May 2, 2016. Richard worked at Jodrell Bank for almost 45 years, contributing to many areas of research, teaching, and technical development. He will be greatly missed by all here, and his many friends and colleagues across the world.

Richard arrived at Jodrell Bank in 1971, when he joined the MSc course in radio astronomy. He proceeded to studying for a PhD, first with Robin Conway as supervisor, and then with Ralph Spencer, when Robin was on sabbatical leave.

Working with Bob Warwick and Ralph Spencer, Richard designed and constructed electronic systems for the first phase-stable interferometer at Jodrell, using the Mk II and Mk III telescopes separated by 24 km. The system automatically compensated for the path-length changes in the radio link between the telescopes. Richard independently worked out the necessary geometric corrections to the phase, which enabled positions of radio sources to be determined to better than 100 milli-arcseconds. It also enabled integrations for hours, allowing, for example, the discovery of radio emission from the parent galaxy of the famous radio source, Cygnus A.

Following the successful completion of his PhD thesis (mostly on the radio polarization properties of quasars), he then worked on MERLIN, where with Bryan Anderson and Mike Bentley, he produced the link-path measuring system still used to this day. During this time (the late 1970s), Richard and Ralph Spencer spent many happy hours working with Sir Bernard Lovell, developing observing systems for the study of red-dwarf flare stars. These used the Mk I (now Lovell) telescope, and the 25-m telescope at Defford at a frequency of 408 MHz. They led to the first unambiguous detection of radio emission from YZ CMi using an interferometer.

With his student, Steve Padin, Richard then went on to design the broadband interferometer using the Lovell and Mk II telescopes operating at 5 GHz. This instrument had one of the highest-speed correlators in existence at the time. It was sensitive enough to detect radio emission from novae and symbiotic stars, leading to a new topic for research.

Richard later worked extensively on the study of the quasar 3C273, leading to a number of important papers in the 1980s and 1990s. He was also project scientist for MERLIN, the 32-m Cambridge Telescope, and the Lovell Telescope, taking responsibility for advising on upgrades, which have kept it at the cutting edge of research.

Most recently, his work focused on studies of the cosmic microwave background with the Very Small Array in Tenerife, and then the Planck spacecraft. He was the United Kingdom's Principal Investigator for the Low-Frequency Instrument (LFI) onboard Planck. He led the team at Jodrell Bank, which designed and built the 30 GHz and 44 GHz space-qualified cryogenic radio receivers, the most sensitive radio-astronomy receivers to date in these bands. The spacecraft was launched in May 2009, and continued operations until the end of its scheduled mission, in October 2013. Planck has provided the most accurate measurements of several key cosmological parameters.

Richard had a wide range of impressive skills in electronics and computing, developing instruments which have led to new areas of research: as he himself said, not bad for a theoretical-physics graduate. Richard could – and did – apply his deep understanding of how radio astronomy really works to a wide variety of problems and projects. His natural insight into the basic physics of what was going on was tremendous. He made it look easy, whether it be electronics, structural engineering, radio-frequency design, astrophysics, or cosmology. His wide-ranging work was recognized with the award in 2011 of an OBE for services to science.

Staff and students at Jodrell Bank remember Richard as a lovely man and a devoted father who was always fun to be around: there was a lot of laughter when working with him. His infectious enthusiasm, commitment to science, and warmth were legendary: he brought humor, understanding, and pin-sharp insight in equal measure to everything he did, and our whole community will miss him greatly.

Friends and colleagues, Jodrell Bank Observatory,
School of Physics and Astronomy,
University of Manchester

International Union of Radio Science (URSI)

3rd URSI Regional Conference on Radio Science

(3rd URSI-RCRS)

1 - 4 March 2017

TIRUPATI, India

Special Session : "25 years of Indian MST Radar"

FIRST CIRCULAR

As part of the silver jubilee of the establishment of the high power Indian MST Radar, National Atmospheric Research Laboratory (NARL), Dept of Space Govt. of India, Gadanki and the Indian Committee for URSI (INCURSI), (which is under the Indian National Science Academy - INSA) are jointly organising the 3rd URSI-RCRS 2017 during March 1-4, 2017 at Tirupati, India. There will be a special session on the progress in MST Radar based science and technological developments. In addition to the regular sessions, there will be a maximum of five Young Scientist Awards (YSA) and five student paper competition (SPC) prizes. Where appropriate, names of YSA recipients could be recommended for being considered for the YSA awards of the XXXII URSI General Assembly and Scientific Symposium - URSI GASS 2017. Details can be found later on our website.

We welcome participation from researchers in India and abroad to this conference. Participants from neighbouring countries in the Asian and African region with whose science academies INSA has an MOU on scientific cooperation and exchange could avail the facilities under those MOUs.

Interested participants are requested to send an email with "interested" in subject line to ursircrs2017@narl.gov.in.

Important Dates

First Circular:	1 May 2016
Second Circular :	14 August 2016
Abstract Submission deadline:	15 November 2016
Acceptance notification:	30 November 2016
Registration Early bird deadline:	15 January 2017
SPC submission deadline:	10 January 2017
YSA submission deadline:	10 January 2017
Conference dates:	1-4 March 2017

Et Cetera

Tayfun Akgül
Istanbul Technical University
Dept. of Electronics and Communications Engineering
Telecommunications Division
80626 Maslak Istanbul, Turkey
Tel: +90 212 285 3605; Fax: +90 212 285 3565
E-mail: tayfun.akgul@ieee.org

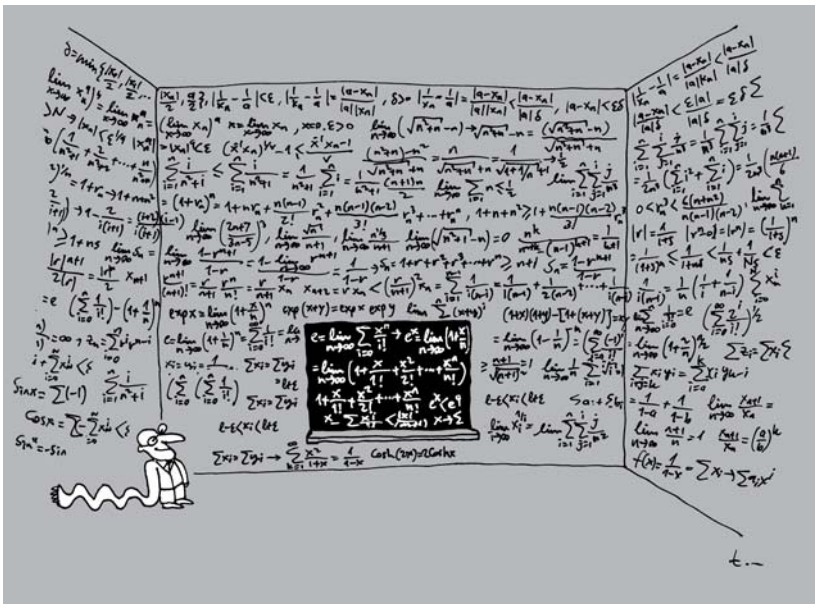

THE CONFERENCE

The European Conference on Antennas and Propagation is owned by the European Association on Antennas and Propagation (EurAAP) and has been organised each year since 2006. The conference is supported by top level Associations on Antennas and Propagation and provides a forum on the major challenges faced by these communities.

Contributions from European and non-European industries, universities, research centres and other institutions are solicited. The conference provides an overview of the current state-of-the-art in Antennas, Propagation, and Measurements topics, highlighting the latest developments and innovations required for future applications.

FORMAT OF THE CONFERENCE

The conference combines the main following features, addressing 38 antenna topics, 21 propagation topics and 14 measurement topics (see www.eucap2017.org):

- Plenary sessions with invited and keynote speakers
- Oral sessions (both convened and regular)
- Poster sessions
- Short Courses and Workshops
- Exhibition

INSTRUCTIONS FOR AUTHORS

Authors are invited to submit their contribution in the form of a FINAL PAPER with a minimum length of two A4 pages and a maximum length of five A4 pages.

The paper must contain enough information for the Technical Programme Committee (TPC) and reviewers to judge on the originality and quality of the work in a single step acceptance/rejection review process. Notice that TPC and reviewers will especially care about plagiarism and self-plagiarism.

During the uploading process, authors will be requested to categorize their paper in terms of conference topic and application track. Accepted papers will be submitted to IEEE Xplore, unless otherwise stated by the corresponding author.

APPLICATION TRACKS

Aiming at increasing the interaction between academia and industry, the conference will feature session tracks focused on applications. The list of application tracks is available at www.eucap2017.org.

EXHIBITION AND SPONSORSHIP

The conference will provide numerous opportunities for exhibitors and sponsors, according to their strategic visibility and publicity targets. Detailed information can be obtained at the conference website.

PARIS AND THE VENUE

Besides its reputation around the world as one of the most cultural and historical cities in the world, Paris also embodies technological progress and is at the heart of scientific discoveries in antennas and propagation!
The "Palais des Congrès" is located downtown in Paris a few minutes away from the city's legendary "Avenue des Champs-Élysées" and is easily accessible by public transport. EuCAP 2017 will be located on a single level and will easily allow meetings and scientific exchanges between participants in a comfortable venue with a view over the city.

CONTACTS

TPC
tpc@eucap2017.org

Exhibitions & sponsorship
exhib-sponsor@b2c-congress.com

Professional Conference Organizer (b2C Congress)
eucap2017@b2c-congress.com

Özgür Ergül
Department of Electrical and Electronics Engineering
Middle East Technical University
TR-06800, Ankara, Turkey
E-mail: ozgur.ergul@eee.metu.edu.tr

SOLBOX-04

Ismail E. Uysal[1], H. Arda Ülkü[2], and Hakan Bağcı[1]

[1]Division of Computer, Electrical, and Mathematical Sciences and Engineering (CEMSE)
King Abdullah University of Science and Technology (KAUST)
Thuwal 23955-6900, Saudi Arabia
E-mail: {ismail.uysal,hakan.bagci}@kaust.edu.sa

[2]Department of Electronics, Gebze Technical University
Gebze, Kocaeli 41400, Turkey
E-mail: haulku@gtu.edu.tr

1. Introduction

We have received a pair of new problems involving plasmonic spheres and their reference solutions in the time domain. The main focus of SOLBOX-04, which was submitted by Ismail E. Uysal, H. Arda Ülkü, and Hakan Bağcı, is computing scattered fields from gold spheres. The challenge is incorporating plasmonic effects that dominate at optical frequencies. In addition to negative permittivity values to be used in the implementations, the submitters had to deal with the highly dispersive properties of the structures in the time domain. Reference solutions were also provided along with the descriptions of the problems. Mie-series solutions were also available for one of them, demonstrating the accuracy of their approach. We are looking forward to receiving alternative solutions for these new, challenging problems, as well as for the previous submissions in the earlier issues (SOLBOX-01, SOLBOX-02, and SOLBOX-03).

2. Problem

2.1 Problem SOLBOX-04 (by I. E. Uysal, H. Arda Ülkü, and H. Bağcı)

This problem involves the computation of fields scattered from metallic (plasmonic) nanostructures at optical frequencies. For this task, time-domain solvers are preferred, since they (i) provide broadband data with a single code execution, and (ii) permit accurate modeling of strong material nonlinearities. However, the direct computation of the fields in the time domain is a challenging task, since the permittivity of metals at optical frequencies is highly dispersive. Two separate examples were considered: A gold sphere of radius 50 nm (inset of Figure 1), and a dimer (inset of Figure 2) consisting of two gold spheres separated by 5 nm. It was assumed that both structures

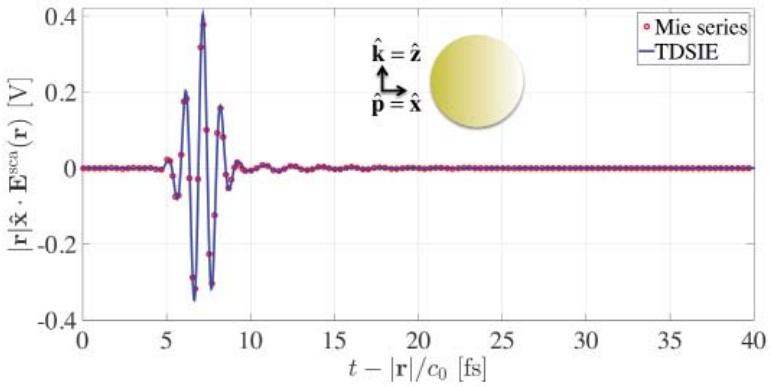

Figure 1. The x component of the range-corrected scattered electric far field, $|\mathbf{r}|\hat{\mathbf{x}} \cdot \mathbf{E}^{\mathrm{sca}}(\mathbf{r},t)$, for the gold sphere in SOLBOX-04.

were centered at the origin and residing in free space. The frequency samples of the gold's permittivity were obtained from the experimental data of Johnson and Christy [1]. The structures were excited by a plane wave with electric field

$$\mathbf{E}_0^{\mathrm{inc}}(\mathbf{r},t) = \hat{\mathbf{x}} G\left(t - \hat{\mathbf{z}} \cdot \mathbf{r}/c_0\right),$$

where c_0 is the speed of light in free space, and

$$G(t) = \cos\left[2\pi f_0 (t - t_0)\right] e^{-(t-t_0)^2/2\sigma^2}$$

is a Gaussian pulse with modulation frequency f_0, duration σ, and delay t_0. In both examples, $f_0 = 900$ THz, $t_0 = 8\sigma$, $\sigma = 3/(2\pi f_{\mathrm{bw}})$, and the effective bandwidth was $f_{\mathrm{bw}} = 600$ THz. It was desired to compute the scattered electric field in the time domain.

3. Solution to Problem SOLBOX-04

3.1 Solution Summary

Solver type (e.g., noncommercial, commercial):
Noncommercial research-based code developed at KAUST, Thuwal, Saudi Arabia.

Solution core algorithm or method:
Time-domain surface integral equation (TDSIE) [2, 3] and marching-on-in-time (MOT).

Programming language or environment (if applicable):
Fortran90/77 + MPI.

Computer properties and resources used:
Four cores, 2.67 GHz, Intel Xeon®, X5650, 48 GB ECC RAM, *Ubuntu*

Total time required to produce the results shown (categories: < 1 sec, < 10 sec, < 1 min, < 10 min, < 1 hour, < 10 hours, < 1 day, < 10 days, > 10 days):
< 10 min (gold sphere) and < 30 min (gold dimer)

3.2 Short Description of the Numerical Solution

To avoid the volumetric discretization and approximate absorbing conditions required by differential-equation-based approaches, a time-domain surface integral equation solver was used to compute the transient fields scattered from plasmonic structures. This time-domain surface integral equation solver made use of the Poggio-Miller-Chang-Harrington-Wu-Tsai (PMCHWT) SIE formulation [4] to construct the scattered fields in the form of a spatio-temporal convolution of equivalent surface electric and magnetic current densities, which were introduced on the surface of the plasmonic structure, with the Green's

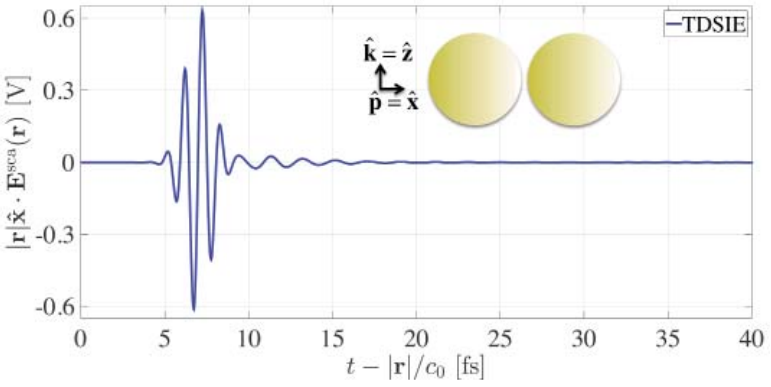

Figure 2. The x component of the range-corrected scattered electric far field, $|\mathbf{r}|\hat{\mathbf{x}} \cdot \mathbf{E}^{\mathrm{sca}}(\mathbf{r},t)$, for the gold dimer in SOLBOX-04.

function of the unbounded dispersive medium. Equivalent currents were expanded using Rao-Wilton-Glisson (RWG) functions [5] in space and polynomial interpolants [6] in time. Inserting these expansions into the time-domain surface integral equation and Galerkin testing, the resulting equation at discrete time steps yielded a matrix system of equations. The samples of the time-domain Green's function and the time-domain permittivity required to compute the matrix entries were obtained from their frequency-domain samples using a fast relaxed vector-fitting algorithm [7]. This matrix system of equations was then solved for the unknown expansion coefficients using an MOT scheme. It should be noted here that the version of the MOT scheme used here was not accelerated. Its memory and CPU requirements could be reduced using blocked FFT-based algorithms [6], or the plane-wave time-domain (PWTD) method [9].

3.3 Results

Figure 1 plots the *x* component of the (range-corrected) electric far fields [8], scattered from the gold sphere along the *z* axis, which are obtained from the (inverse Fourier transformed) Mie series solution and the time-domain surface integral equation solution. The results agreed well, verifying the accuracy of the time-domain surface integral equation solver. Similarly, Figure 2 plots the *x* component of the (range-corrected) electric far field [8] scattered from the gold dimer along the *z* axis, which is obtained from the time-domain surface integral equation solution. It should be noted here that there is no analytical solution for this problem.

4. References

1. P. B. Johnson and R.-W. Christy, "Optical Constants of the Noble Metals," *Phys. Rev. B*, **6**, pp. 4370-4379, 1972.

2. I. E. Uysal, H. A. Ulku, and H. Bagci, "MOT Solution of the PMCHWT Equation for Analyzing Transient Scattering from Conductive Dielectrics," *IEEE Antennas Wireless Propag. Lett.*, **14**, pp. 507-510, 2015.

3. I. E. Uysal, H. A. Ulku, and H. Bagci, "Transient Analysis of Plasmonic Nanostructures Using an MOT-PMCHWT Solver," IEEE International Symposium on Antennas and Propagation, Vancouver, BC, 2015, pp. 1508-1509.

4. B. Shanker, M. Lu, J. Yuan, and E. Michielssen, "Time Domain Integral Equation Analysis of Scattering from Composite Bodies via Exact Evaluation of Radiation Fields," *IEEE Trans. Antennas Propag.*, **57**, 5, May 2009, pp. 1506-1519.

5. S. M. Rao, D. R. Wilton, and A. W. Glisson, "Electromagnetic Scattering by Surfaces of Arbitrary Shape," *IEEE Trans. Antennas Propag.*, **30**, 3, May 1982, pp. 408-418.

6. H. Bagci, A. E. Yilmaz, V. Lomakin and E. Michielssen, "Fast Solution of Mixed-Potential Time-Domain Integral Equations for Half-Space Environments," *IEEE Trans. Geosci. Remote Sens.*, **43**, 2, February 2005, pp. 269-278.

7. B. Gustavsen and A. Semlyen, "Rational Approximation of Frequency Domain Responses by Vector Fitting," *IEEE Trans. Power Delivery*, **14**, 3, July 1999, pp. 1052-1061.

8. S. M. Rao, *Time Domain Electromagnetics*, San Diego, CA, Academic Press, 1999.

9. P. -L. Jiang and E. Michielssen, "Multilevel Plane Wave Time Domain Enhanced MOT Solver for Analyzing Electromagnetic Scattering from Objects Residing in Lossy Media," IEEE International Symposium on Antennas and Propagation, Washington, DC, 2005, 3B, pp. 447-450.

XXI[st] International Seminar/Workshop
DIRECT AND INVERSE PROBLEMS OF ELECTROMAGNETIC AND ACOUSTIC WAVE THEORY
(DIPED-2016)

Tbilisi, Georgia, September 26-29, 2016

FIRST CALL FOR PAPERS

General Information

The XXI[st] International Seminar/Workshop on Direct and Inverse Problems of Electromagnetic and Acoustic Wave Theory (DIPED-2016) will be held at the Tbilisi State University, Georgia, on September 26-29, 2016. The IEEE MTT/ED/AP/EMC Georgian and MTT/ED/AP/CPMT/SSC West Ukraine Chapters are co-organizers of the DIPED-2016. The DIPED seminar series was started in 1982, it began newly as the IEEE ED, MTT, and AP Societies technical co-sponsored event since 1995.

Suggested Topics

- Theoretical aspects of electrodynamics
- Diffraction theory
- Propagation and scattering in complex media
- Numerical methods in the electrodynamics
- Waveguide and photonic crystal structures
- Inverse problems and synthesis
- Antennas and antenna arrays
- Acoustics: theory and applications

Instruction for Authors

1. The instruction for preparing the papers will be presented in the Web Site of the DIPED-2016 Seminar/Workshop.
2. The WinWord doc or LaTeX files should be sent to Dr. Mykhaylo Andriychuk, Program Committee Secretary, via e-mail andr@iapmm.lviv.ua.

Important Dates

August 1, 2016	Deadline for reception of camera-ready papers.
August 15, 2016	Notifications of authors about acceptance of the papers.
September 26-29, 2016	Seminar/Workshop DIPED-2016.

Organizing Committee

Chairman: *Prof. Revaz S. Zaridze*
Ivane Javakishvili Tbilisi State University
3, Chavchavadze Ave.
0179, Tbilisi, Georgia
Tel.: +995 32 2290 821, fax: +995 32 2290 845
e-mail: revaz.zaridze@tsu.ge

Secretary: *Dr. Tamar Gogua*
Ivane Javakishvili Tbilisi State University
1, Chavchavadze Ave.
0179, Tbilisi, Georgia
Tel: +995 32 2222 473, fax: +995 32 2222 473
E-mail: tamar.gogua@tsu.ge

Program Committee

Chairman: *Prof. Nikolai N. Voitovich*
Pidstryhach Institute for Applied Problems in Mechanics and Mathematics, NASU
3"B" Naukova St., Lviv, 79060, Ukraine
Tel: +38 032 258 51 44, fax: +38 032 263-72-70
E-mail: voi@iapmm.lviv.ua

Secretary: *Dr. Mykhaylo Andriychuk*
Pidstryhach Institute for Applied Problems in Mechanics and Mathematics, NASU
3"B" Naukova St., Lviv, 79060, Ukraine
Tel: +38 032 258 96 46, fax: +38 032 263-72-70
E-mail: andr@iapmm.lviv.ua

For detailed information, please visit web site: **http://www.ewh.ieee.org/soc/cpmt/ukraine/** or **http://ewh.ieee.org/r8/ukraine/georgian/DIPED/**

Randy L. Haupt
Colorado School of Mines
Brown Building 249
1510 Illinois Street, Golden, CO 80401 USA
Tel: +1 (303) 273 3721
E-mail: rhaupt@mines.edu

How Full is Your Glass

A popular philosophical/psychoanalytical question is, "Is the glass half full or half empty?" If you answer, "Half empty," then you are pigeon-holed as a pessimist. You think about subtraction: what could have been. You do not appreciate what you have. If you answer, "Half full," then you are pigeon-holed as an optimist. You see possibilities to add something: you appreciate what you have.

The *Merriam-Webster Dictionary* defines "pigeon hole" as "a neat category which usually fails to reflect actual complexities." In other words, some prejudice is involved. We want to brand someone as behaving in a certain way all the time. Do you behave one way all the time? I know I don't. If I just drank half a glass of iced tea, and you asked me if it was "half empty" or "half full," I would say "half empty." That response does not make me pessimistic, just realistic. I just drank half of the tea! On the other hand, if I was pouring the iced tea into a glass and my phone rang before I filled it, I would say that it was "half full." Why? Because I was filling the glass when I stopped. That does not mean that I am optimistic.

Many of our attitudes are situational. A soldier or athlete may be brutal in battle, but may be kind and gentle at other times. If you eat meat, does that mean that you hate or like animals? The fallacy of the "half full"/"half empty" branding is demonstrated by the pro-/anti-abortion argument. A large survey of the American public from 1972 to 2012 reported the attitudes of people towards abortion [1]. The question, "Are you for or against abortion," is not easy to answer for all people. About 40% of the respondents over the years felt that abortion was fine for any reason (glass "half full"). That does not mean that the rest of the people were against abortion under any circumstances (glass "half empty"). In reality, factors such as birth defects, a woman's health, and rape are significant factors that determine a person's attitude towards abortion. You may be on one side or the other, except for....

We seem to want to categorize people by an arbitrary test. You will often hear, "If you do or say ***," then "You are ###." "If you are not for us, then you are against us." This type of attitude discourages people from thinking. Rather than looking at the situation and applying good judgment and ethics, you are expected to always adhere to some predetermined course of action. We who think and analyze for a living should cringe at this attitude. Our motto should be, "I will not be pigeon holed, because I am not a pigeon!"

The glass "half full"/"half empty" question is not as simple as it seems. The idea of a "half full" glass is absurd, because the glass is always full: half liquid and half air. If it is "half full" of liquid, is it "half empty" of air? Sometimes our glass is 30% or 60% full or empty. It might be milk instead of water. Nobody is always an optimist. Nobody is always a pessimist. Human beings are for the most part situational. It depends – and that is okay.

Reference

1. T. W. Smith and J. Son, "General Social Survey 2012 Final Report Trends in Public Attitudes Towards Abortion," NORC at the University of Chicago, May 2013.

RFI 2016

Coexisting with Radio Frequency Interference

October 17-20, 2016

Hosted by the
National Radio Astronomy Observatory (NRAO)
at the New Mexico Tech Macey Center
in Socorro, New Mexico (USA)

Radio Frequency Interference (RFI) has become a critical issue for many users of the electromagnetic spectrum. This is especially true for observational sciences such as radio astronomy, microwave remote sensing of the Earth, and Solar and ionospheric studies where highly sensitive measurements are necessary.

Following the previous successful workshops held in Bonn (Germany, 2001), Penticton (Canada, 2004) and Groningen (The Netherlands, 2010), RFI 2016 aims to bring together researchers, engineers and users from all radio science disciplines to consider how RFI affects their respective fields, to develop mitigation strategies, and to foster cooperation and collaboration. Attention will also be given to the impact of new and future sources of RFI, spectrum management challenges, and new technology developments.

RFI 2016 will represent a step forward in the ongoing efforts to achieve meaningful scientific observations in the presence of significant and growing Radio Frequency Interference, and will offer an opportunity for the Radio Astronomy and Remote Sensing communities to interact and exchange ideas. More details are available on the workshop website **http://go.nrao.edu/rfi2016**.

Prospective authors are invited to submit an abstract no later than **August 1, 2016**, on the following topics:

- Defining and quantifying RFI
- Spectrum management and frequency allocations
- Radio Quiet Zones, electromagnetic interference
- SETI: separating terrestrial and extra-terrestrial transmissions
- RFI detection, prediction
- Calibration, direction-of-arrival estimation
- RFI in passive and active microwave remote sensing
- Mono and multi antenna signal processing
- Progresses in flagging and excision techniques
- Signal subtraction approaches
- Time/frequency/spatial filtering
- Pre- and post-correlation techniques
- Towards a real-time implementation of identification and mitigation
- Future sources of RFI

Selected authors will be offered the opportunity to submit an extended paper for follow on publication in a dedicated book.

Important dates:

Abstract submission deadline	August 1, 2016
Paper acceptance notification	September 4, 2016
Author registration	September 15, 2016
Conference	October 17-20, 2016
Proceeding paper submission	November 11, 2016

Scientific Organizing Committee:

Willem Baan (ASTRON - URSI)
Frank Gronwald (U Siegen)
Joel Johnson (OSU)
Paolo de Matthaeis (NASA, IEEE-GRSS)
Roger Oliva (ESA)
Albert-Jan Boonstra (ASTRON)
Gregory Hellbourg (CSIRO)
David Le Vine (NASA)
Amit Kuma Mishra (UCT)
Richard Prestage (NRAO)
Elena Daganzo-Eusebio (ESA)
Brian Jeffs (BYU)
Harvey Liszt (IUCAF, NRAO)
Sidharth Misra (JPL-NASA, IEEE-GRSS)
Hannah Rothkaehl (CBK)

Local Organizing Committee:

Lori Appel (NRAO)
Rick Perley (NRAO)

James C. Lin
University of Illinois at Chicago
851 South Morgan Street, M/C 154
Chicago, IL 60607-7053 USA
E-mail: lin@uic.edu

Minimally Invasive Transcranial Magnetic Stimulation (TMS) Treatment For Major Depression

The brain may be seen as an electronic network made of neurons and their connections. The structure of a neuron consists of both higher conducting "passive" membranes, and an "active" component of trans-membrane voltage mediated by intra- and extra-cellular ion concentrations in a water milieu. Higher conducting neuronal membranes maintain a voltage of about −60 mV to −70 mV when the cell is in its resting state. Any changes in voltage are facilitated by trans-membrane flow of electrically charged ions, which are mostly potassium, sodium, chloride, and calcium. Firings of excitable neurons are modulated by repetitive discharges. Electromagnetic fields of different frequencies, strengths, and waveforms could affect neurological systems by induced-current or direct-field effects on ionic flows and molecular interactions, resulting in neural excitation in the brain.

Transcranial magnetic stimulation (TMS) is a minimally invasive (or noninvasive) treatment procedure that uses transient, high-strength, pulsed magnetic fields to stimulate nerve cells in the brain to improve symptoms of depression or other psychiatric diseases resistant to drug therapy. Currently, TMS is typically used when common depression drug treatments are ineffective – especially for major depressive disorders [1, 2].

The first demonstration of TMS involving the motor cortex in the human brain took place in 1985 [3]. A high-strength, transient electric current is passed through a single, circular coil positioned over the head of a human subject. The coil generates a brief, time-varying magnetic field, which induces an eddy-current pulse and associated electric field in the underlying brain tissue by Faraday's law of electromagnetic induction. This electric field causes central system neurons to depolarize, which leads to muscular action potentials with identifiable amplitudes, conduction velocities, and latencies, as well as motor muscular responses in the human body. The specific location and extent of induced electric fields resulting in neuronal excitation differ according to the positioning of the TMS coil on the head.

However, a relatively large region of the brain is affected by the wide, induced electric field of a single coil. The figure-eight coil was introduced to give rise to more focused (~ mm in size) induced electric fields [4]. The peak electric field in the brain induced by a pair of opposing currents flowing through a figure-eight coil occurs directly under the coil's center: the crossover point of two circular coils.

Besides electric currents, coil shape, winding geometry, and the distance of the coil from the scalp can all affect the resultant induced fields that evoke responses from neural substrates. Indeed, as expected, biological parameters such as skin, fat, and skull thickness, along with neural-tissue types, geometry, and structure will also impact the location and extent of induced fields, and TMS treatment outcome.

Repetitive TMS, or rTMS, applied to treat depression involves delivering repetitive magnetic pulses.

The procedure uses repetitive stimulations at different frequencies to modulate cortical brain activity.

In October 2008, rTMS was first approved for clinical practice by the US Food and Drug Administration (FDA) as a treatment for major depression for patients who have not responded to antidepressant medication. It is also currently used in other countries as a treatment for drug-resistant depression. The FDA guidelines for rTMS were updated in 2011 [5].

Current evidence suggests that major depression is associated with prefrontal cortex asymmetry: relative hypoactivity in the left dorsolateral prefrontal cortex of the brain, and relative hyperactivity in the right dorsolateral prefrontal cortex. The clinical efficacy of rTMS is related to either high-frequency stimulation of the left prefrontal cortex, or low-frequency inhibition of the right prefrontal cortex in major depressive disorder, which, in addition to prefrontal cortex, involves cingulate gyrus, amygdala, ventral striatum, and medial thalamus. These regions are known to control executive functioning and mood regulation. High-frequency rTMS stimulation increases cortical excitability, while low-frequency stimulation is inhibitory.

During a typical 30- to 60-minute rTMS treatment session, a figure-eight coil is placed against the scalp, near the forehead. The coil delivers a pulsed magnetic field that stimulates target nerve cells to a typical depth of 1.5 cm to 2.5 cm in the frontal cortex region of the brain. The procedure is painless, and does not require anesthesia. It is efficacious and safe when recommended protocols are followed in the acute or serial treatment of major depression [6].

A study of rTMS practice in 42 clinical settings indicated that rTMS is an effective treatment for drug-resistant depressions [7]. Among 42 clinical sites, which were all located in the United States, 32 (76%) were private clinical practices, seven (17%) were academic medical centers, and three (7%) were nonacademic institutional settings. The study involved 307 outpatients with major depressive disorder diagnoses, and who had persistent symptoms despite antidepressant pharmacotherapy. Patients had a mean age of 48.6 years (SD: 14.2 years; range 18 to 90 years), and 205 patients (66.8%) were female. Treatments were delivered using the same rTMS therapy system and standard treatment protocol: pulse frequency of 10 Hz; stimulation at 120% of motor threshold; and a cycle of 4 sec on (active stimulation) and 26 sec off (no stimulation). The TMS system provided default parameters that generated 75 stimulation cycles, resulting in 3,000 pulses per treatment session.

Outcome assessments were obtained at baseline, two weeks, at point of maximal treatment benefit, and again at six weeks in cases where the course of rTMS extended beyond six weeks. Efficacy measures included clinician-reported Clinical Global Impressions-Severity of Illness Scale (CGI-S), and patient-reported Inventory of Depressive Symptoms-Self Report version (IDS-SR), and the 9-Item Patient Health Questionnaire (PHQ-9).

The primary-outcome measure was the change from baseline to endpoint on the CGI-S. Secondary outcome measures included baseline-to-endpoint change on the PHQ-9 and IDS-SR scales. For the CGI-S, response was defined as achieving an endpoint rating of 3 or less (corresponding with "mildly ill" or better), whereas remission on that scale was defined as achieving an endpoint rating of "borderline mentally ill" or "normal/not at all ill." For the PHQ-9, response was defined as achieving an endpoint score less than 10, whereas remission was defined as achieving an endpoint score less than 5. Finally, for the IDS-SR, response was defined as achieving a 50% or greater drop in endpoint score compared to the patient's baseline rating, whereas remission was defined as an endpoint score of less than 15.

The average number of rTMS sessions was 28.3 (SD: 10.1, range: 2 to 94), corresponding to an average duration of treatment of 42 days (SD: 14.2, range: 2 to 130) per patient. 280 (91.2%) patients received treatment over the left dorsolateral prefrontal cortex only. The average number of pulses per session was 3,216 (SD: 466).

Results showed a significant change in CGI-S from baseline to end of treatment. Clinician-assessed response rate (CGI-S) was 58.0%, and remission rate was 37.1%. Patient-reported response rate ranged from 56.4% to 41.5%, and remission rate ranged from 28.7% to 26.5% for PHQ-9 and IDS-SR, respectively.

It is noted that there was one medical event, which was related to the device. A generalized tonic-clonic seizure (formerly known as a *grand mal seizure*) occurred in a female patient during her 10th rTMS treatment session. The patient had no prior history of seizure; however, she had several clinical factors that may have contributed to altering her seizure threshold. The patient recovered fully from the event without neurologic sequelae. Seizure is thus a known, but rare, medical risk associated with rTMS. The estimated risk of seizure is approximately 0.003% per treatment exposure, and <0.1% per treatment course.

References

1. J. C. Lee, D. B. Blumberger, P. B. Fitzgerald, Z. J. Daskalakis, and A. J. Levinson, "The Role of Transcranial Magnetic Stimulation in Treatment-Resistant Depression: A Review," *Current Pharmaceutical Design*, **18**, 36, 2012, pp. 5846-5852.

2. K. A. Johnson, M. Baig, D. Ramsey, S. H. Lisanby, D. Avery, W. M. McDonald, X. B. Li, E. R. Bernhardt, D. R. Haynor, P. E. Holtzheimer, III, H. A. Sackeim, M. S. George, and Z. Nahas, "Prefrontal rTMS for Treating Depression: Location and Intensity Results from the OPT-TMA Multi-Site Clinical Trial," *Brain Stimulation*, **6**, 2, 2013, pp. 108-117.

3. A. T. Barker, R. Jalinous, and I. L. Freeston, "Non-Invasive Magnetic Stimulation of Human Motor Cortex," *Lancet*, **1**, 8437, 1985, pp. 1106-1107.

4. S. Ueno, T. Tashiro, and K. Harada, "Localized Stimulation of Neural Tissue in the Brain by Means of a Paired Configuration of Time-Varying Electric Fields," *J. Appl. Phys.*, **64**, 10, 1988, pp. 5862-5864.

5. FDA, "Guidance for Industry and FDA Staff – Class II Special Controls Guidance Document: Repetitive Transcranial Magnetic Stimulation (rTMS) Systems," Bethesda, MD, **July 26, 2011;** http://www.fda.gov/RegulatoryInformation/Guidances/ucm265269.htm#2.

6. J. P. O'Reardon, H. B. Solvason, P. G. Janicak, S. Sampson, K. E. Isenberg, Z. Nahas, W. M. McDonald, D. Avery, P. B. Fitzgerald, C. Loo, M. A. Demitrack, M. S. George, and H. A. Sackeim, "Efficacy and Safety of Transcranial Magnetic Stimulation in the Acute Treatment of Major Depression: A Multisite Randomized Controlled Trial," *Biol. Psychiatry.*, **62**, 11, 2007, pp. 1208-1216.

7. L. L. Carpenter, P. G. Janicak, S. T. Aaronson, T. Boyadjis, D. G. Brock, I. A. Cook, D. L. Dunner, K. Lanocha, H. B. Solvason, and M. A. Demitrack, "Transcranial Magnetic Stimulation (TMS) for Major Depression: A Multisite, Naturalistic, Observational Study of Acute Treatment Outcomes in Clinical Practice," *Depress. Anxiety*, **29**, 2012, pp. 587-596.

Please note that the URSI Secretariat

has moved to a new address

since15 March 2016:

URSI Secretariat
Ghent University - INTEC
Technologiepark-Zwijnaarde 15
B-9052 Gent
BELGIUM

The telephone and fax number remain the same :
Tel. : +32 9-264 3320
Fax: +32 9-264 4288

Early Career Representative Column

Stefan J. Wijnholds
Netherlands Institute for Radio Astronomy
Oude Hoogeveensedijk 4
7991 PD Dwingeloo, The Netherlands
E-mail: wijnholds@astron.nl

Introduction by the Associate Editor

Like many other researchers, I can still remember the euphoric feelings after receiving the acceptance notification for my first journal article. I also remember the large amount of time invested in finding out how academic publishing works, in practice. Every university graduate probably has a global idea of how academic publishing works, but there are many details involved that are usually not part of that global picture, such as the scope of a journal, the actors involved in the reviewing process, efficient ways of dealing with reviewer comments, etc. A proper understanding of such details can save time and can increase the chances of getting a paper accepted. I am very grateful to Ross Stone. He pointed me to a recent column he and Levent Sevgi wrote on academic publishing in the *IEEE Antennas and Propagation Magazine*, and he suggested taking that column as a starting point for this column on the academic-publishing process. I would also like to thank Phil Wilkinson, Editor-in-Chief of the URSI-logo journal *Radio Science*, for adding specific details for the *Radio Science* journal.

Readers who have also read the original *Antennas and Propagation Magazine* column may notice that we have reduced the scope to the process of academic publishing, leaving out the material on the ethical issues involved. These ethical issues are important matters that we plan to address in a future column.

One of the ideas that was brought up while brainstorming about the contents of this ECR column was the possibility of including short announcements for events that are of particular interest to young scientists. If you are organizing such an event, please let me know. The same holds for any idea that you may have for URSI to reach out to early-stage researchers. I am looking forward to your suggestions!

The Academic Publishing Process: From Manuscript to Publication

W. Ross Stone[1], Stefan J. Wijnholds[2], and Phil Wilkinson[3]

[1]Stoneware Ltd.
840 Armada Terrace
San Diego, CA 92106 USA
E-mail: r.stone@ieee.org

[2]Netherlands Institute for Radio Astronomy
Oude Hoogeveensedijk 4
7991 PD Dwingeloo, The Netherlands
E-mail: wijnholds@astron.nl

[3]Past President of URSI
Editor-in-Chief, *Radio Science*
E-mail: phil_wilkinson@internode.on.net

Abstract

This paper presents an overview of the process of academic and scientific publishing, using the URSI-logo journal *Radio Science* as a specific example. The intent is to provide a brief tutorial for those new to academic publishing. The importance of a publication's scope is explained. The steps in the publication process are described in detail, along with the roles of the Editor-in-Chief, Associate Editors, reviewers, and authors.

1. Introduction

The purpose of this column is to provide an overview of the academic and scientific publication process in general terms, specifically tailored towards people who are new to academic publishing. This column is an adaptation from a similar column that recently appeared in the *IEEE Antennas and Propagation Magazine* [1]. We will use the URSI-logo journal *Radio Science* as a concrete example of a specific implementation of the general process, which is very similar for many scientific journals. Most of the comments also apply to the URSI *Radio Science Bulletin*.

2. Basic Concepts

2.1 Publication Types

Radio Science is a *peer-reviewed* scholarly journal. This means that the technical material in *Radio Science* has been critically reviewed by at least one (usually three) independent subject-matter experts before being accepted for publication (see the discussion of the peer-review process, below). Journals typically publish technical papers reporting new results, usually with a relatively narrow focus. In what follows, the term "paper" and "article" will be used interchangeably to describe what journals publish.

Radio Science measures the length of a paper in publishing units (PU). This will be discussed in more detail in the section on publishing models and page charges. Other journals, such as IEEE *Transactions*, measure the length of the paper in the number of printed pages. Many journals impose a restriction on the maximum length of a paper. This can be a hard limit or a soft limit. In the first case, articles longer than the imposed limit will simply be rejected for that reason. In the case of a soft limit, the author should declare that he or she is willing to pay charges for the excess length. These limits are quite useful, as they encourage brevity. If you find yourself struggling with the length constraint, it is usually a good idea to critically review the scope of your manuscript, and to check whether it is well focused towards its key points. On most occasions, the subject matter of a well-focused manuscript will fit within the constraints imposed by most journals.

Besides journal papers, *Radio Science* publishes *comments* (other journals may use different names, e.g., *correspondence* or *letters (to the editor)*). These are shorter papers, typically with a narrower scope than a regular paper. Comments typically expand on a previously published result, or comment on (or reply to comments on) other published material.

Some journals, such as the *IEEE Signal Processing Letters*, specialize in the rapid publication of shorter papers,

typically with a maximum length of four pages. There are also journals that specialize in review papers, or publications that not only contain peer-reviewed technical content, but also contain non-peer-reviewed material of general interest to their intended audience. The *Radio Science Bulletin* is an example of the latter.

2.2 The Importance of a Publication's Scope

Each publication has a statement of its scope. This is a very important tool for both the publication and for potential authors. The scope specifies the technical field that articles in the publication must cover. The scope of a publication is important for authors, because it provides guidance to an author regarding whether the topic of an author's paper is appropriate for the publication. The publication's scope usually also gives guidance regarding the types of articles a publication will accept. One of the biggest problems Editors-in-Chief (EiCs) have is receiving articles that are out of scope for their publication. For some journals, it is not unusual for as many as 10% of the submissions received by a publication to be out of scope.

In the case of *Radio Science*, all submissions pass through a quality-control stage that includes a check on all authors, paper formatting, and a pass through Crosscheck to identify recycled text and potential evidence of plagiarism. Submissions that satisfy this level are passed to the EiC, who provides further screening of articles to verify that the subject and contents of the article fit within the scope of *Radio Science*, and that the article is comprehensible (in other words, not so poorly written that it is unreadable).

If these criteria are not met, the EiC may reject the paper without review. It is incumbent on authors to be sure that their submission falls within the scope of the publication. If uncertain, an author may contact the EiC of a publication before submitting an article to check to see if both the scope and type of article being considered for submission are appropriate.

3. Publishing Process

This section will review the process typically followed in processing a paper, from submission to publication. While the process described is typical for most publications, there are variations. Authors are urged to consult the Web pages for the publication to which they are considering submitting a paper in order to gain an understanding of the process used by that publication. *Radio Science* is a publication of the American Geophysical Union (AGU), so for *Radio Science* (and other AGU journals), this can be found on the AGU Web page under "publications." The following subsections trace the processing of the paper in chronological order.

3.1 Paper Submission

As discussed in Section 2.2, it is very important for an author to be sure that a paper falls within the scope of the publication to which it is submitted. If it doesn't, the paper is likely to be rejected before ever being sent for review. If the paper is other than a "standard" submission for the publication, it is wise to check with the publication's Editor-in-Chief before submitting the paper to see if it is appropriate to submit the paper. Examples might include tutorials, reviews, and papers that are unusually long. It is important to understand what audience a publication is trying to reach, and to make sure that the article being submitted is appropriate for the audience of the publication to which it is submitted.

Radio Science uses the submission system of the AGU, a Web-based paper-submission system, called GEMS. This system will accept papers in a variety of common file formats. *Radio Science* provides both *Word* and *LaTeX* templates to help authors preparing their manuscript in following the *Radio Science* style guidelines. These templates are available in the AGU author resource center at http://publications.agu.org/author-resource-center. This includes templates for preparing articles using *Word* and *LaTeX*, information on the style used in *Radio Science*, help with editing, and formats for references. There is extensive information on how to provide figures and graphics for articles.

Once the article has been prepared, it is submitted via an online submission system. Very few journals accept submissions via e-mail (the *Radio Science Bulletin* is an example of one journal that does accept submissions via e-mail). The online submission process typically involves uploading the manuscript file for the article, and answering a series of questions. These questions typically include assurances on the part of the author that policies related to duplicate submission and publication, plagiarism, conflict of interest, data availability, and authorship have been followed.

3.1.1 Importance of Abstracts and Keywords

Two important elements that are requested as part of the submission process are an abstract for the article and a series of keywords. These may not seem very important. It turns out that they can be critical to the future success of getting an article found by researchers, and getting it read (and therefore, getting the article cited).

In this day of digital libraries, articles are found by using search engines. While some digital libraries support full-text searching of articles, the default searching mode uses index terms. Most of the other major scientific indices (e.g., INSPEC, *Ei Compendex) also index the abstracts*

of articles, and use keywords to aid searching. A good abstract and the right keywords can (and often do) make the difference between a highly read and cited article, and one that is rarely found. An author who wants to have his or her work cited and used will spend at least as much time preparing a good abstract as writing the introduction and conclusions to the paper. Again, the likelihood of others reading and citing your work may well depend on the choice of good keywords to describe the article.

In addition to keywords, *Radio Science* asks for a list of up to three key points made in the article. These key points are very brief sentences (100 characters) that should highlight the most-important results from the paper. Besides their role in the indexing process for digital libraries, these keywords and key points also play a crucial role in the assignment of an appropriate Associate Editor by the Editor-in-Chief, as well as assisting the Associate Editor in finding additional independent reviewers for the paper.

3.2 The Role of the Associate Editor and the Review Process

Submitted articles typically undergo a prescreening process. This was described in Section 2.2. If the article passes the prescreening process, it is usually assigned to an Associate Editor. The Associate Editors typically report to the Editor-in-Chief (in the case of *Radio Science*, the Associate Editors typically report to an Editor, who in turn reports to the Editor-in-Chief). Each Associate Editor deals with a separate technical area under the scope of the publication. The Associate Editor assigns the article to reviewers, and monitors the progress of the reviewing process.

In the case of an article with multiple authors, one author serves as the corresponding author. It is the responsibility of this corresponding author to handle all correspondence with the publication, and to also keep all of the other authors of the article informed of all correspondence. The corresponding author should receive a prompt acknowledgment of the receipt of the submission.

An article submitted to a peer-reviewed journal will be reviewed by at least one subject-matter expert (and almost all peer-reviewed journals require a minimum of two such reviews). In the case of *Radio Science*, Associate Editors typically strive to have each paper reviewed by three experts. This is commonly done either to insure that at least two reviews are received in a timely fashion, and/or that there are sufficient reviews to allow a decision on the paper to be easily made. The Associate Editor combines the reviewers' comments with his or her own judgment, and makes a recommendation to the Editor-in-Chief regarding a decision on the article. The Editor-in-Chief makes the final decision, and transmits that decision and the comments of the reviewers and the Associate Editor to the author.

Most publications allow several possible categories of outcome to the reviewing process. In the case of *Radio Science*, these categories are:

- Publish in the present form: the article is accepted without any requirement for revision, and will appear on the *Radio Science* Web site as a published paper. This is extremely rare in most publications upon first submission. It is unusual for less than a few percent of all articles submitted to ever be accepted "as submitted."

- Return to the author for minor revisions: the reviewers have recommended modifications that are straightforward and do not involve significant technical issues. The Editor-in-Chief may indicate whether adequately making the recommended modifications will likely result in the article being accepted for publication, or if additional review will be required. Authors are expected to provide a revised manuscript within 21 days.

- Return to the author for major revisions: the reviewers have identified significant problems with the article. These can be technical issues, problems with the organization and writing of the article, or both. Again, the Editor-in-Chief will indicate whether additional review will be required after the recommended modifications are made, but in most cases where major revisions are asked for, additional review is needed. Authors are expected to provide a revised manuscript within 45 days.

- Reject and encourage resubmission: as with "return to authors for major revisions," the reviewers have identified a number of significant issues. In this case, it is the judgment of the EiC that the required revisions are of such substantial nature that it will be hard for the authors to make such a revision within a reasonable timeframe allowed for the submission of the revised version.

- Reject: the paper is unlikely to be suitable for publication even after possible revisions are made. For example, this may be because the ideas presented in the paper are not sufficiently novel, or because of fundamental technical errors.

Most journals have a similar range of acceptance/rejection categories. Rapid-publication journals, such as letters journals, may use different (typically fewer) categories to facilitate a rapid-publication process.

In the broadest sense, most publications review articles based on three criteria: quality, novelty, and significance. Quality involves both technical quality (the material has to be technically correct) and quality of presentation (the material has to be understandable and adequately well presented). Novelty is a requirement that the material be new: it should not repeat what is already in the literature.

Significance implies that the results reported should be of value and importance to the field. The weightings of these three factors may differ among different journals. For example, review journals may not weight novelty as heavily as a journal that reports the latest results in the same field.

3.2.1 Single-Blind and Double-Blind Review

Most publications employ single-blind review: the identities and affiliations of the reviewers are kept from the authors of the article, but the identities and affiliations of the authors of the article are known to the reviewers and the editors. *Radio Science* and the *Radio Science Bulletin* use single-blind review processes. The reviewers remain anonymous to authors, unless the reviewer chooses to waive anonymity. Some publications employ double-blind review, in which the authors' identities and affiliations also remain hidden until after the final acceptance or rejection decision has been made. Some publications allow double-blind review to be requested by submitting authors (the *Radio Science Bulletin* will accommodate such requests).

Snodgrass [2] has provided a thoughtful analysis and comparison of these two reviewing methods. His conclusions and those in the references he cites make a rather strong case that double-blind reviewing removes several potential biases from the process, including biases related to gender, and related to prominence or publishing history in the field.

It should also be noted that upon submission, *Radio Science* and the *Radio Science Bulletin* allow authors to request specific persons to be excluded as reviewers or editors for the submitted paper. *Radio Science* also asks authors to suggest potential reviewers. Experience has shown that authors typically provide very good reviewer suggestions.

3.3 The Role of the Editor-in-Chief

Note that in the above description of the review process, it was the Editor-in-Chief who made the final decision regarding the disposition of the article. However, the degree to which the Editor-in-Chief becomes involved with a particular article can vary among publications, and among articles within a given publication. For publications with a very large number of articles, the Editor-in-Chief must heavily rely on the recommendations of the Associate Editors. For such publications, the Editor-in-Chief may only take the time to carefully look at an article when there is a significant disagreement among the reviewers of an article, or when the Associate Editor asks for more involvement – or when an author appeals a decision.

One of the measures of the quality of an Editor-in-Chief is how he or she handles situations in which reviewers (and/or reviewers and an Associate Editor) are not in agreement as to what should be done with an article. The key issues here are the willingness and ability of the Editor-in-Chief to become directly involved (and sometimes, to make a difficult decision). In such cases of disagreement, an Editor-in-Chief needs to first assess whether he or she is technically competent to decide among the differing opinions presented by the reviewers and/or the Associate Editor. If so, then it is the responsibility of the Editor-in-Chief to read the article and make a decision. That may involve overruling reviewers and/or an Associate Editor. If the Editor-in-Chief does not feel technically competent to make such a decision without additional help, then it is incumbent on the Editor-in-Chief to independently obtain additional input from one or more competent reviewers to resolve the issue.

Interestingly, if an Editor-in-Chief gets directly involved in such situations, makes a decision based on specific criteria, and communicates those criteria to the author, there usually are no significant problems. Authors may disagree with the result, but if the criteria are reasonable, it is hard to disagree with the fairness of the process. In contrast, problems almost always arise when an Editor-in-Chief does not become involved in such situations. The result is that a decision is made where there obviously are conflicting criteria, and such a decision is likely to appear arbitrary to the author. That rarely is interpreted as a fair process by an author. Problems also often arise when the reasons for a decision are not fully and clearly communicated to an author.

3.4 Revisions, Acceptance, and Rejection

If an article isn't immediately accepted or rejected, some level of revision is almost certainly required. Reviewers are usually reasonably specific regarding what revisions they feel are needed (and a good Associate Editor or Editor-in-Chief will ask a reviewer to be specific, if that is needed).

The manuscript, together with the reviewers' comments, is passed back to the authors, who are expected to take these suggestions into account and prepare a new version of their paper. It is now common practice, and expected by *Radio Science*, for authors to provide a detailed response to all comments on their paper when submitting their revised text. They also need to demonstrate that their responses have indeed affected the revised text by providing a highlighted copy of the paper. Incidentally, preparation of this rebuttal is made harder by the recent tendency for some reviewers to annotate an electronic version of the paper but not provide a covering review. This highlights the tension between the Associate Editor's task of identifying reviewers for papers and securing good reviews and the workloads this imposes on reliable reviewers.

If the authors agree with the suggested revisions, then the article can be revised, and the next important step is resubmitting the revised article. If the authors do not agree with a suggested revision, they will need to be very specific in explaining why they are refusing to make the revision. If what has been suggested is technically incorrect, then this may be straightforward. If what has been suggested involves adding or removing material, reorganizing or clarifying the text, or performing additional work to support the claims made in the article, the authors probably need to give careful consideration to what has been requested. At least two independent authorities (a reviewer and the Associate Editor) have agreed that the request is needed. It is unlikely that a refusal to respond to the request will be readily accepted, no matter how good a justification is provided by the authors. The authors may need to consider deciding between responding to the request and submitting the article to another publication.

3.4.1 Two Keys to Getting a Paper Accepted

When responding to reviews with a revised paper, there are two key steps authors can take that in many instances and with most editors will significantly increase the likelihood of the revised paper being accepted. These involve making it easy to evaluate the revisions, and making sure that the requested revisions are actually included in the paper.

When a revised version of the article is submitted, it is a good idea to make it very easy for the Associate Editor to understand what revisions were made, and how they relate to the revisions that were requested. One of the best ways to do this is to provide a list. Each item in the list should be one of the quoted specific requests from a reviewer. Following each item should be an explanation of what change was made to the article to respond to the request, including the quoted revised text. This makes it extremely easy and quite quick for an Associate Editor to verify that the reviewers' requests have been addressed. This is far better than forcing an Associate Editor to compare original and revised versions of a manuscript to determine what changes have been made, even if a description of those changes is provided.

It is much more likely that an article will be accepted if an Associate Editor can easily verify that all of the changes requested by the reviewers have been made by going down a list such as this. In some cases, this may even allow the Associate Editor to avoid the need for additional review.

A second key factor is to insure that the responses to the reviewers' comments are actually included in the revised article. It is not uncommon for authors to provide quite good responses to reviewers' suggestions in the material provided with a revised article, but to fail to actually include the responses in the article. Apparently, in such cases the authors feel that providing the response to the Associate Editor is sufficient. That rarely is true. If the reviewer had the question or concern, readers are likely to have the same question or concern, and the response should be incorporated into the revised article.

3.4.2 Subsequent Review and Acceptance or Rejection

Hopefully, the revised article will be accepted for publication. If it is not, it may be sent out for additional review. If the scope of the additional review is limited to the issues raised in the initial review and any changes made to the article, and if the same reviewers are used as were used in the initial review, that is fine. However, sometimes either different reviewers are used – often because some reviewers are unavailable for later revisions – or reviewers decide to expand the scope of their reviews beyond what they were concerned about in the initial review. There is nothing fundamentally wrong about this. Unfortunately, it can result in an iterative situation in which authors are repeatedly asked to address new issues with each round of revision and review, and the process fails to converge. That is unfair to the authors, the reviewers, and the editors, although it may also be indicative of a fundamental problem with the paper (e.g., due to grammar and presentation problems it is ambiguous). Whatever the reason, it is best if the editors involved can use the same reviewers wherever possible, and limit the scope to the same issues as were raised in the initial review. This may require the Associate Editor to become directly involved in evaluating whether a revision has adequately addressed a reviewer's concerns. That is better than a non-converging iterative process.

If the review of the revised article results in recommendations for additional changes, the Associate Editor and Editor-in-Chief have to decide if such changes are likely to result in an article that can be published, or if the article should be rejected. Most publications have a limit on the number of cycles of revision and review that will be permitted for an article. If that limit is exceeded, the article is rejected. If the authors resubmit the article, it is treated as a new submission (and this may well mean that it will be reviewed by a new set of reviewers). In principle, *Radio Science* does not have a limit on the number of revisions it may ask authors to provide. In practice, it is unusual to have more than three or four iterations. Often, the last iterations may be rapidly handled, as they involve minor changes that save authors from adding changes at the proofing stage of publication.

If an article is rejected, there generally is little opportunity for appeal, unless the authors believe that some bias or impropriety was involved in the process. From a practical standpoint, once an article has been rejected by a publication, it is usually best to try to address the issues that were the basis for the rejection, and find a different publication to which to submit the article.

3.5 Final Submission

Once an article is accepted for publication, the final version of the manuscript has to be submitted. The author tools discussed in Section 3.1 should be used. In particular, it is very important to follow the style guidelines and citation and reference formats for the particular publication in which the article will appear. Careful attention should also be given to the preparation of figures and equations in articles.

One of the most-common mistakes authors make is to fail to use a sufficiently large font in labeling the axes and other data on plots and other figures. The best way to avoid this is to print a copy of the figure at the size it would appear if printed, and measure the resultant size of any fonts. Figures are typically sized to be either one or two columns in width. With a figure adjusted to this size, for most publications the fonts used should be no smaller than 9 pt (9/72 in, or one-eighth inch, or 3.2 mm). The font size used in the figure should certainly be no smaller than the standard font size for body text in the journal in which the figure is to appear. Experience has shown that most people are rather poor at estimating font sizes: it is best to measure this.

Articles are typically submitted using the same submission system that is used for initial article submission, and for tracking reviews and revisions. When submission of an accepted article is made, the author will probably be asked several questions regarding the type of publishing model to be used, and various page charges.

When the EiC for *Radio Science* recommends that a paper be accepted without further change, the manuscript then appears on the *Radio Science* Web page in its current form, and a proof copy is generated. At this stage all authors will be requested to provide AGU with their ORCID, if they have not already done so. ORCIDs will now be *required* for all corresponding authors, and strongly encouraged for coauthors. AGU officially joined with seven other publishers in a commitment to include the ORCID (Open Researcher and Contributor ID) for authors of all papers published in 2016 (see statement: https://eos.org/agu-news/agu-opens-its-journals-to-author-identifiers). The IEEE will also require that all authors submitting papers to its journals include their ORCID by the end of 2016. The ORCID is a unique publisher-independent identification mechanism for authors that solves the author disambiguation problem. More information can be found at orcid.org.

3.5.1 Publishing Models and Page Charges

Different journals use different publishing models. Open-access journals make accepted papers available for free, i.e., potential readers do not need a subscription to the journal to get access to the full paper. The costs involved in running the publication are paid for by using publication or article-processing fees for the authors. Some journals use a hybrid open-access publishing model. This allows the author to choose whether his or her paper will appear as part of a subscription package, or will be available to all readers for free. If the subscription model is chosen, there may be no charge to the author. However, a reader may have to have a subscription in order to view and download the article.

If an author cannot afford to pay the article-processing fee, some journals have provisions under which a journal may waive the fee, if a request is made. However, this is usually only done where circumstances require that the article be published using an open-access model and the author does not have the resources to pay the article-processing fee. *Radio Science* does not require an author to make any decision on this until the paper has been accepted for publication.

Whether a subscription or open-access model of publishing is chosen, an author may also be asked to pay some or all of three types of page charges: voluntary, mandatory over-length, and color.

Voluntary page charges do not arise if an open-access model of publishing is chosen. Voluntary page charges are indeed voluntary: they are a per-page charge requested from authors to help offset the costs associated with processing and publishing the paper.

Mandatory over-length page charges are imposed if the published length of a paper exceeds a limit established by the publication. These charges serve at least two purposes: they help to encourage authors to limit papers to a desired maximum length, and they pay the costs associated with papers that would otherwise cause the publication to exceed its budgeted number of pages. Again, the amounts vary by publication, and are given in the same list with the voluntary page charges.

Color page charges are imposed by most publications when an author desires that material on a page appear in print in color. Note that these charges apply only to color in print. If the material appears in color in the online version and in black-and-white in the print version, there typically is no additional charge. The amounts for such charges are discussed in the Web site of the publication.

Radio Science uses a combination of mandatory fees and over-length charges. To determine the total charges, *Radio Science* measures the length of the paper in publishing units (PU). One PU corresponds to 500 words, one figure, or one table. An article containing 3700 words (including text, abstract, and figure captions only, excluding titles, author lists and affiliations, tables, and references), three figures, and one table will thus count as having twelve PUs. Authors of papers with a length of at most 25 PU are only charged the base publication fee of USD1000. Excess PUs are charged USD125 per PU. If the author(s) opt for

open-access publication, *Radio Science* charges USD3500. This open-access fee replaces the base publication fee, but not the over-length charges.

The *Radio Science Bulletin* is totally open access, and is unusual in that it does not charge any author-processing fees or over-length page charges. There are no charges to authors for publishing in the *Radio Science Bulletin*, and the issues are available for downloading from the URSI Web site without charge.

3.6 Proofing

Almost all publications edit accepted articles prior to publishing them. After editing and formatting, a proof copy in PDF format is sent to the author. The author typically has a few days in which to go through the proof and return any corrections. *It is very important that this proofreading step be carefully and thoroughly done*. While the people doing the editing have experience in editing technical material, they are usually not scientists or engineers, and they are usually not subject-matter experts in the field of the article. Changes that are made to correct problems with English can affect the technical meaning. Symbols and equations may not appear as they should after being formatted. Depending on the file format in which the original manuscript was provided by the author, it may be necessary for the publication to re-key all of the equations and symbols. The degree of accuracy with which that is done is amazingly high, but it is not perfect. Proofreading the proof copy of an article is a critical step, and it needs to be carefully done.

3.7 A Note About English

With very few exceptions, articles are to be written in English. English is not the first language for the majority of the world, although it arguably is the language shared most in common, at least in technical fields. Regardless, it is estimated that over half of the articles submitted to most technical journals published in English are written by authors for whom English is not the first language. Even where English is the first language of the author(s), many scientists and engineers are often lacking in English skills. The editing done by most publications helps with this, but it is intended primarily to correct basic issues of grammar, punctuation, and style. This editing usually cannot overcome problems with unclear meaning.

There are a number of English resources available to authors. There are also fee-based editing services that will perform several different levels of English editing on manuscripts. If English is not your first language and you cannot have your article proof-read by a native English speaker or another person who is proficient in English, it may actually improve the odds of having your paper accepted to have your paper edited prior to first submission. It is not uncommon for articles to be rejected in the pre-screening stage or by the reviewers for lack of clarity caused by poor command of the English language. AGU offers some English-language assistance suggestions along with their Advice to Authors.

3.8 Reprints and Posting

Once an article has been accepted, authors typically want to be able to start sharing the article with their technical community. The issue of author posting of accepted (and published) articles on the Web is tremendously complicated, and the policies of academic publishers are the topics of a great deal of controversy. The SHERPA/RoMEO Web site (http://www.sherpa.ac.uk/romeo/index.php) permits comparing posting policies for journals and publishers.

The AGU allows an author to

- To present the material orally;
- To reproduce figures, tables, and extracts, properly cited;
- To make paper copies of all or part of the contribution for classroom use;
- To deny subsequent commercial use of the contribution;
- To place the contribution or its abstract on his/her personal Web site.

The last usage requires some care, since *Radio Science* needs to be properly acknowledged. The precise format for such a proper citation is provided on the "Usage Permissions" page of the AGU Web site.

The *Radio Science Bulletin* allows non-commercial posting and presentation of published materials so long as proper citation, acknowledgment, and copyright statements are included.

Authors can order printed reprints of an article from most publications that publish in print. This tends to be rather expensive. Information on ordering reprints for *Radio Science* is available in the author tools mentioned above. Reprints are substantially more expensive if they are not ordered at approximately the time of final article submission.

3.9 A Final Comment About Timing

Most authors are very anxious to get their papers published. This can lead to authors querying editors about the status of their papers. If such a query is received when the paper is undergoing normal processing, that query will

only divert people from more productive work and will, at best, be irritating for all concerned. Irritating editors usually does not benefit authors. If such a query alerts the editor to something that has gone astray in the processing of the paper, then it is a useful query. Knowing when to send a query regarding a paper requires that the author have some idea of the timeline associated with the steps in publishing.

Authors submitting to *Radio Science* can check the status of their paper in their account in the online submission system. This system will automatically send reminders to Associate Editors and reviewers when a paper is waiting for an action from their side. *Radio Science* asks reviewers to complete their review within 21 days after they accept reviewing the paper. Over the last year, the median time between original submission and the first decision was about 60 days. This measure is composed of the quality-control stage, the time it takes the EiC and Associate Editors to assign papers to reviewers, the time it takes to secure three willing reviewers, the time the reviewers take to process the paper, and, finally, the time both Associate Editors and the EiC take to form their opinions about the outcome of these reviews.

Many publications post the statistics on the time to first decision (and in some cases, on the times to other steps in the process) on the publication's Web page. If the information isn't there, it may be useful to ask the production editor or editorial assistant for the average times when the article is first submitted. If an article has been under submission for a time significantly longer than the average time to first decision for the publication involved, then a polite query checking on the status may well be appropriate. Please remember, there will always be a tension between author enthusiasm and reviewer workloads. Also, at *Radio Science*, usually long before an author starts worrying about the time taken processing their paper, the *Radio Science* Editors' Assistant has been sending reminders to reviewers asking when they will complete their review, and to the Associate Editors and the EiC asking if there is sufficient information already collected to make a decision. Those of us who are familiar with their work certainly appreciate their efforts.

The *Radio Science Bulletin* asks that reviews be returned within 30 days. The current median time from submission to first decision is somewhat less than 60 days, although there is substantial variation.

If an editor asks for a response from an author by a certain time, the author should either meet that schedule, or at least provide an explanation as to why the schedule can't be met and an estimate of when the response will be provided. Ignoring such requests can mean that nothing happens on your paper until the editor finally hears from you, regardless of how long that may be.

4. Conclusions

This article has presented a brief tutorial on the major aspects of the academic-publishing process. Although we have presented this process in general terms, the URSI-logo journal *Radio Science* and the URSI journal *Radio Science Bulletin* were used as specific examples to illustrate specific steps in the process. The importance of a publication's scope was explained. The steps in the publishing process were described in detail, along with the roles of the Editor-in-Chief, Associate Editors, reviewers, and authors.

5. References

1. W. R. Stone and L. Sevgi, "Aspects of Academic Publishing," *IEEE Antennas and Propagation Magazine*, **57**, 6, December 2015, pp. 134-145.

2. R. T. Snodgrass, "Editorial: Single Versus Double-Blind Reviewing," *ACM Transactions on Database Systems*, **32**, 1, March 2007, pp. 1-29.

National Radio Science Meeting

The National Academies of SCIENCES · ENGINEERING · MEDICINE

◆ January 4-7, 2017 ◆ University of Colorado at Boulder
◆ Meeting website: www.nrsmboulder.org
◆ USNC-URSI website: www.usnc-ursi.org

This open scientific meeting is sponsored by the U.S. National Committee (USNC) of the International Union of Radio Science (URSI). The USNC-URSI is appointed by the National Academies of Sciences, Engineering and Medicine, and represents U.S. radio scientists in URSI. Through technical co-sponsorship of the meeting by the IEEE Antennas and Propagation Society, authors will have their choice of submitting one-page abstracts that are not archived on IEEE Xplore, or two-page summaries that are archived on IEEE Xplore. At least one author is required to register for each presented abstract or summary. Papers must be presented for their corresponding summaries to be archived on IEEE Xplore. Abstracts or summaries on any topic in the interest area of a Commission are welcome. Contact the appropriate USNC-URSI Commission Chair listed below or visit the meeting website for further information.

Meeting Plenary Highlights

(1) Electromagnetic Spectrum Coexistence and Codesign
Contacts: Gregory H. Huff (Commission C Chair), ghuff@tamu.edu
Charles Baylis (Commission E Chair), Charles_Baylis@baylor.edu

(2) Fast Radio Bursts and the Discovery of Missing Matter
Contact: David DeBoer (Commission J Chair), ddeboer@berkeley.edu

USNC-URSI Chair: David R. Jackson, (713) 743-4426, djackson@uh.edu
USNC-URSI Secretary: Sembiam Rengarajan, (818) 677-3571, srengarajan@csun.edu

COMMISSION A, Electromagnetic Metrology

Steven J. Weiss, (301) 394-1987,
steven.j.weiss14.civ@mail.mil

TOPICS

Antennas
Bioeffects and medical applications
EM-field metrology
EMC and EM pollution
Impulse radar
Interconnect and packaging
Materials
Microwave to submillimeter measurements/standards
Millimeter-wave and sub-mm wave communications
Noise
Planar structures and microstrip circuits
Quantum metrology and fundamental concepts
Time and frequency
Time domain metrology

COMMISSION B, Fields and Waves

John L. Volakis, (614) 292-5846, volakis@ece.osu.edu

TOPICS

Antenna arrays
Antenna theory, design and measurements
Cognitive radio
Complex media (metamaterials, bandgap structures, biological and geophysical media, and others)
Educational methods and tools
Electromagnetic interaction and coupling
Guided waves and waveguiding structures
High-frequency techniques
Inverse scattering and remote sensing
Microstrip and printed devices and antennas
Nano-electromagnetics
Nonlinear electromagnetics
Numerical methods (differential- and integral-equation based, hybrid and other techniques)
Propagation phenomena and effects
Rough surfaces and random media
Scattering
Theoretical electromagnetics
Transient fields, effects, and systems
Ultra-wideband electromagnetics
Wireless communications

COMMISSION C, Radio-communication Systems and Signal Processing

Gregory H. Huff, (979) 862-4161, ghuff@tamu.edu

TOPICS

Cognitive radio
Computational imaging and inverse methods
Distributed sensor networks
Physics-based signal processing
Radar systems
Radar target detection, localization, and tracking
Sensor array processing and calibration
Signal processing for radar remote sensing
Statistical signal processing of waves in random media
Synthetic aperture and space-time processing

COMMISSION D, Electronics and Photonics

Zoya Popovic, (303) 492-0374,
Zoya.Popovic@colorado.edu

TOPICS

Electronic devices, circuits, and applications
Photonic devices, circuits, and applications
Physics, materials, CAD, technology and reliability of electronic and photonic devices, in radio science and telecommunications
Wide bandgap materials

Abstract / Summary Submissions
and
Student Paper Competition Submissions
are due by
September 19, 2016
This is a FIRM DEADLINE!
Please visit *www.nrsmboulder.org*

COMMISSION E, Electromagnetic Environment and Interference

Charles Baylis, (254) 710-4306, Charles_Baylis@baylor.edu

TOPICS

Communication in the presence of noise
Effects of natural and intentional emissions on system performance
Electromagnetic compatibility in: computational electromagnetics, education, measurement technologies, standards, and radiation hazards
High-power electromagnetic effects of transients on electronic systems
Spectrum management and utilization

COMMISSION F, Wave Propagation and Remote Sensing

Michael H. Newkirk, (240) 228-6976, Michael.Newkirk@jhuapl.edu

TOPICS

Point-to-point propagation effects:
Measurements — *Mobile/fixed paths*
Propagation models — *Horizontal/slant paths*
Multipath/mitigation — *Surface/atmosphere interactions*
Land or water paths — *Numerical weather prediction*
Scattering/diffraction — *Dispersion/delay*
Indoor/outdoor links — *Natural/man-made structures*
Microwave remote sensing of the earth:
Atmospheric sensing — *Ocean and ice sensing*
Field campaigns — *Interferometry and SAR*
Subsurface sensing — *Scattering/diffraction*
Radiation and emission — *Propagation effects*
Urban environments — *Soil moisture & terrain*
Propagation and remote sensing in complex and random media

COMMISSION G, Ionospheric Radio and Propagation

Sigrid Close, (650) 725-2863, sigridc@stanford.edu

TOPICS

Ionospheric imaging
Ionospheric morphology
Ionospheric modeling and data assimilation
Meteoroids and orbital debris
Radar and radio techniques for ionospheric diagnostics
Space weather – radio effects
Transionospheric radio propagation and systems effects

COMMISSION H, Waves in Plasmas

Anatoly V. Streltsov, (386) 226-7137, streltsa@erau.edu

TOPICS

Chaos and turbulence in plasmas
Plasma instabilities
Spacecraft-plasma interactions
Solar/planetary-plasma interactions
Space as a research laboratory
Wave-wave and wave-particle interactions
Waves in space and laboratory plasmas

COMMISSION J, Radio Astronomy

David DeBoer, (510) 520-9077, ddeboer@berkeley.edu

TOPICS

CMB polarization
New telescopes, techniques and technology
Observatory reports
Planets
Timely technical tutorials

COMMISSION K, Electromagnetics in Biology and Medicine

Mahta Moghaddam, (213) 740-4712, mahta@usc.edu

TOPICS

Biological effects
Dosimetry and exposure assessment
Electromagnetic imaging and sensing applications
Human body interactions with antennas and other electromagnetic devices
Therapeutic, rehabilitative and other biomedical applications

ERNEST K. SMITH USNC-URSI STUDENT PAPER COMPETITION

Prizes will be awarded to three student papers. Awards will be made for First Prize in the amount of $1000, Second Prize at $750, and Third Prize at $500. The deadline for submission of ***full papers*** on the meeting website is ***September 19, 2016***. Please see *www.nrsmboulder.org* for additional information, or contact the Student Paper Chair, Prof. Erdem Topsakal, Dept. of ECE, Virginia Commonwealth University, etopsakal@vcu.edu. Student papers and awards will be presented at the Plenary Session on Thursday morning, January 5, 2017. Student Paper Competition participants will have the option of submitting their full papers for publication in a special section of the journal *Radio Science*.

ABSTRACT AND SUMMARY SUBMISSION

The organizers of this meeting require the use of electronic submission. Details and instructions may be found at the conference website, *www.nrsmboulder.org*. Authors may choose to submit to special sessions in addition to the general topics listed above. A list of special sessions will be available on the conference website. All abstracts or summaries must be submitted online by **Monday, September 19, 2016**. If you have any questions on abstract/summary submission or the technical program, please direct them to the USNC-URSI Secretary, Sembiam Rengarajan, at srengarajan@csun.edu. Abstracts must have a minimum of 250 words. You will not be able to submit an abstract that does not meet the minimum length requirements. After abstract or summary submission is complete, please note that registration is required to attend any session of the meeting or to present a paper. More information about USNC-URSI is available at *www.usnc-ursi.org*.

Questions about the conference: For questions concerning conference logistics, please contact: Christina Patarino, Phone: (303) 492-5151, Fax: (303) 492-5959, E-mail: christina.patarino@colorado.edu

Asta Pellinen-Wannberg
Umeå University, Department of Physics and
Swedish Institute of Space Physics
S-90187 Umeå, Sweden
Tel: +46 90 786 7492
E-mail: asta.pellinen-wannberg@umu.se

Introduction from the Associate Editor

This time, I present a contribution from Anthea Coster, PhD, Assistant Director for the Haystack Observatory at the Massachusetts Institute of Technology, and a Fellow of the Institute of Navigation.

I met Anthea for the first time some 15 years ago, while visiting the Haystack Observatory. After that, we have met at various URSI meetings around the world. In addition to her various involvements in radio science, radars, and GPS systems, I was impressed by her travels to Africa for teaching space-weather issues to students in Rwanda. I later understood that she had received this kind of dedication from her heritage, since her grandfather was involved in helping Lise Meitner in leaving Germany in the late 1930s. You can read below about her path through her research in her own words.

Reflections on a Career in Radio Science

Anthea Coster

Haystack Observatory
Massachusetts Institute of Technology
Route 40, Westford, MA 01469, USA
Tel: +1 (781) 981-5753
E-mail: acoster@haystack.mit.edu

It has been almost 40 years since I started graduate school in Space Physics and Astronomy at Rice University, which I count as the beginning of my career. At the time, I never would have imagined that I would complete my PhD doing research in Puerto Rico at the Arecibo Observatory. I also never imagined that I would move to Boston and work at MIT for 30-plus years, first in the space surveillance group at Lincoln Laboratory, and later in the atmospheric science group at the MIT Haystack Observatory. Along the way, I have deployed radars in St. Croix and Guadeloupe, launched radiosondes from the Haystack parking lot, deployed Global Navigation Satellite System (GNSS) receivers in Alaska, installed an ionospheric calibration system in Florida, collected GNSS data with cell phones in Brazil, and taught space-weather classes to students in Zambia and Rwanda. When I began my studies at Rice, I envisioned none of the above. Nevertheless, by the time I started at Rice, I was convinced that I had found where I belonged.

I did not start out with the plan of studying radio science, although some of my earliest memories are of sitting in front of the radio that my father built, with its different-colored glowing tubes. My father had learned to build radios during WWII using parts bought off the black market, and, being Dutch, arranged to power them with bicycles. He was a geophysicist, and throughout my childhood, he always encouraged me to take math and science.

I grew up in Texas and attended the University of Texas at Austin, where I majored in mathematics, within a liberal-arts honors program there. Most of my friends in the honors program had plans to become lawyers or doctors. For the majority of my time at UT Austin, I was very uncertain about what lay ahead for me. At the time, there were very few female role models. In fact, I had no female mathematics or science professors during my entire time at university, both as a graduate and as an undergraduate student. The majority of students in my math classes were also male. However, perhaps because there were so few of us, I did form lasting friendships with several women in my math and science classes. We supported each other by being study buddies, working through homework sets together, studying for exams, and offering each other support and friendship. As a group these women have all gone on to fulfilling careers: several are now university professors, one became an astronaut, and another a managing director and senior portfolio manager at Prudential. Most of them also managed the balancing act of motherhood and career. So, the first piece of advice I have for any student, male or female, is to reach out and find other students who can support you and help you along the way.

While at the University of Texas, I had a strong preference for applied mathematics courses. As these were the math courses required for engineering, one would have thought that studying engineering might have been suggested to me. Yet, in the early 1970s at the University of Texas – which at the time had a student population of over 40,000 students – there were only a handful of women students in the engineering school (I believe the number was about five). I wish I had saved the letter that the engineering department sent me in response to my inquiries about transferring into their program. To say the tone of the letter was discouraging was an understatement. Engineering in those days was deemed too hard and too demanding a major for women students. At the end of my undergraduate studies, I took time off to work. This was primarily because I did not see a path ahead.

I accepted a position at an oil company in downtown Houston, and quickly realized that the engineers were being paid twice the salary I was. Within six months, while working, I started taking physics and computer science courses at night at the University of Houston. It was the physics course that started the wheels spinning for me. My University of Houston physics professor told me about the Rice University Space Physics program, and encouraged me to consider it. For me, those words of encouragement came at a critical time. As fate would have it, during my second year of taking physics courses at night, I met a professor from the Rice Space Physics Department on a plane to Washington DC. This was just luck, or perhaps fate. Nevertheless, by the end of the flight, he encouraged me to apply to their graduate program that year, even though I had not finished the undergraduate physics curriculum. I did apply, and I was accepted, and I started graduate school in the Fall of 1977. Later that year, I applied and was accepted by Prof. W. E. Gordon, the founder of the Arecibo Observatory, as one of his graduate students. I spent my first summer at Arecibo in 1978. My graduate research was in ionospheric heating, and I analyzed data from a 50 MHz radar that we deployed to the Caribbean islands of St. Croix and Guadeloupe. I learned about digitizing magnetic tapes, FFTs, and issues with timing between remote sites. I also learned about the plasma physics involved with ionospheric heating, and the various instabilities set into motion when the additional energy of the HF heater was transferred into the local plasma.

Upon graduation, I eventually landed in the space surveillance group at the MIT Lincoln Laboratory. There, I worked with Dr. Mike Gaposchkin, the son of the famous woman astronomer, Prof. Celia Payne-Gaposchkin. From him I learned the intricate details of orbit determination, atmospheric drag, and satellite tracking. In 1985, Lincoln Laboratory invested in a Global Positioning System (GPS) receiver, hoping to develop its potential for real-time ionospheric modeling in the satellite-tracking program. For me, this was lucky, because I was able to start working with GPS in the very early days of ionospheric discovery. Later, I was also able to work with Dr. Pratap Misra's group on Globalnaya Navigazionnaya Sputnikovaya Sistema (GLONASS) studies. Lincoln Laboratory also sponsored my water-vapor campaign in 1995, utilizing GPS, radiosondes, water-vapor radiometers, and very-long-baseline interferometry (VLBI). My appreciation for what could be done to enhance atmospheric science with GNSS drew me more and more into what became the central focus of my career: helping to introduce GNSS data to the ionospheric science community.

In the mid-1990s, I oversaw the introduction of yearly Commission G sessions at the US National Radio Science Meeting in Boulder, Colorado, focused on GNSS science. I transferred full time to the MIT Haystack Observatory's atmospheric science group in 2003. We began putting gridded 1° by 1° TEC maps online through the Madrigal database. By the end of this year, we hope to produce a higher resolution line-of-sight TEC product from the almost 5000 GNSS receivers' data that we download every day. We have seen signatures of multiple atmospheric disturbances, ranging from large geomagnetic disturbances, earthquakes, and meteors. In the future, my prediction is that the study of small-scale signatures in the ionosphere will become a rapidly developing research area.

To conclude this, I want to say a few words to students, especially to women students who may wonder how to juggle a career and family, and for those who may not see a straight path forward. To them I say: it is okay. Career paths do not always follow a straight line: graduate school, post-doc, professor, and tenure. I know of one very successful female scientist who took eight years off when her children were small. As for myself, I am grateful that I was able to work at Lincoln Laboratory, where the proposal-writing stress was minimal during my children's early years, when I did have less energy to focus full-time on my career.

It is worth remembering that careers last a long time, and have their ebbs and flows. I have an aunt, who finished her PhD when she was 60, and became a full professor when she was 65. She retired when she was 78. So, always remember, women typically have longer life spans than men. What is more important is to find something that you are excited about, and to keep pushing forward in that area. As for myself, I enjoy working with other people on large projects. I have made wonderful lifelong connections and friendships within this field. I love the stimulation of experimental campaigns, of watching new results appear on the screen, of getting something new to work.

As for being a woman working in a primarily male environment, I think one should always remind yourself that you bring a different and important perspective to the table. You should also remind yourself that if you think something is right, then try to make it happen. Finally – my very last piece of advice – always remember that words of encouragement can make a profound difference in the lives of others.

Introducing the Author

Anthea Coster is a principal research scientist and an Assistant Director at MIT Haystack Observatory, USA. She received her BA in Mathematics at University of Texas at Austin, and the MSc and PhD in Space Physics and Astronomy at Rice University, by running ionospheric-modification experiments at the Arecibo Observatory in

Figure 1. Anthea Coster in front of the Millstone Hill UHF Radar at the Haystack Observatory.

Puerto Rico. After her doctorate in 1983, she received a Research Scientist II position at Georgia Tech Research Institute, and the next year, a researcher position at the Lincoln Laboratory at MIT. From 2003, she has worked as Research Scientist, Principal Research Scientist, and as the Assistant Director at the Haystack Observatory. She is a past Commission G Chair of USNC-URSI, and was recently elected a Fellow of the Institute of Navigation.

Anthea's research interests are physics of the ionosphere, magnetosphere, thermosphere, space weather and storm-time effects, coupling between the lower and upper atmosphere, as well as between the magnetosphere and the ionosphere, GPS positioning and measurement accuracy, radio-wave propagation effects, and meteor detection and analysis. Her current work comprises the primary responsibility for various aspects of the Haystack Observatory's communications, strong engagement in the planned evolution of the Northeast Radio Observatory Corporation (NEROC) in terms of both membership and activities, and helping to coordinate and manage Haystack's growing interactions with researchers and educators on campus. It includes responsibility for overseeing education and public outreach matters, taking a lead in international outreach at Haystack, and responsibility for working with other observatory staff members to proactively address diversity issues at the Observatory on a broad front.

Frequencies and Radioscience 2016 Workshop May 3rd, 2016, Paris, France

The Radio Regulations (RR) Treaty, which established the rules for how worldwide radio communications functions, is regularly updated every three to four years by the World Radiocommunication Conference (WRC) of ITU-R. One of the issues of WRC-15 was the agenda of the next conference (WRC-19). In addition, the provisional agenda of WRC-23 was published. Both agendas tackle scientific and technical matters of high importance.

More specifically, many applications tend to be shifted towards higher and higher frequencies. It therefore appears necessary to deepen our knowledge on propagation of:

1. Fixed links in the 275-450 GHz band,

2. Links between basic stations and mobiles in the 24-86 GHz band, and

3. Evaluation of the loss due to penetration and propagation inside buildings in the 24-86 GHz band.

A precise knowledge of subjects such as propagation and their underlying physical phenomena, and the construction of reliable models, are necessary to the conception of future systems, either fixed, mobile, ground-based, or spatial.

Earth exploration can have many different applications, and WRC-15 enlarged the bandwidth attributed to Earth exploration by SAR operating in the X band onboard satellites. Future needs with respect to Earth exploration in the 45 MHz band have already been envisaged in the WRC-23 agenda.

The Radio Astronomy Service (RAS), which has occupied a specific position among the Services of ITU-R from the beginning, presently has to cope with more and more interference from emissions resulting from various new systems, which require more and more bandwidth. Taking into account frequencies (> 300 GHz), which up to now were not taken into account by the Radio Regulations for radio communications applications, may have important consequences for passive Earth observation by radiometers and spectrometers.

A workshop on Frequencies and Radioscience took place on May 3, 2016, on the Telecom-ParisTech premises. It was co-organized by the technical club RSSR of SEE and the Agence Nationale des Fréquences (ANFR: French National Agency of Frequencies). This workshop emerged from WRC-15. WRC-15 ended in November 2015 in Geneva, after a long month of negotiations. WRC-15 gathered more than 130 nations in order to update the Radio Regulations, which aim at determining the different usages of the radio-electrical spectrum.

WRC-15 was marked by several important regulatory evolutions. The agendas of WRC-19 and WRC-23 aim at preparing major evolutions of the radio communications landscape. For instance, one can note a new high limit of attributed spectrum, which might be pushed up from 275 GHz to 450 GHz. The main aim of this workshop was to invite engineers and scientists working on these issues to exchange their views on subjects that should be studied in depth for the period until the next WRC.

The conclusions of WRC-15 and analysis of the agendas of the next two conferences led to selecting some issues and to defining the agenda of this workshop. The workshop was organized around some main issues: propagation models for fixed or mobile radio communications in high bands, possible evolutions of the radio-electrical environment and possible consequences, stakes and technological challenges. These issues gathered various participants: scientists, industry representatives, representatives from institutions, and also economists. They had the opportunity to exchange and to confront their viewpoints on shared access to spectrum.

Joel Lemorton (ONERA), President of the Scientific Committee, welcomed participants and introduced the workshop. He did this just before Jean-Pierre Le Pesteur, Chair of the ANFR Board, who recalled the stakes of WRC-19, and underlined the need to update and deepen the required knowledge for the work of the ITU-R Study Groups (SG) preparing the conference. He underlined that given the international nature of the process and the need to reach global consensus, four years of preparations for WRCs was rather a short period.

Alexandre Vallet (ANFR) presented the in-depth functioning of ITU-R, in particular, WRCs and Radio Regulations. He explained the significant technical work accomplished by ITU-R Study Groups on a large spectrum of issues in order to reach consensus at WRCs.

Having recalled the hypotheses on which various empirical and theoretical models allowing the description of terrestrial propagation in terms of millimeter waves are based, Hervé Sizun (URSI-France) focused his contribution on the influence of the components of the atmosphere, particularly rain, on point-to-point links.

Nicolas Jeannin (ONERA), winner of the Général Ferrié price in 2015, presented his work on the Earth/space links, so as to face up to the increasing need for bandwidth due to an ever-increasing volume of data.

Laurent Dolizy (Huawei) presented the perspectives of the forthcoming 5G standards, taking into account services simultaneously rendered to users, and resulting bandwidth needs.

Hervé Boeglen (Poitiers University, Laboratory XLIM) presented an experimental means based on software digital radio (SDR) to measure the channel capacity.

In order to illustrate the great variety of techniques currently being developed, Marc Maso (Huawei) described technologies for microwave energy recovery. These allow coping with the data-explosion constraint along with that of energy saving.

Thibaut Caillet (ANFR) presented spectrum-engineering studies led by ANFR with respect to scientific services. Stéphane Kemkemian (Thales) underlined spectrum needs, and the specific constraints of radars for both surveillance and SAR imagery.

Vincent Pietu (IRAM) and Ivan Thomas (Paris Observatory) underlined the importance of the upper part of the spectrum for the Radio Astronomy Service, and the risks related to the overall/general increase of ambient noise level in these bands. This aspect was then followed up by Monique Dechambre (LATMOS), who described the techniques used for passive observation of continental and ocean surfaces by means of microwave radiometry. She showed the serious disturbances of parasite emissions in L band coming from out-of-band emissions, or even prohibited emissions.

Michel Bourdon (RFMB) presented future technologies required for the design of active microwave circuits.

Various contributions were summarized. The scientific and technical nature of the workshop did not prevent participants from enthusiastically taking part in the discussions of the roundtable, which took place at the end of the workshop, on the theme, "Technical Performance and Economic Aspects." The discussions were conducted by Eric Fournier (ANFR), Spectrum Planning and International Affairs Director, and Joëlle Toledano, Professor for Economic and Social Affairs, co-Chair of the Master "Innovation Company and Society" at the University Paris-Saclay.

The organizers of the Workshop wholeheartedly thanked the partner organizations (URSI-France, ONERA, Telecom-ParisTech, IEEE-AESS, SFPT, ANFR), and particularly ANFR, for the contributions of their experts.

The workshop was a unique opportunity for young scientists to learn more about the issue of frequency-spectrum access, along with the procedures put into place by ITU in order to reach a global consensus on Radio Regulations (URSI Working Group 2014-2017 – F1 – Education and Training in Remote Sensing and Related Aspects of Propagation/Next-Generation Radar Remote Sensing)

Jean Isnard
URSI-France
E-mail: jisnard-isti@club-internet.fr

URSI Conference Calendar

July 2016

MMET 2016
16th International Conference on Mathematical Methods in Electromagnetic Theory
Lviv, Ukraine, 5-7 July 2016
Contact: Dr. Alexander Nosich, MMET 2016 TPC Co-Chairman, Laboratory of Micro and Nana Optics, IRE NASU, vul. Proskury 12, Kharkiv 61085, Ukraine, Fax (380-57) 315-2105, E-mail anosich@yahoo.com
http://www.mmet.org/2016

ISPRS-URSI session
SpS15 - URSI-ISPRS Joint Special Session: "Disaster and Risk Management"
Prague, Czech Republic, 12-19 July 2016
Contact: Prof. Tullio Joseph Tanzi (URSI) E-mail: tullio.tanzi@telecom-paristech.fr and Prof Orhan Altan (ISPRS 1st Vice President) E-mail:oaltan@itu.edu.tr
http://www.isprs2016-prague.com/

COSPAR 2016
41st Scientific Assembly of the Committee on Space *Research (COSPAR) and Associated Events*
Istanbul, Turkey, 30 July – 7 August 2016
Contact: COSPAR Secretariat, 2 place Maurice Quentin, 75039 Paris Cedex 01, France, Tel: +33 1 44 76 75 10, Fax: +33 1 44 76 74 37, E-mail: cospar@cosparhq.cnes.fr
https://www.cospar-assembly.org/

August 2016

EMTS 2016
2016 URSI Commission B International Symposium on Electromagnetic Theory
Espoo, Finland, 14-18 August 2016
Contact: Prof. Ari Sihvola, Aalto University, School of Electrical Engineering, Department of Radio Science and Engineering, Box 13000, FI-00076 AALTO, Finland, E-mail: ari.sihvola@aalto.fi

HF13
Nordic HF Conference with Longwave Symposium LW 13
Faro, Sweden (north of Gotland in the Baltic Sea), 15-17 August 2016
Contact: Carl-Henrik Walde, Tornvägen 7, SE-183 52 Taby, Sweden, tel +46 8 7566160 (manual fax switch, E-mail info@walde.se
http://www.ursi.org/img/website24x24.jpg

AP-RASC 2016
2016 URSI Asia-Pacific Radio Science Conference
Seoul, Korea, 21 - 25 August 2016
Contact: URSI AP-RASC 2016 Secretariat, Genicom Co Ltd, 2F 927 Tamnip-dong, Yuseong-gu, Daejeon, Korea 305-510, Fax.: +82-42-472-7459, E-mail: secretariat@aprasc2016.org
http://www.ursi.org/img/website24x24.jpg

September 2016

International Symposium on Turbo Codes and Iterative Information Processing
Brest, France, 5-9 September 2016
Contact: If for submission issues, please contact istc@mlistes.telecom-bretagne.eu
https://conferences.telecom-bretagne.eu/turbocodes

Next-GWiN Workshop 2016
4th International Workshop on Next Generation Green Wireless Networks
Dublin, Ireland, 12-13 September 2016
Contact: Prof. Jacques Palicot, Supelec, Rennes, France, E-mail: Jacques.Palicot@supelec.fr
http://www.next-gwin.org/

ICEAA 2016
Eighteenth edition of the International Conference on Electromagnetics in Advanced Applications
Cairns, Australia, 19-23 September 2016
Contact: Prof. Guido Lombardi, Politecnico di Torino, E-mail: iceaa16@iceaa.polito.it
http://www.iceaa-offshore.org/j3/

Metamaterials 2016
10th International Congress on Advanced Electromagnetic Materials in Microwaves and Optics
Chania, Greece, 19-22 September 2016
Contact: http://congress2016.metamorphose-vi.org/
http://congress2016.metamorphose-vi.org

VERSIM 2016
VLF/ELF Remote Sensing of Ionospheres and Magnetospheres Workgroup
Hermanus, Western Cape, South Africa, 19-23 September 2016
Contact: VERSIM@sansa.org.za
http://events.sansa.org.za/versim-information

October 2016

RFI 2016
Radio Frequency Interference 2016
Socorro, NM, USA, 10-13 October 2016
Contact: Prof. Willem Baan, Asserweg 45, NL-9411 LP Beilen, The Netherlands, E-mail: baan@astron.nl
(website in preparation)

RADIO 2016
IEEE Radio and Antenna Days of the Indian Ocean 2016
Réunion Island, 10-13 October 2016
Contact: radio2016@radiosociety.org
http://www.radiosociety.org/radio2016/

ISAP 2016
2016 International Symposium on Antennas and Propagation
Okinawa, Japan, 24-28 October 2016
Contact: Prof. Toru Uno, Tokyo Univ. of Agriculture & Technology, Dept of Electrical and Electronic Engineering, 2-24-16 Nakamachi, Koganei 184-8588, Japan, Fax +81 42-388 7146, E-mail: uno@cc.tuat.ac.jp
http://isap2016.org/

November 2016

SCOSTEP/ISWI International School on Space Science
Sangli, India, 7-17 November 2016
Contact: Dr. Dadaso Jaypal Shetti, Department of Physics, Smt. Kasturbai Walchand College, Sangli, Maharashtra-416416, India, E-mail:- iswi2016@gmail.com, Fax: +91-233-2327128
http://www.iiap.res.in/meet/school_meet/index.php

August 2017

URSI GASS 2017
XXXIInd URSI General Assembly and Scientific Symposium
Montreal, Canada, 19-26 August 2017
Contact: URSI Secretariat, Ghent University - INTEC, Technologiepark - Zwijnaarde 15, 9052 Gent, Belgium, E-mail info@ursi.org

May 2018

AT-RASC 2018
Second URSI Atlantic Radio Science Conference
Gran Canaria, Spain, 28 May – 1 June 2018
Contact: Prof. Peter Van Daele, URSI Secretariat, Ghent University – INTEC, Technologiepark-Zwijnaarde 15, B-9052 Gent, Belgium, Fax: +32 9-264 4288, E-mail address: E-mail: peter.vandaele@intec.ugent.be
http://www.at-rasc.com

May 2019

EMTS 2019
2019 URSI Commission B International Symposium on Electromagnetic Theory
San Diego, CA, USA, 27-31 May 2019
Contact: Prof. Sembiam R. Rengarajan, California State University, Northridge, CA, USA, Fax +1 818 677 7062, E-mail: srengarajan@csun.edu

Information for Authors

Content

The *Radio Science Bulletin* is published four times per year by the Radio Science Press on behalf of URSI, the International Union of Radio Science. The content of the *Bulletin* falls into three categories: peer-reviewed scientific papers, correspondence items (short technical notes, letters to the editor, reports on meetings, and reviews), and general and administrative information issued by the URSI Secretariat. Scientific papers may be invited (such as papers in the *Reviews of Radio Science* series, from the Commissions of URSI) or contributed. Papers may include original contributions, but should preferably also be of a sufficiently tutorial or review nature to be of interest to a wide range of radio scientists. The *Radio Science Bulletin* is indexed and abstracted by INSPEC.

Scientific papers are subjected to peer review. The content should be original and should not duplicate information or material that has been previously published (if use is made of previously published material, this must be identified to the Editor at the time of submission). Submission of a manuscript constitutes an implicit statement by the author(s) that it has not been submitted, accepted for publication, published, or copyrighted elsewhere, unless stated differently by the author(s) at time of submission. Accepted material will not be returned unless requested by the author(s) at time of submission.

Submissions

Material submitted for publication in the scientific section of the *Bulletin* should be addressed to the Editor, whereas administrative material is handled directly with the Secretariat. Submission in electronic format according to the instructions below is preferred. There are typically no page charges for contributions following the guidelines. No free reprints are provided.

Style and Format

There are no set limits on the length of papers, but they typically range from three to 15 published pages including figures. The official languages of URSI are French and English: contributions in either language are acceptable. No specific style for the manuscript is required as the final layout of the material is done by the URSI Secretariat. Manuscripts should generally be prepared in one column for printing on one side of the paper, with as little use of automatic formatting features of word processors as possible. A complete style guide for the *Reviews of Radio Science* can be downloaded from http://www.ips.gov.au/IPSHosted/NCRS/reviews/. The style instructions in this can be followed for all other *Bulletin* contributions, as well. The name, affiliation, address, telephone and fax numbers, and e-mail address for all authors must be included with

All papers accepted for publication are subject to editing to provide uniformity of style and clarity of language. The publication schedule does not usually permit providing galleys to the author.

Figure captions should be on a separate page in proper style; see the above guide or any issue for examples. All lettering on figures must be of sufficient size to be at least 9 pt in size after reduction to column width. Each illustration should be identified on the back or at the bottom of the sheet with the figure number and name of author(s). If possible, the figures should also be provided in electronic format. TIF is preferred, although other formats are possible as well: please contact the Editor. Electronic versions of figures *must* be of sufficient resolution to permit good quality in print. As a rough guideline, when sized to column width, line art should have a minimum resolution of 300 dpi; color photographs should have a minimum resolution of 150 dpi with a color depth of 24 bits. 72 dpi images intended for the Web are generally *not* acceptable. Contact the Editor for further information.

Electronic Submission

A version of Microsoft *Word* is the preferred format for submissions. Submissions in versions of T_EX can be accepted in some circumstances: please contact the Editor before submitting. *A paper copy of all electronic submissions must be mailed to the Editor, including originals of all figures.* Please do *not* include figures in the same file as the text of a contribution. Electronic files can be send to the Editor in three ways: (1) By sending a floppy diskette or CD-R; (2) By attachment to an e-mail message to the Editor (the maximum size for attachments *after* MIME encoding is about 7 MB); (3) By e-mailing the Editor instructions for downloading the material from an ftp site.

Review Process

The review process usually requires about three months. Authors may be asked to modify the manuscript if it is not accepted in its original form. The elapsed time between receipt of a manuscript and publication is usually less than twelve months.

Copyright

Submission of a contribution to the *Radio Science Bulletin* will be interpreted as assignment and release of copyright and any and all other rights to the Radio Science Press, acting as agent and trustee for URSI. Submission for publication implicitly indicates the author(s) agreement with such assignment, and certification that publication will not violate any other copyrights or other rights associated with the submitted material.

Application for an URSI Radioscientist

APPLICATION FOR URSI RADIOSCIENTIST

I have not attended the last URSI General Assembly & Scientific Symposium, and wish to remain/become an URSI Radioscientist in the 2014-2017 triennium. This application includes a subscription to *The Radio Science Bulletin* and inclusion in the URSI mailing lists.

(Please type or print in BLOCK LETTERS)

Name : Prof./Dr./Mr./Mrs./Ms. _____
Family Name First Name Middle Initials

Present job title: _____

Years of professional experience: _____

Professional affiliation: _____

I request that all information be sent to my ☐ home ☐ business address, i.e.:

Company name: _____

Department: _____

Street address: _____

City and postal/zip code: _____

Province/State: _____ Country: _____

Tel: _____ ext. _____ Fax: _____

E-mail: _____

Areas of interest *(Please tick)*

- ☐ A Electromagnetic Metrology
- ☐ B Fields and Waves
- ☐ C Radio-Communication Systems & Signal Processing
- ☐ D Electronics and Photonics
- ☐ E Electromagnetic Environment & Interference
- ☐ F Wave Propagation & Remote Sensing
- ☐ G Ionospheric Radio and Propagation
- ☐ H Waves in Plasmas
- ☐ J Radio Astronomy
- ☐ K Electromagnetics in Biology & Medicine

☐	By signing up, you agree to be included into the URSI mailing list. You can unsubscribe at any time.
☐	I agree that my contact details will be used by URSI only and will never be transferred to other parties.

Please return this signed form to :

The URSI Secretariat
Ghent University - INTEC
Technologiepark - Zwijnaarde
B-9052 GHENT, BELGIUM
E-mail: info@ursi.org